

**C H A P T E R - 3**

**RESULTS AND DISCUSSION**

**(RANDOM COPOLYMERS)**

## CHAPTER - 3

### Results and Discussion (random copolymers)

	Page
3.1 Optimisation of reaction conditions	84
3.1.1 Monomer : Monomer ratio	84
3.1.2 Reaction time	86
3.1.3 Initiator concentration	89
3.1.4 Reaction temperature	91
3.2 Characterisation	91
3.2.1 IR	91
3.2.2 NMR	95
3.2.3 Solubility of copolymers	95
3.2.4 Monomer reactivity ratio	96
3.2.5 Rate of copolymerisation	103
3.2.6 Viscosity studies	103
3.2.7 Differential scanning calorimetry	122
3.2.8 Thermogravimetric analysis	124
3.2.9 Differential thermal analysis	137
3.2.10 Wide angle X-ray diffraction	142
3.2.11 Microscopy	143
3.2.12 Contact angle measurements	149
3.2.13 Solubility parameters of copolymer	154
3.2.14 Swelling	158
3.2.15 Differential refractometry	163
3.2.16 Adiabatic compressibility	167
3.2.17 Zeta potential	167
3.2.18 Hydrolysis of copolymers	169
References	175

### 3. RESULTS AND DISCUSSION :

From literature survey it is observed that majority of the work in synthesising MMA-AN copolymers is done in DMF medium. Here we are systematically optimising the reaction conditions for the synthesis of MMA-AN copolymers in a relatively inexpensive toluene medium.

#### 3.1 Optimisation of reaction conditions :

The reaction conditions for random copolymerisation of methyl methacrylate and acrylonitrile have been optimised by varying the composition of the monomers in the feed, and also by varying reaction time, initiator concentration and reaction temperature.

##### 3.1.1 Monomer : Monomer ratio :

In the industrial production of copolymers it is important to know what a composition the monomer mixture is needed to give a copolymer with a desired composition. Hence the study of effect of monomer : monomer concentration in feed ratio was undertaken. The results obtained are given in Table 3.1. From the results we can summarise that percentage yield is almost independent of monomer : monomer feed ratio provided all other experimental conditions are identical. From the nitrogen analysis it was observed that the copolymers always showed higher mole-fractions of MMA than AN when compared with the mole fraction values taken in the feed composition. This is due to the higher reactivity of MMA. Further it has been observed that with an increase in MMA concentration in the feed, the copolymers formed were colourless and transparent and resembled PMMA. On the other hand with the increase in AN concentration

Table - 3.1

Effect of monomer : monomer ratio on percentage yield.

Reaction time : 6 h

Reaction temperature : 75°

Initiator concentration :  $5 \times 10^{-3}$  M

Total Volume : 100 cm<sup>3</sup>

Medium : toluene

Sample Code	Ratio of MMA:AN (v/v) in the feed	Mole fraction of MMA in the feed	Mole fraction of AN in the feed	Mole fraction of MMA in the copolymer	Mole fraction of AN in the copolymer	Percentage yield (%)
A <sub>1</sub>	3:1	0.65	0.35	0.68	0.32	70.00
A <sub>2</sub>	2:1	0.55	0.45	0.64	0.36	65.00
A <sub>3</sub>	3:2	0.48	0.52	0.60	0.40	62.00
A <sub>4</sub>	1:1	0.38	0.62	0.55	0.45	62.00
A <sub>5</sub>	2:3	0.29	0.71	0.41	0.59	68.00
A <sub>6</sub>	1:2	0.24	0.76	0.38	0.62	66.00
A <sub>7</sub>	1:3	0.17	0.83	0.28	0.72	70.00

in the feed, the copolymers formed exhibited decreased solubility in toluene and yellow to orange colouration. This colouration is due to the formation of a system of several conjugated double bonds - C=N- [ 1 ]. The viscosity studies of these copolymers are discussed in details in section 3.2.6. The data obtained for the effect of variation in monomer : monomer ratio on intrinsic viscosity of the resulting copolymers is presented in Fig. 3.1. It is observed that with the increase of MMA/AN ratio (W/W), intrinsic viscosity and hence viscosity molecular weight graphs show a parabolic nature. The initial sharp decrease in intrinsic viscosity is observed with initial incorporation of MMA in copolymer and further increase in MMA/AN ratio in the feed composition shows marginal increase in intrinsic viscosity. This may be due to the lower molecular weight of PMMA formed and higher reactivity of MMA which influences the viscosity property of the resulting copolymer. The copolymers resulting from the very high ratios of MMA/AN are very much similar to PMMA and vice-versa. However, the viscosity molecular weights calculated for the copolymers rich in MMA were much lower than the molecular weight of PMMA (Table 3.6 ). The details of viscosity molecular weight are discussed in section 3.2.6

### 3.1.2 Reaction time :

The results obtained for the effect of reaction time on percentage yield and intrinsic viscosity of the resulting copolymers are given in Fig.3.2. It is observed that with the increase in reaction time percentage yield increases. This is due to the increased extent of decomposition of benzoyl peroxide with time resulting into higher percentage yield. After an optimum time quantitative decomposition and consumption of free radicals results into a constant percentage yield; whereas the graph for intrinsic viscosity passes through a maxima. Initial increase in intrinsic viscosity is due to increased size of polymer chain

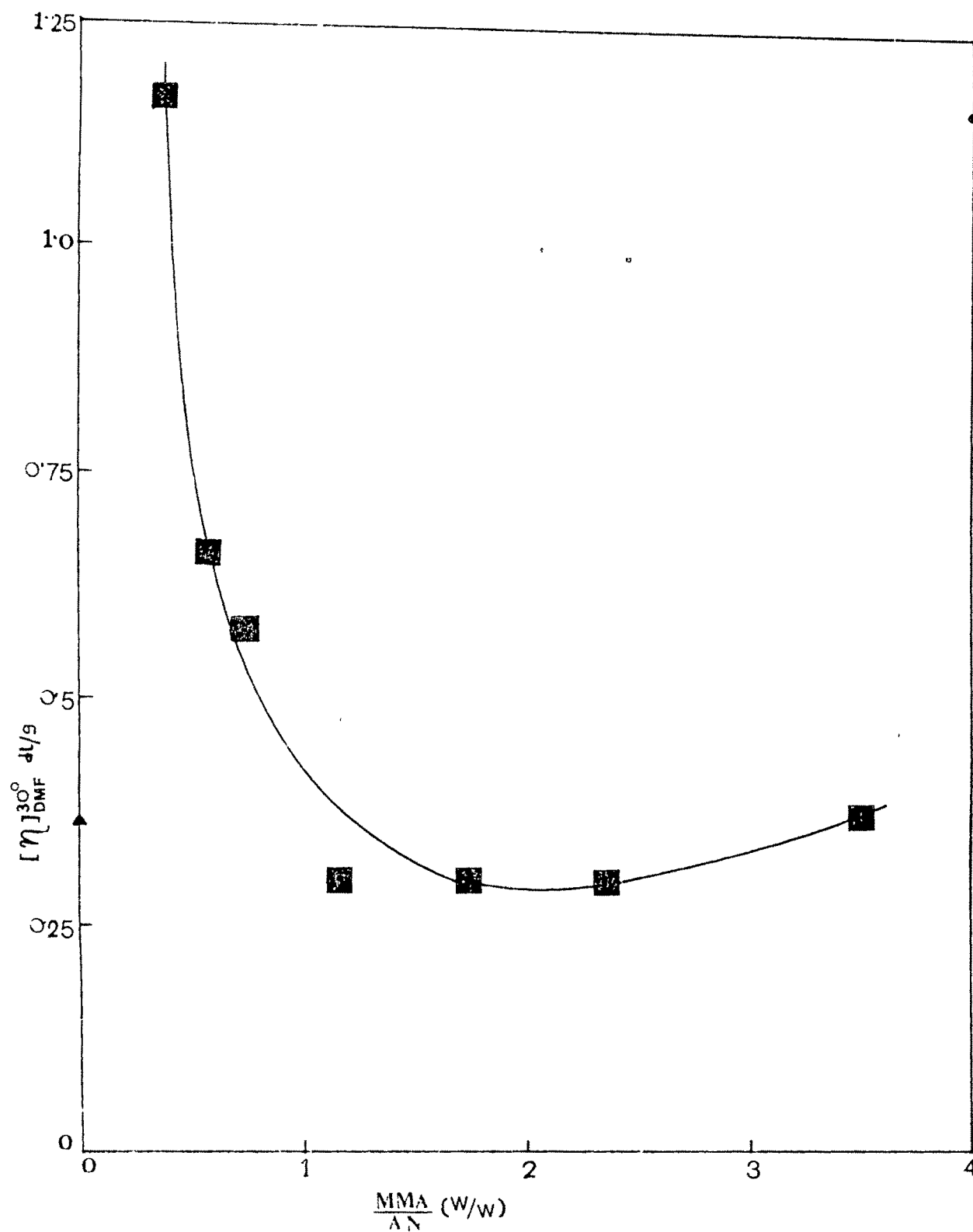


Fig.3.1. Effect of monomer: monomer ratio on intrinsic viscosity of copolymers in DMF at 30°. Reaction time: 6h, Benzoylperoxide concentration:  $5 \times 10^{-3}$  M, reaction temperature : 75°. ● PAN and ▲ PMMA.

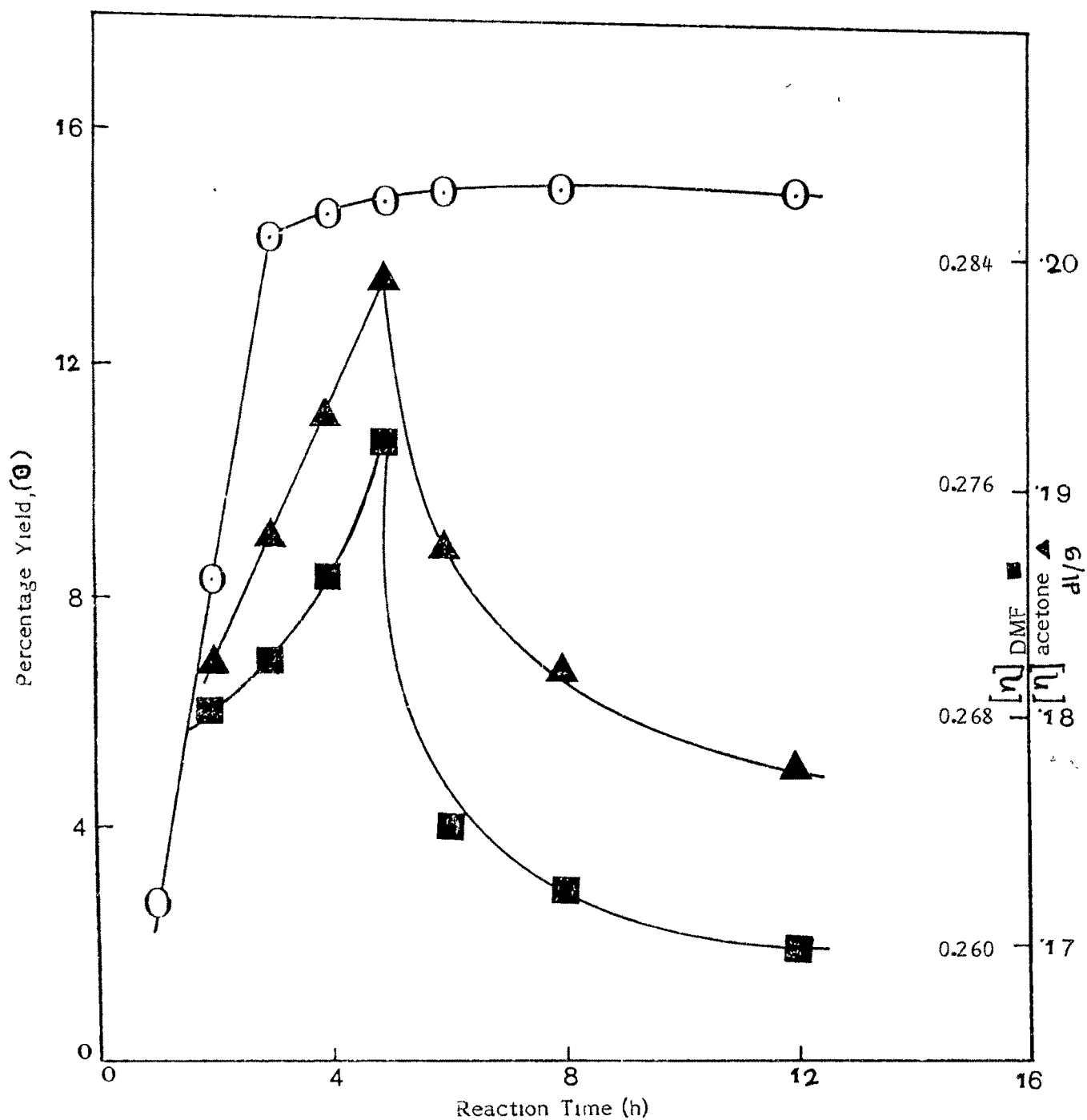
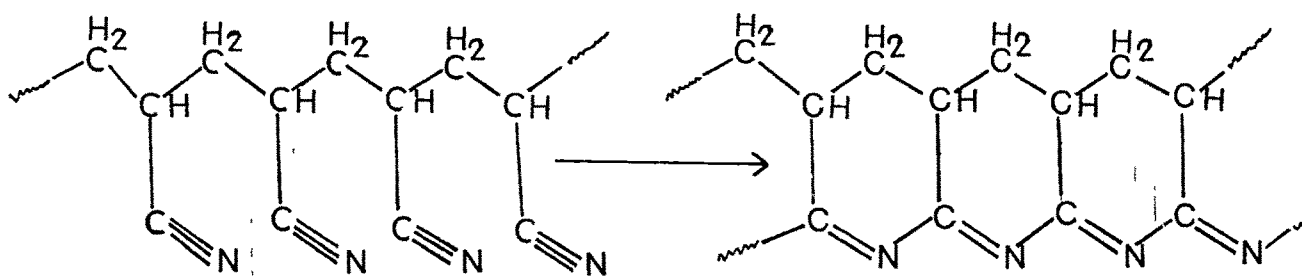


Fig.3.2 Effect of reaction time on percentage yield and intrinsic viscosity. Benzoyl peroxide concentration:  $5 \times 10^{-4} M$ , reaction temperature:  $75^\circ$ , MMA: AN 2:1 (v/v). percentage yield,  $\blacktriangle$  intrinsic viscosity in acetone at  $30^\circ$ ,  $\blacksquare$  intrinsic viscosity in DMF at  $30^\circ$ .

and hence molecular weight with time. Due to higher reactivity of MMA, the copolymers formed at lower reaction time show higher composition of MMA whereas for longer reaction times the initially unreacted AN is predominantly incorporated into the copolymer. Hence products are relatively rich in AN. Acetone being a non-solvent for PAN during viscosity measurements, PAN segments of the poly(methyl methacrylate-co-acrylonitrile) develop a theta ( $\theta$ ) solvent with respect to copolymer and for that the intrinsic viscosity decreases. Hence the copolymers synthesised at higher reaction time show decreasing intrinsic viscosity in acetone. The intrinsic viscosity data in DMF also exhibits similar pattern. In this case the decrease in intrinsic viscosity may be due to the cyclisation of the PAN segments of the copolymer to pseudo-naphthylidenes [2,3] as shown below. As a result the copolymer exhibits reduced interactions with solvent and hence resulting into lower intrinsic viscosities.



### 3.1.3 Initiator Concentration :

The results of the effect of concentration of benzoyl peroxide on copolymerisation are presented in Fig. 3.3. It is observed that as the concentration of benzoyl peroxide increases percentage yield initially increases and then remains constant. This is because, with increasing initiator concentration, the number of free radicals formed are increased accelerating the copolymerisation. A stage is attained when all the active monomers take part in copolymerisation reaction and further addition of benzoyl peroxide does not affect the reaction, thereby giving constant percentage yield. But with increase of benzoyl peroxide

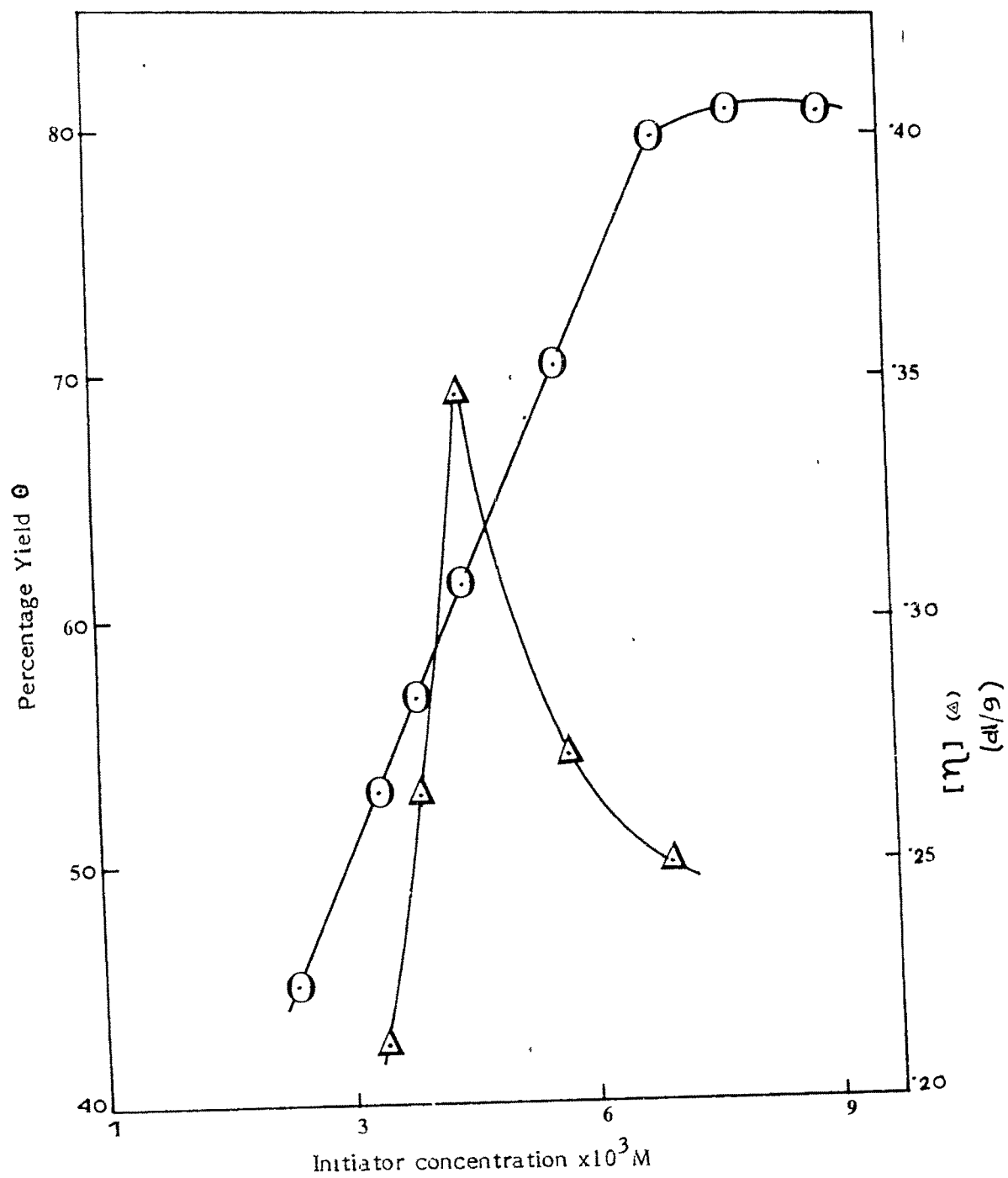


Fig.3.3 Effect of initiator concentration on percentage yield and intrinsic viscosity in DMF at 30°, reaction time:6h, temperature:75°,MMA:AN 2:1(v/v)

concentration, the intrinsic viscosity of the resulting copolymer in DMF initially increases and then decreases. The initial increase in intrinsic viscosity is due to the increase of molecular weight of copolymer with higher degree of polymerisation due to accelerated propagation. Further increase in the concentration of benzoyl peroxide causes the mutual termination by disproportionation between the active monomers sites, hence resulting into a polymer with a lower molecular weight exhibiting lower intrinsic viscosity. Hence the overall result is the appearance of maxima.

#### 3.1.4 Reaction temperature :

Table 3.2 shows the results of the effect of reaction temperature on the copolymerisation of MMA and AN. It is observed from the results that with the increase of reaction temperature the percentage yield increases and then remains constant. This may be due to the increased number of free radicals formed at higher temperature, which accelerates the copolymerisation reaction thus increasing the percentage yield. A temperature is attained when initiator is quantitatively decomposed into free radicals and further increase in temperature causes no effect on the formation of free radicals. Hence the percentage yield remains constant.

### 3.2 Characterisation :

#### 3.2.1 I R analysis:

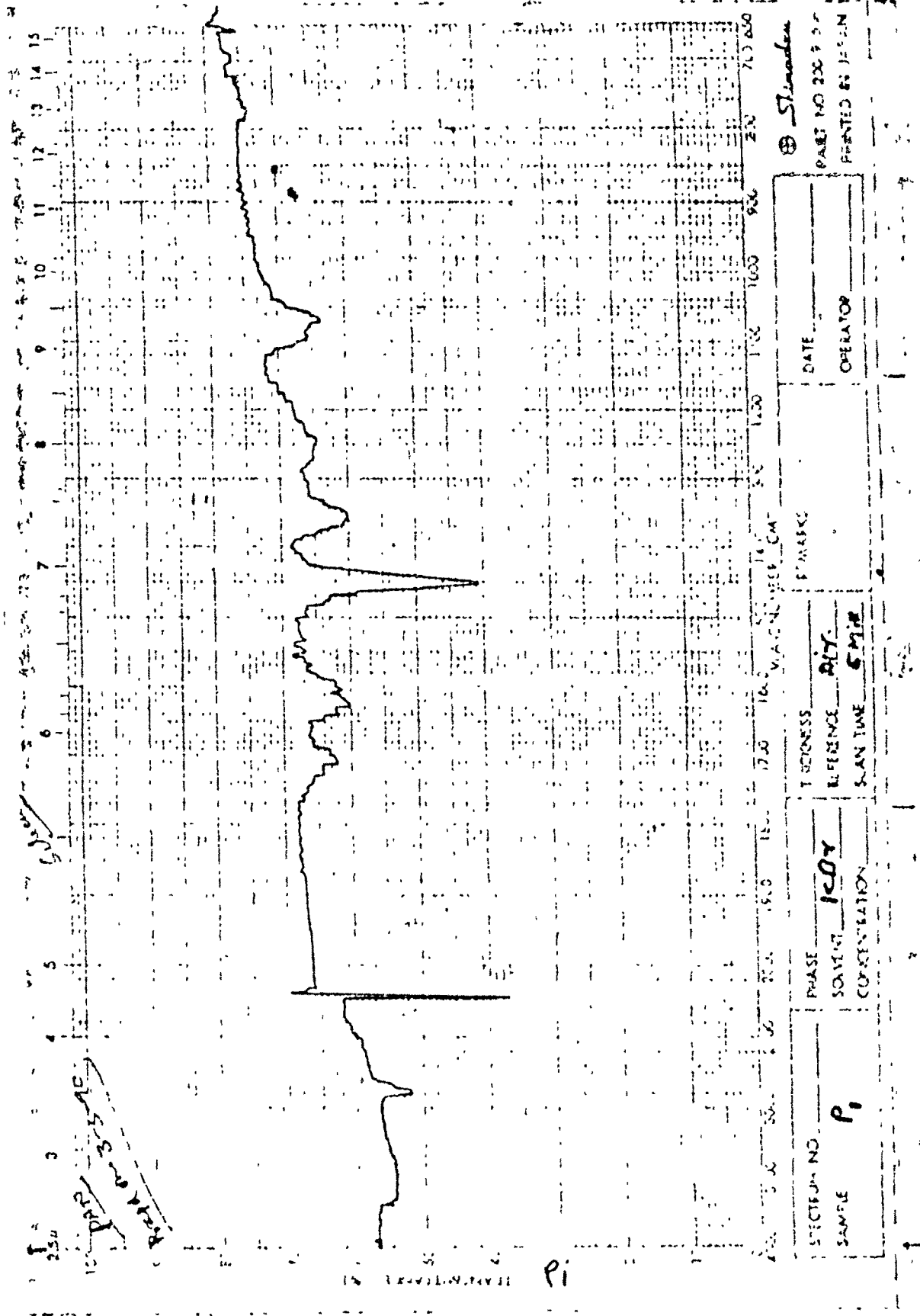
The i.r. spectra of PAN, PMMA, and a representative copolymer of MMA and AN are given in Figs.3.4-3.6. The i.r. spectra of PAN (Fig. 3.4) shows the sharp distinct peak at  $2250\text{ cm}^{-1}$  corresponding to  $\text{-C}\equiv\text{N}$  stretching, whereas i.r. spectra of PMMA (Fig. 3.5) exhibits the bands at  $1735\text{ cm}^{-1}$  and  $2930\text{ cm}^{-1}$  corresponding

Table - 3.2

Effect of reaction temperature on percentage yield.

Monomer : monomer ratio	: 2:1 (MMA:AN) (v/v)
Reaction time	: 6 h
Initiator concentration	: $5 \times 10^{-3}$ M
Total volume	: $100 \text{ cm}^3$
Medium	: toluene

Temperature (°C)	Percentage yield (%)
70	60
75	65
80	73
85	74
90	75
100	75



SPECTRUM NO. _____ SAMPLE <b>Pi</b>	PHASE _____ SOLVENT <b>PCOY</b> CONCENTRATION _____	T REFERENCE _____ REFERENCE <b>Pi</b> SCAN TIME <b>5 MIN</b>	DATE _____ OPERATOR _____
--	---	--	------------------------------

PART NO 35510  
 PRINTED BY JESUN  
 © *Stinson*

Fig.3.4 IR spectra of PAN

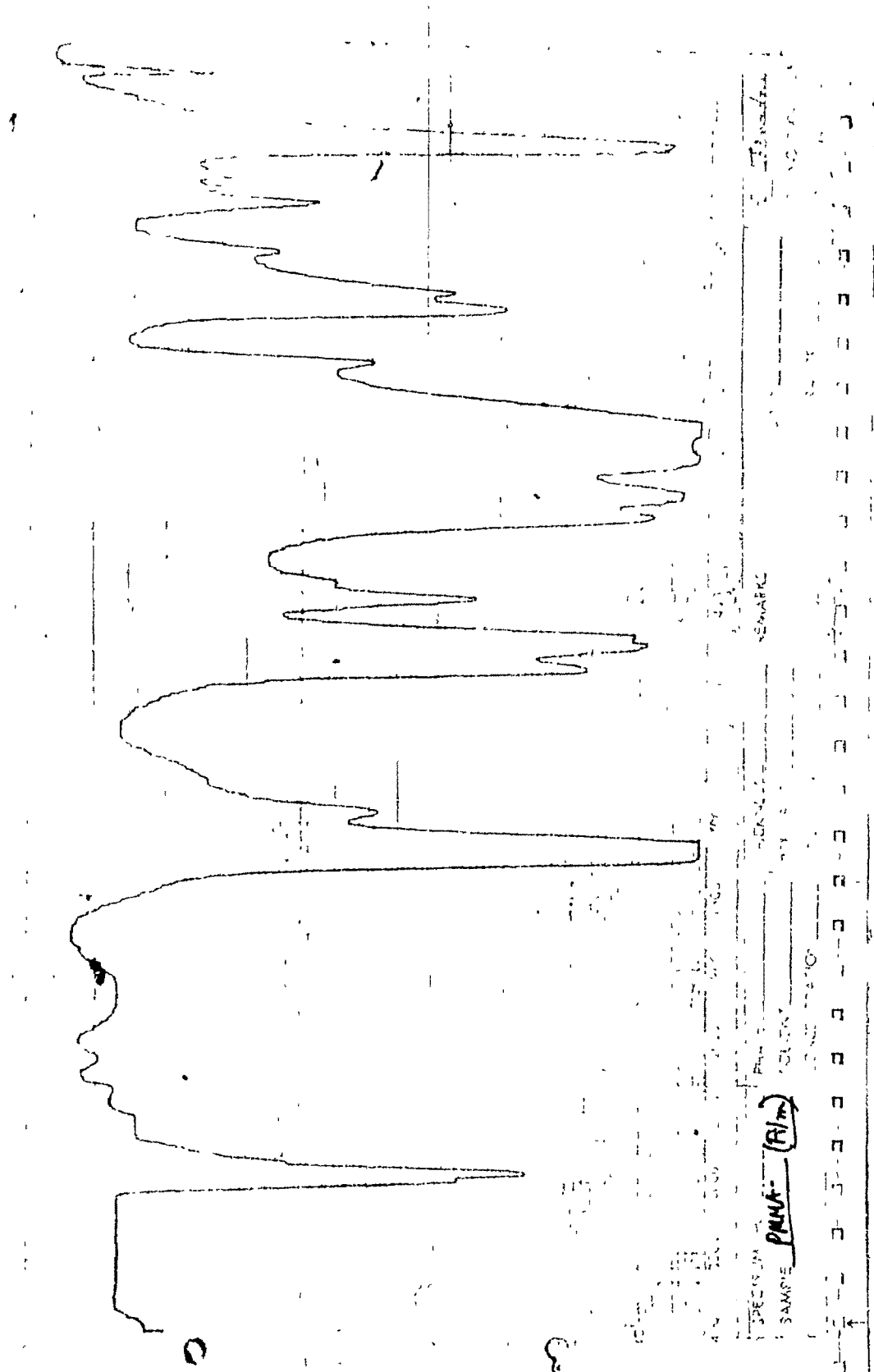


Fig.3.5 IR spectra of PMMA

to carbonyl and methyl stretching vibrations of  $-\text{COCH}_3$ . In Fig. 3.6, for the copolymers of MMA and AN the presence of AN unit in copolymer is confirmed by the sharp peak exhibited at  $2250 \text{ cm}^{-1}$  for  $\text{C}\equiv\text{N}$  stretching vibration and the presence of MMA unit is confirmed by the i.r. bands at  $1735 \text{ cm}^{-1}$  and  $2930 \text{ cm}^{-1}$  for carbonyl stretching and methyl stretching vibrations respectively from  $-\text{COCH}_3$ .

### 3.2.2 $^1\text{H}$ NMR analysis :

The  $^1\text{H}$  NMR spectrum of copolymer is given in Fig.3.7. In the spectrum the ester methyl proton ( $\text{OCH}_3$ ) appeared at 3.65 ppm, the  $\beta$ -methylene protons ( $-\text{CH}_2-$ ) appeared in the range 1.8 - 2.2 ppm,  $\beta$ -methyl protons ( $-\text{CH}_3$ ) gave peaks at 1.3 ppm. The methine proton from acrylonitrile unit appeared at 4.05 ppm. These signals which are characteristic of MMA and AN clearly showed their presence in the copolymer. The peak at 3.3 is for solvent DMSO.

### 3.2.3 Solubility of Copolymers

Solubility behaviour of the copolymers and PMMA as well as PAN was studied using various solvents. PMMA is soluble in chloroform acetone, benzene and toluene, whereas PAN is insoluble in the above solvents. However, the copolymers with mole fraction of AN upto 0.59 are soluble in the above solvents. The synthesised PMMA is insoluble in DMSO but the copolymers of MMA and AN irrespective of their composition are soluble in DMSO. These solubility tests confirm the formation of true copolymers from the monomers MMA and AN. The results for solubility behaviour of the copolymers are given in Table 3.3.

### 3.2.4 Determination of monomer reactivity ratios :

For the determination of reactivity ratios, copolymers synthesised at lower

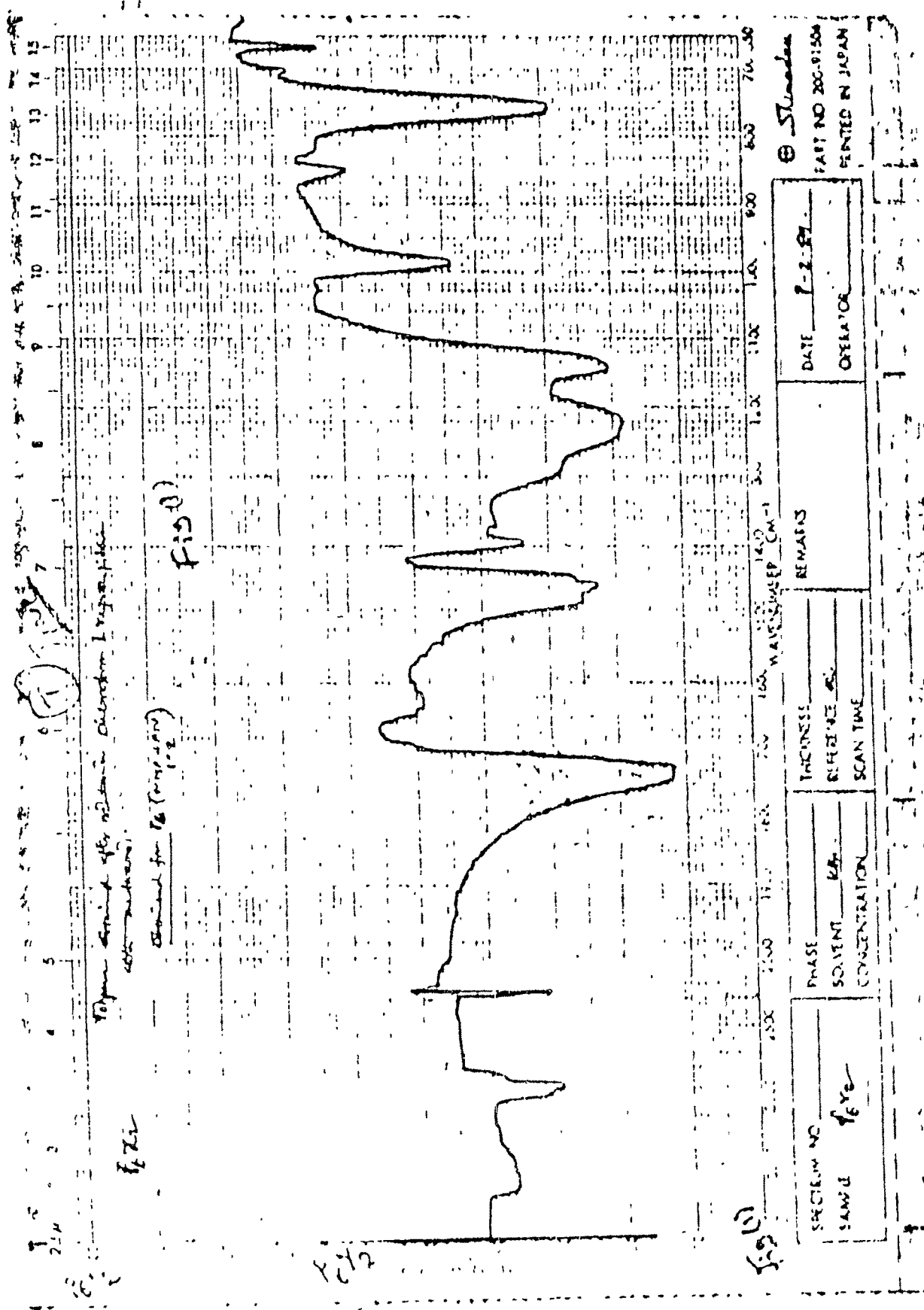


Fig.3.6 IR spectra of copolymer: MMA:AN 1:2 (v/v), sample A<sub>6</sub>

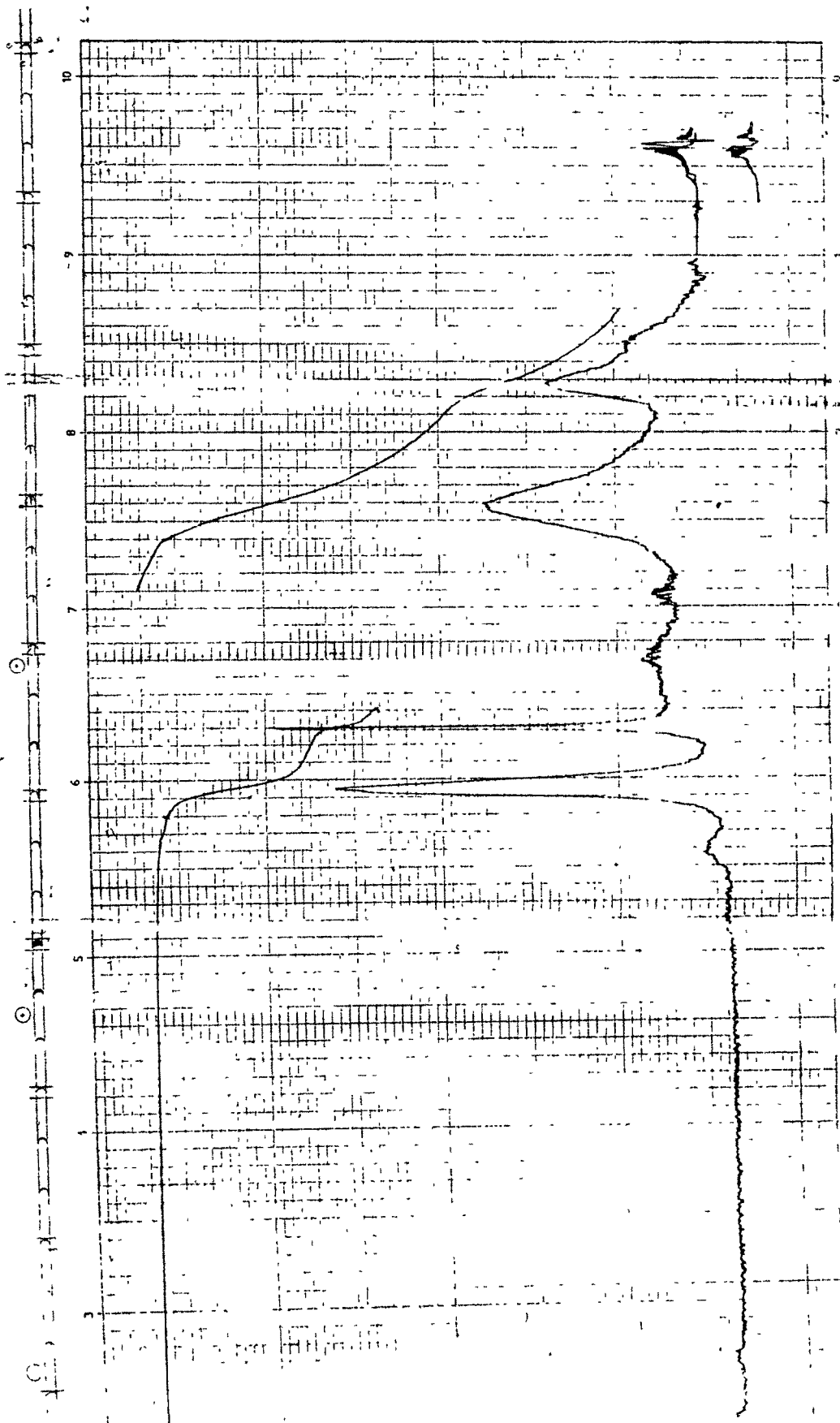


Fig.3.7 : NMR spectra of copolymer ( sample A )

© 1971 PERKIN-ELMER, INC. PART NO 5600 6671 MADE IN GREAT BRITAIN

Table-3.3

Solubility behaviour of random copolymers in various solvents at 30°

Solvents	Mole fraction of AN in the copolymer									
	0	0.26	0.32	0.36	0.40	0.45	0.59	0.62	0.72	1.0
Acetone	+	+	+	+	+	+	+	-	-	-
CHCl <sub>3</sub>	+	+	+	+	+	+	+	-	-	-
Toluene	+	+	+	+	+	+	+	-	-	-
CCl <sub>4</sub>	-	-	-	-	-	-	-	-	-	-
DMF	+	+	+	+	+	+	+	+	+	+
Ether	-	±	±	±	-	-	-	-	-	-
THF	-	+	+	±	-	-	-	-	-	-
IBMK	+	+	+	+	+	+	+	-	-	-
Heptane	-	-	-	-	-	-	-	-	-	-
Ether + Heptane mixture	-	-	-	-	-	-	-	-	-	-
DMSO	-	+	+	+	+	+	+	+	+	+
DMA	+	+	+	+	+	+	+	+	+	+
Xylene	+	-	-	-	-	-	-	-	-	-
Nitro- benzene	+	+	+	+	+	+	+	+	+	-

+ soluble

- insoluble

± swelling

conversion rates (<5%) were used. The composition of the monomers in the copolymers was determined from acrylonitrile content in the copolymer through nitrogen analysis by Dumas method. The results are given in Table 3.4 and Fig. 3.8. From Fig. 3.8 it is seen that with increased acrylonitrile content in the feed ratio, the copolymers show increased mole fraction of AN which is expected. The observed increase is almost linear with correlation coefficient of 0.974. Several methods [4-6] are available for the determination of reactivity ratios all depends of course, on careful analysis of the copolymers formed from monomer mixtures at a series of compositions. Since the composition changes with conversion, it is necessary either to limit the copolymerisation to low conversion or to treat the integral composition, using, for example, the integral composition equation of Skeist [ 7 ] as given below.

$$\ln \left( \frac{[M]}{[M]_0} \right) = \int_{f_2}^{f_1} \frac{df_1}{(F_1 - f_1)}$$

Since the calculations involved in the latter method are excessively cumbersome, we have used the former procedure. Fineman - Ross [8] and Kelen-Tudos [9] methods are used to determine the reactivity ratios. Details of the process are discussed in section 2.4.8. The data of the copolymer composition were treated according to these two methods. The conversion of the copolymers was maintained below 5% to ensure the homogeneity of the resulting copolymers. The various parameters required for the calculations are given in Table 3.5. The reactivity ratios  $r_1$  (MMA) and  $r_2$  (AN) evaluated by Fineman-Ross method are 1.20 and 0.15 respectively and by Kelen-Tudos method are 1.20 and 0.16 respectively. The product of the reactivity ratios (i.e.  $r_1 r_2$ ) in the present system is less than one confirming the random nature of the resulting copolymers. The monomer reactivity ratios calculated by the above two methods are in good agreement with the literature values [10].

Table - 3.4

Copolymer composition from nitrogen analysis (Dumas method)

Reaction time	: 45 minutes
Reaction temperature	: 75°
Initiator concentration	: $5 \times 10^{-3}$ M
Total volume	: 100 cm <sup>3</sup>
medium	: Toluene

Run	Feed composition mol/dm <sup>3</sup> [MMA] [AN]		Weight of copolymer (g)	Conversion (%)	Nitrogen in the copoly- mer (%)	Mole of AN in the copoly- mer $\times 10^4$
1	2.83	1.52	0.4955	2.72	4.82	17.06
2	2.64	2.13	0.3435	1.82	5.27	12.93
3	1.89	3.04	0.3805	2.18	7.32	19.90
4	1.51	3.65	0.5630	3.27	8.51	34.22
5	1.32	4.25	0.5820	3.26	10.79	44.87
6	0.94	4.56	0.5040	3.00	12.37	44.55

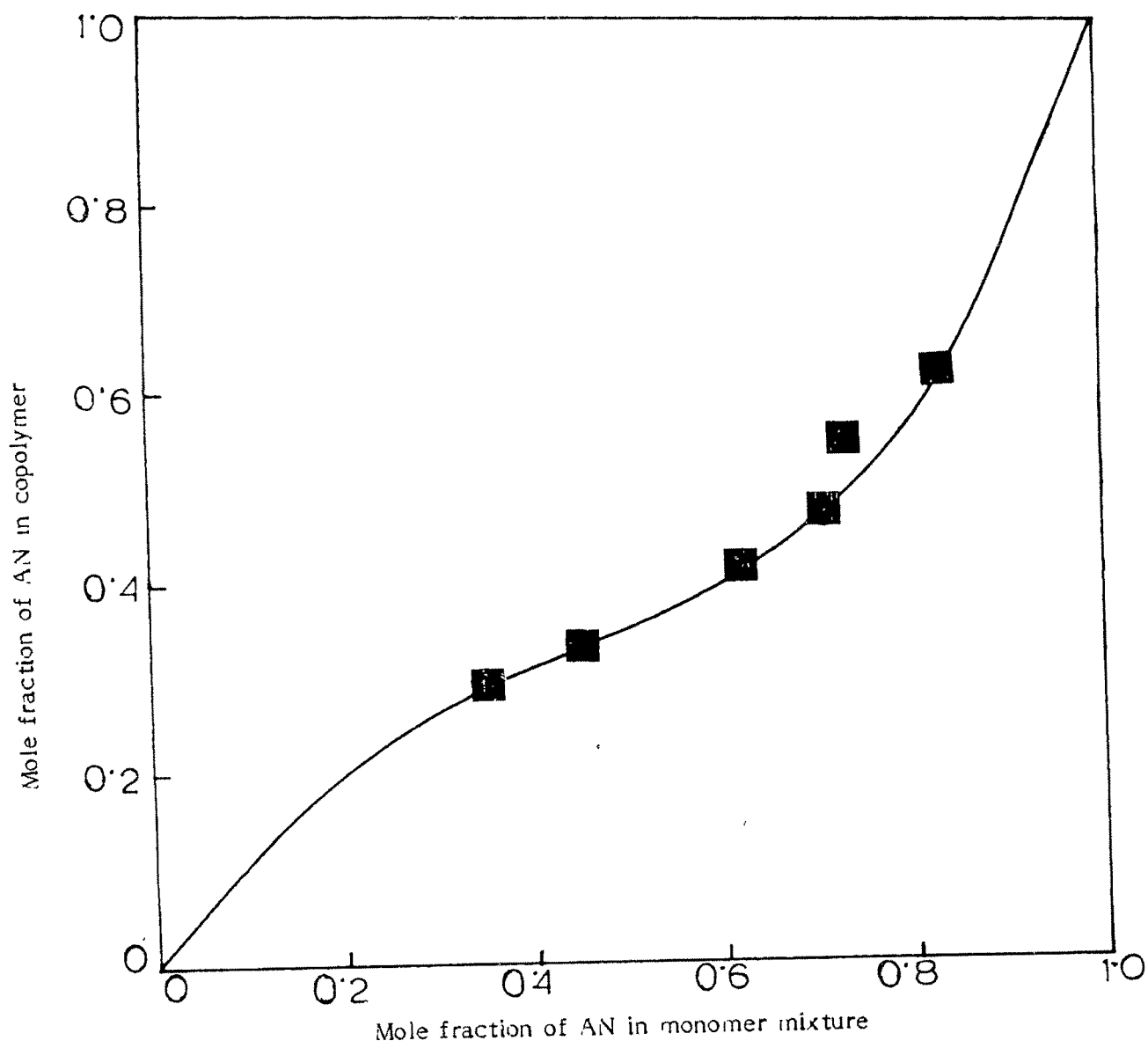


Fig.3.8 Copolymer composition curve. Reaction time:45min. Benzoyl peroxide concentration:  $5 \times 10^{-3}$  M, temperature:  $75^{\circ}$ , medium: Toluene.

Table - 3.5

Parameters for Fineman-Ross and Kelen-Tudos equations for the copolymer of MMA and AN.  $\alpha = 0.322$

Run	F	f	$G=F(f-1)/f$	$H=F^2/f$	$\eta=G/(\alpha+H)$	$\xi=H/(\alpha+H)$
1	1.8636	2.3740	1.0786	1.4630	0.6040	0.8196
2	1.2417	2.1265	0.6577	0.7250	0.6280	0.6924
3	0.6212	1.3824	0.1718	0.2790	0.2860	0.4642
4	0.4139	1.1152	0.0428	0.1540	0.0895	0.3235
5	0.3104	0.7671	-0.0942	0.1260	-0.2100	0.2813
6	0.2069	0.6014	-0.1371	0.0710	-0.3490	0.1807

### 3.2.5 Rate of copolymerisation :

The rate of copolymerisation of MMA and AN is determined by using the copolymerisation equation 1.21 mentioned earlier in section 1.4 . The rate of homopolymerisation was also determined under identical conditions to get value of  $\delta_2/\delta_1$  and  $R_1^{1/2}/\delta_1$  required for calculation of rate of copolymerisation ( $R_p$ ). The values of reactivity ratios  $r_1$  and  $r_2$  were calculated as discussed above (section 3.2.4). The only indeterminable factor in our experiment in the determination of rate of copolymerisation was the value of  $\phi$ , the ratio of termination rate constant. For the system MMA-AN, the value of  $\phi$  has been determined by Luskin [11] and is given as  $\phi = 6 - 24$ . We have used the highest and lowest values of  $\phi$  (i.e.  $\phi = 24$  and 6) for calculation of rate of copolymerisation. Fig. 3.9 shows the plot of rate of copolymerisation against mole fraction of AN. It is evident from the graph that the rate of copolymerisation increases with increase of AN concentration (mole fraction) in the feed. It is also observed from the figure that the rate of copolymerisation lies between the homo polymerisation rates when the value of  $\phi = 24$  (Fig.3.9.a), When  $\phi = 6$  ( Fig.3.9.b ) the rate of copolymerisation is higher in comparison with that obtained when  $\phi = 24$ .

### 3.2.6 Viscosity Studies :

From viscosity measurements in DMF and DMSO, the intrinsic viscosities of the homopolymers and copolymers are calculated. Fig.3.10-3.12 show the plots of intrinsic viscosities of copolymers in DMF at 30°. Huggins [ 12 ] and Kraemer equations [ 13 ] (discussed in section 2.4.4) have been used to calculate the intrinsic viscosities of the polymers. The correlation coefficients for the plots of  $\eta_{sp}/C$  Vs. C and  $\ln \eta_r/C$  Vs.C were found to be  $0.9994 \pm 0.0004$  for all the systems and for all the temperatures studied. Fig. 3.13 shows the temperature dependence of the intrinsic viscosities in DMF and DMSO for some repre-

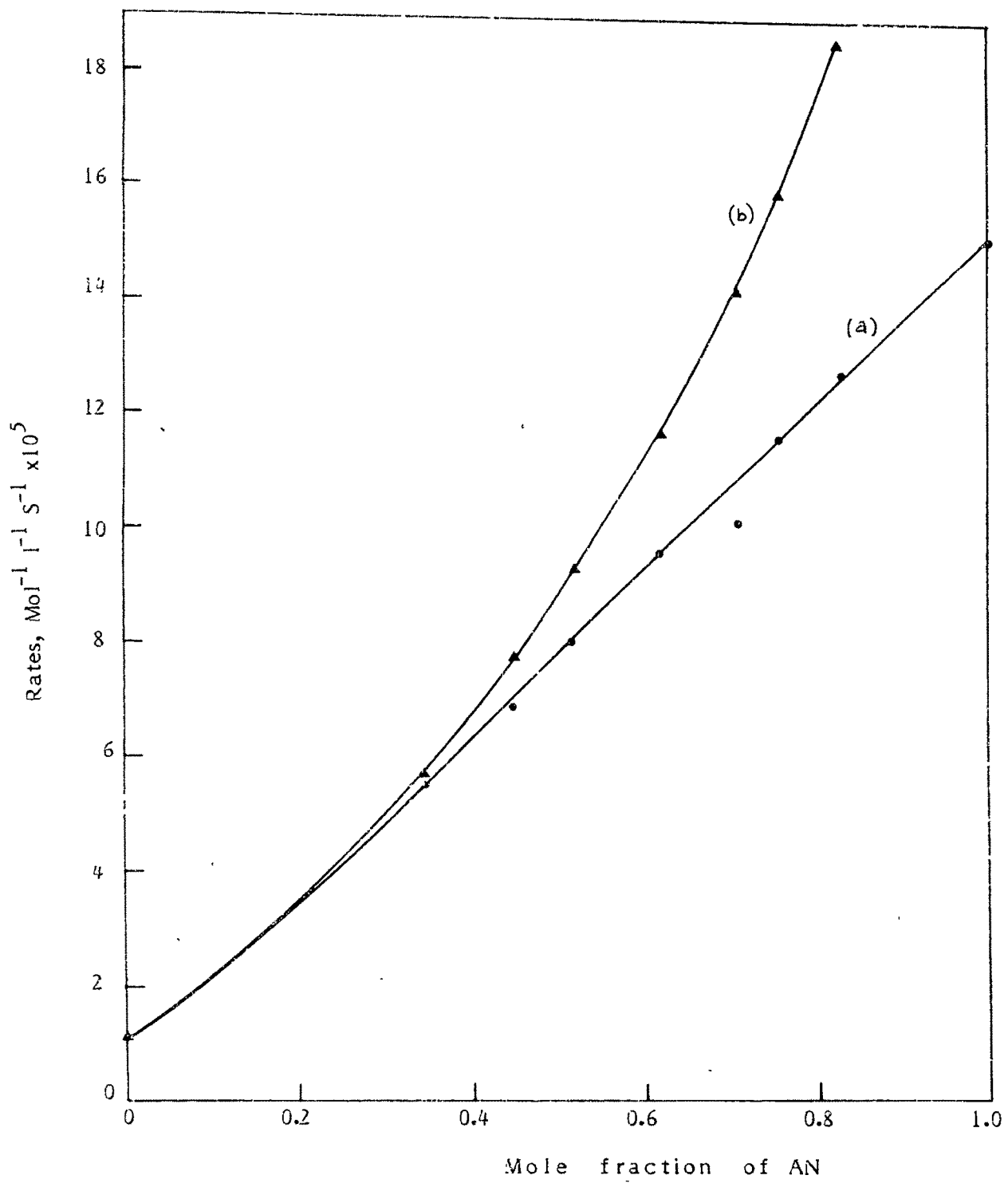


Fig.3.9 Rate of copolymerisation.  
▲ for  $\phi = 6$ , ● for  $\phi = 24$

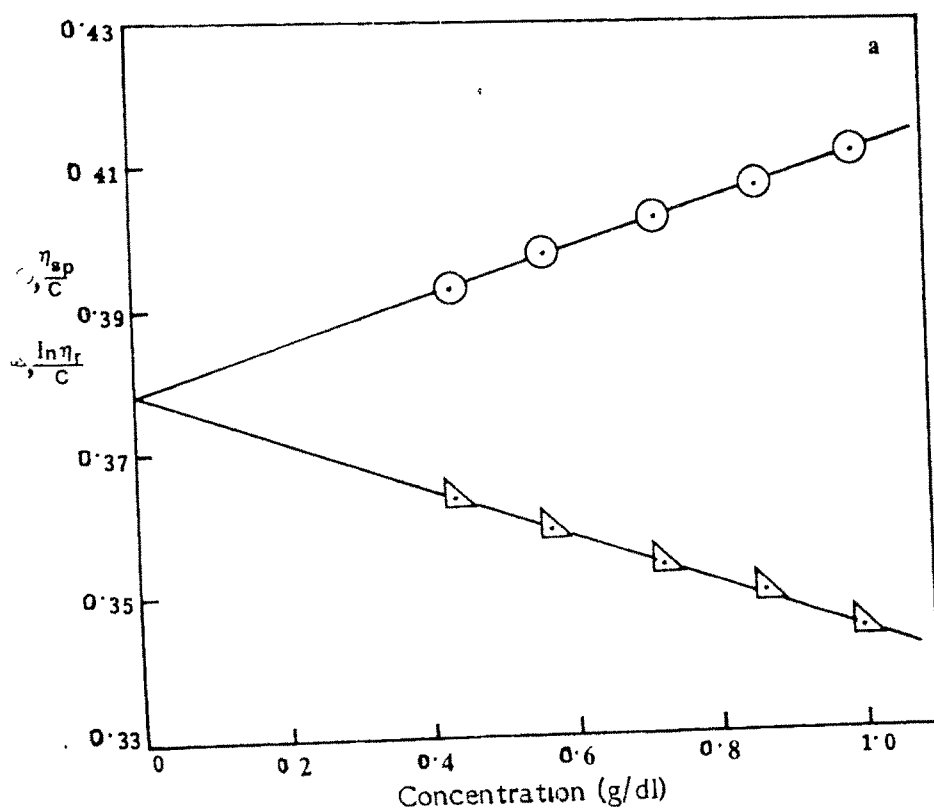
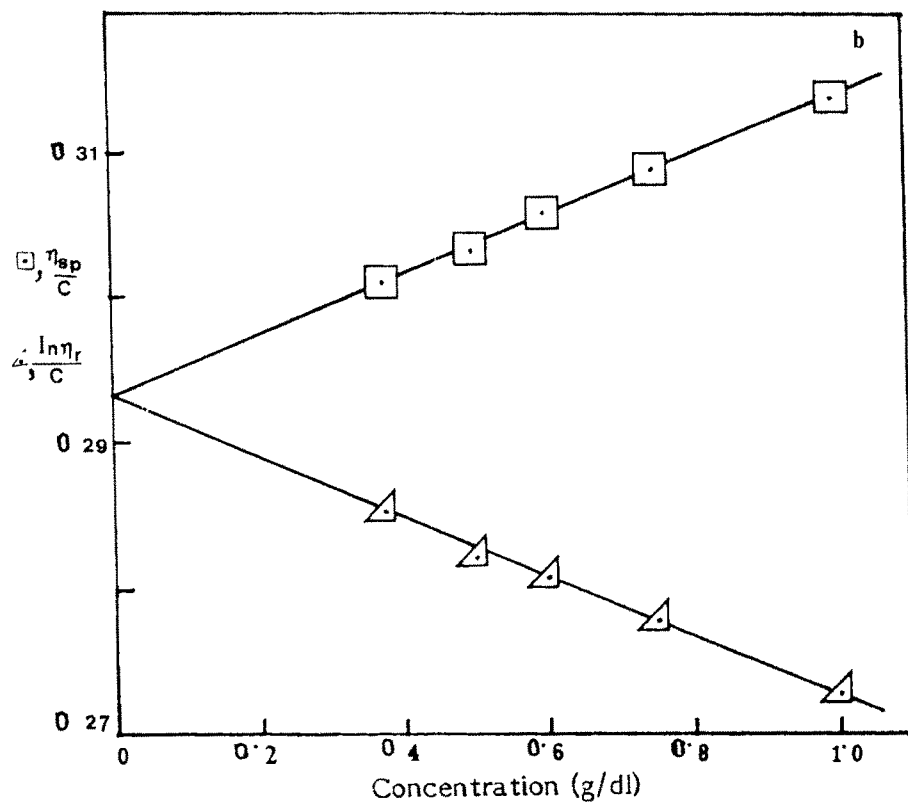


Fig.3.10 Intrinsic viscosity in DMF at 30°  
 (a) 3:1 (MMA:AN), A<sub>1</sub>, (b) 2:1 (MMA:AN), A<sub>2</sub>

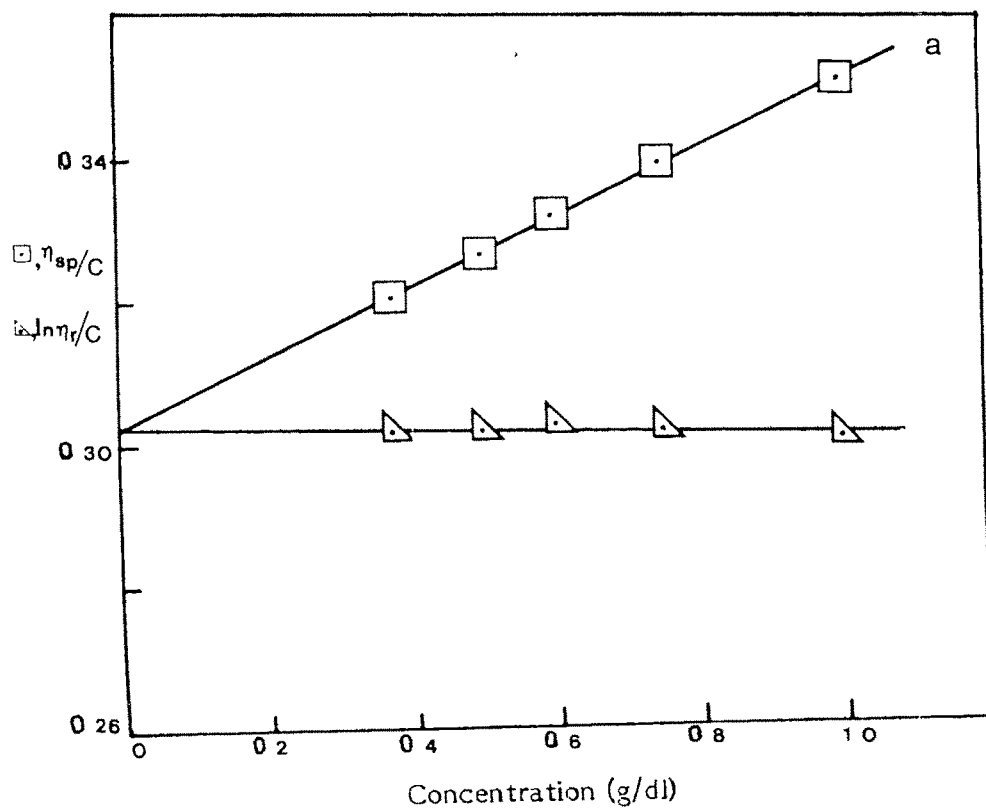
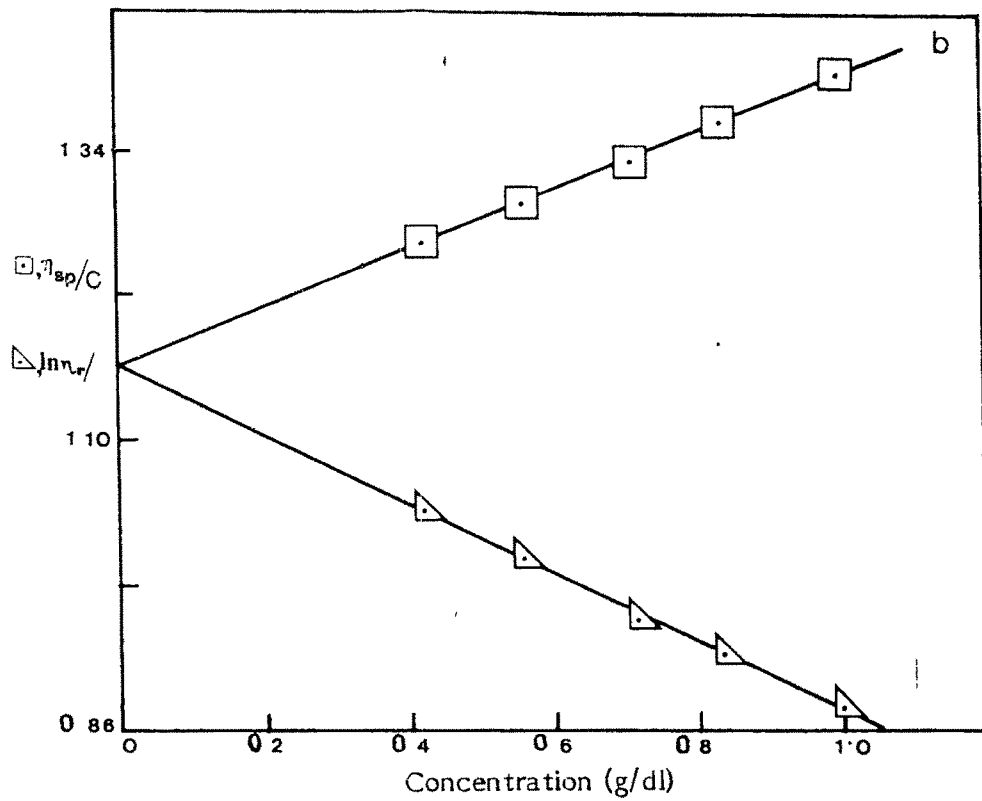


Fig. 3.11 Intrinsic viscosity in DMF at 30°  
 (a) 3:2 (MMA:AN),  $A_3$  (b) 1:3 (MMA:AN),  $A_7$

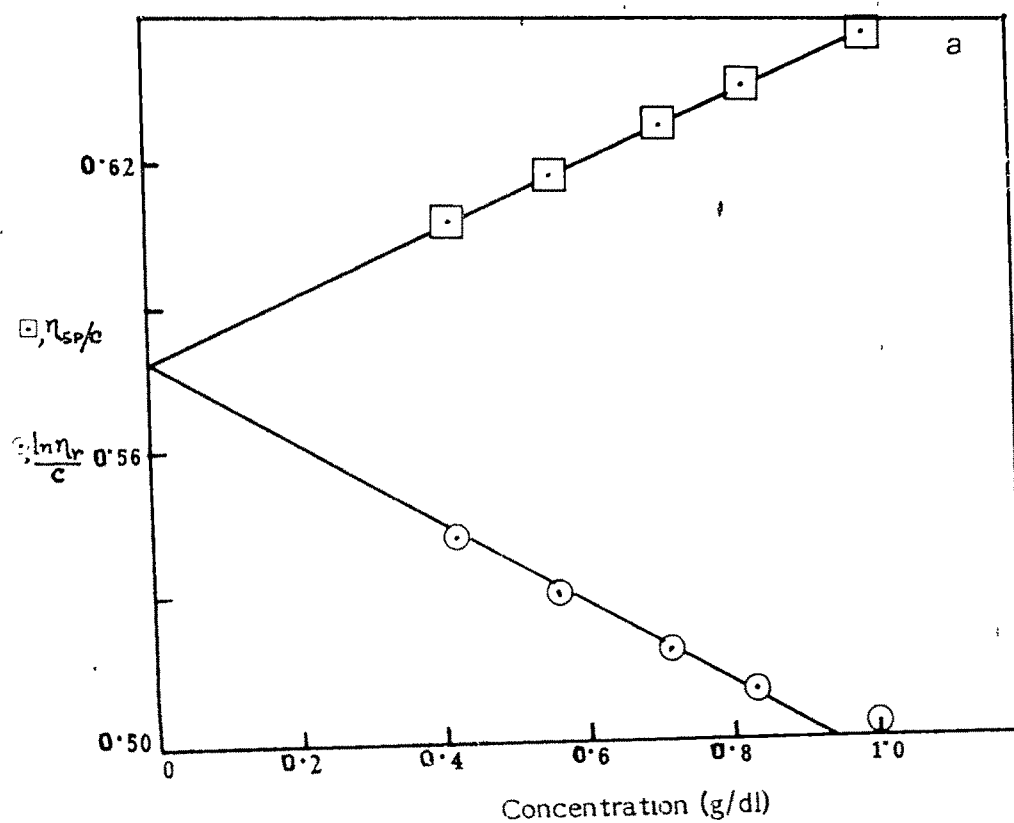
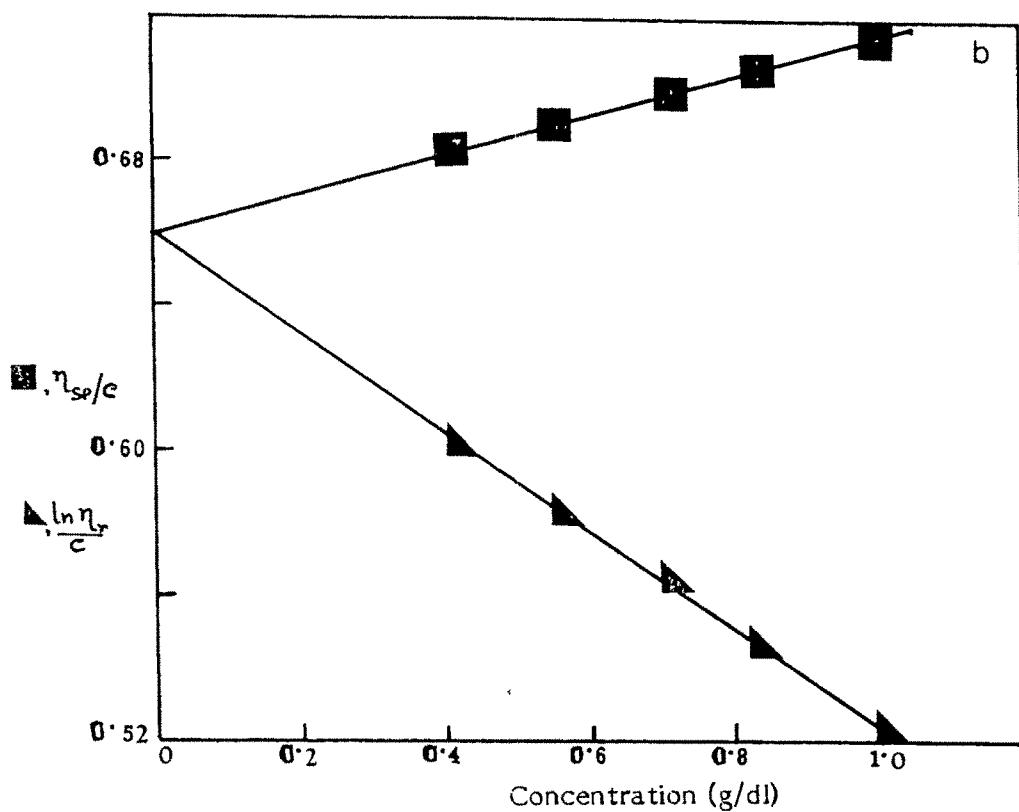


Fig.3.12 Intrinsic viscosity in DMF at 30°, (a) 2:3 (MMA:AN),  $A_5$ , (b) 1:2 (MMA:AN),  $A_6$ .

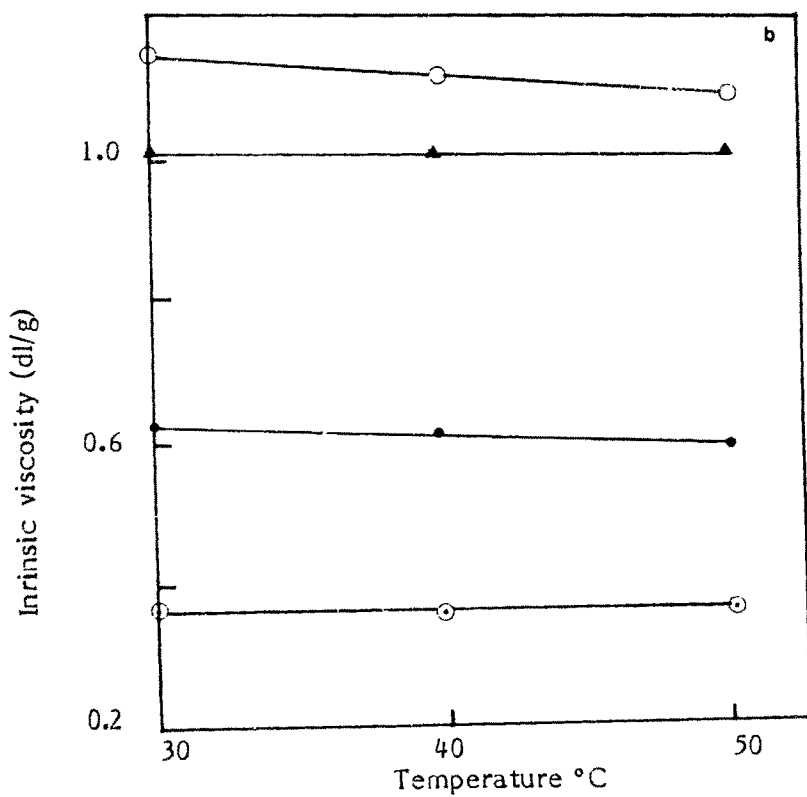
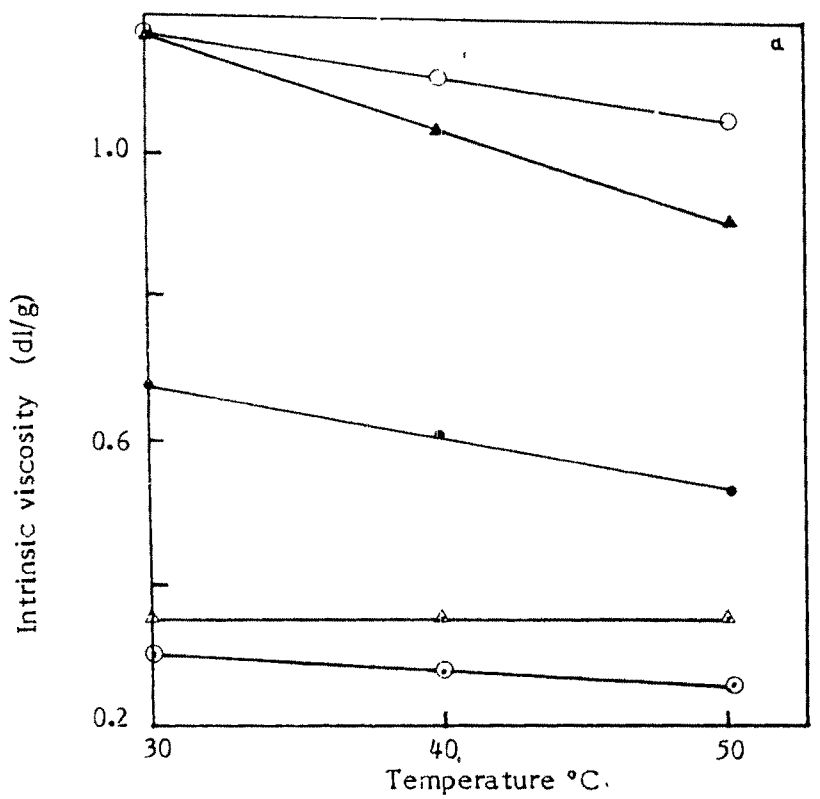


Fig.3.13 Effect of temperature on intrinsic viscosity of copolymers and homopolymers, a. in DMF, b. in DMSO,  $\circ$   $A_2$ ,  $\bullet$   $A_6$ ,  $\blacktriangle$   $A_7$ ,  $\circ$  PAN,  $\triangle$  PMMA.

sentative copolymers and homopolymers of MMA and AN, synthesised under similar reaction conditions. It is observed that the intrinsic viscosity decreases with the increase in temperature giving a good linear relationship with a negative slope. The decrease in the value of intrinsic viscosity is more pronounced in DMF (17 to 33% decrease) than in DMSO (2-4% decrease). The negative slopes indicate that swelling of the polymer coils in solution is not considerable due to decreased thermodynamic affinity with increased temperature and hence the system exhibits lower critical solution temperature (LCST) [14] which is particularly true for the DMF system. We have also observed decreasing swelling extent for the copolymers in less polar solvents ( section 3.2.14 ). DMF being less polar in comparison with DMSO, lower swelling is expected. Decreased intrinsic viscosity values at higher temperatures particularly in DMF medium also indicates poor solubility and poor polymer solvent interaction at higher temperature. From comparison of intrinsic viscosities of copolymers in DMF and DMSO (Table 3.6 ) it was observed that, at 30°, the intrinsic viscosities of copolymers and of PAN show overall lower values in DMSO than in DMF. This suggests that DMSO behaves as the poorer solvent at lower temperature for PAN as well as for the copolymers. At higher temperatures intrinsic viscosity values of PAN and copolymers rich in PAN are higher in DMSO indicating that at higher temperature DMSO acts as a better solvent for PAN as well as for the copolymers rich in PAN than does DMF. Due to less polar DMF, interaction of nitrile group of PAN with DMF is lesser as well as cyclisation of PAN segments into pseudo-naphthylidene results into lower intrinsic viscosities. PMMA is insoluble in DMSO, but its copolymers with AN, developed in this study are soluble in DMSO. Insolubility of PMMA in DMSO may be due to comparatively polar nature of DMSO for less polar PMMA. Improvement in the solubility of copolymers is probably due to micellar solubilisation. Several reports are available [15-17] which deal with the solubility of block copolymers in a solvent which acts as a bad solvent for one of the components. Hence

Table - 3.6

Intrinsic viscosities of homo and copolymers of AN and MMA

Reaction time : 6 hours, Reaction temperature : 75°

initiator concentration :  $5 \times 10^{-3}$  M, Total volume = 100 cm<sup>3</sup>, medium : toluene

Sample No.	Mole fraction of AN		Intrinsic viscosity in DMF (dl/g)			Intrinsic viscosity in DMSO (dl/g)			Mol.Wt. $\bar{M}_n \times 10^{-3}$
	taken in reaction mixture	found in copolymer	30°	40°	50°	30°	40°	50°	
A <sub>1</sub>	0.35	0.32	0.38	0.35	0.33	0.32	0.31	0.30	8.40
A <sub>2</sub>	0.45	0.36	0.30	0.28	0.26	0.26	0.25	0.26	6.94
A <sub>3</sub>	0.52	0.40	0.31	0.31	0.30	0.30	0.29	0.29	7.63
A <sub>4</sub>	0.62	0.45	0.30	0.26	0.26	0.30	0.29	0.29	6.91
A <sub>5</sub>	0.71	0.59	0.58	0.55	0.50	0.58	0.58	0.55	17.64
A <sub>6</sub>	0.76	0.62	0.66	0.63	0.53	0.61	0.61	0.59	30.51
A <sub>7</sub>	0.83	0.72	1.16	1.00	0.91	1.00	1.10	1.00	38.86
PAN	-	-	1.16	1.10	1.05	1.14	1.11	1.09	71.72 <sup>a</sup>
PMMA	-	-	0.35	0.36	0.36	insoluble			40.30 <sup>b</sup>

\* Calculated using intrinsic viscosity and K and  $\alpha$  values :

for copolymers at 25° in DMF

a. at 30° in DMF

b. at 30° in acetone

it is stated that the copolymer molecules can associate to form micellar aggregates with the insoluble blocks, comprising micellar cores. This explanation may be of some relevance to the present study in which some of the PMMA blocks may be forming a central core of micelles with the PAN segments on the outer surface interacting with DMSO. Overall lower values of hydrodynamic volume in DMSO than in DMF for majority of the copolymers rich in MMA also support the above explanation [Table 3.8].

To study the temperature dependence of viscosity of copolymers Frenkel-Eyring equation for viscous flow can be used in the form:

$$\eta = (Nh/V) \cdot e^{\Delta G^\ddagger/RT}$$

Where V is the molar volume and other symbols have the normal meaning.  $\Delta G^\ddagger$  is the overall activation free energy of polymer solution flow which is a function of polymer-solvent interaction.

Hence,

$$\ln(\eta V/Nh) = \Delta G^\ddagger/RT = \Delta H^\ddagger/RT - \Delta S^\ddagger/R$$

Where  $\Delta H^\ddagger$  and  $\Delta S^\ddagger$  are the overall activation enthalpy and entropy changes due to polymer solution flow and hence polymer solvent interaction. Therefore plotting  $\ln(\eta V/Nh)$  against  $1/T$ , overall  $\Delta H^\ddagger$  and  $\Delta S^\ddagger$  values for the copolymer systems in DMF and DMSO were calculated (Figs 3.14-3.19), V (molar volume of copolymer solution) was taken as the molar volume of the solvent at that temperature, due to little difference in the density of the copolymer solutions and that of solvent [18]. The plots obtained were linear. The values of  $\Delta G^\ddagger$ ,  $\Delta H^\ddagger$  and  $\Delta S^\ddagger$  were calculated from the slopes and intercepts of the linear plots and are given in Table 3.7. It was observed from the copolymers

Table - 3.7

Activation parameters for copolymeric systems

concentration of solutions, 0.5 g/dl

Sample No.	$\Delta H^\ddagger$ KJ mol <sup>-1</sup>	$\Delta S^\ddagger$ J mol <sup>-1</sup> deg <sup>-1</sup>	$\Delta G^\ddagger$ KJ mol <sup>-1</sup>		
			30°C	40°C	50°C
In DMF					
A 1	9.97	10.65	13.20	13.30	13.41
A 2	10.27	9.45	13.13	13.23	13.32
A 3	9.64	11.58	13.15	13.26	13.38
A 4	9.66	11.33	13.09	13.21	13.32
A 5	12.12	4.64	13.53	13.57	13.62
A 6	11.75	6.04	13.58	13.64	13.70
A 7	14.32	-0.60	14.14	14.13	14.13
PAN	10.87	10.30	13.99	14.09	14.20
PMMA	9.37	12.68	13.21	13.34	13.47
In DMSO					
A 1	15.06	-1.17	14.71	14.70	14.68
A 2	15.17	-1.71	14.65	14.63	14.62
A 3	14.87	+0.17	14.92	14.92	14.92
A 4	15.21	-1.75	14.68	14.66	14.64
A 5	15.61	-1.96	15.02	15.00	14.98
A 6	15.28	-0.76	15.05	15.04	15.03
A 7	15.11	+1.31	15.51	15.52	15.53
PAN	16.24	-1.31	15.85	15.83	15.82
PMMA	insoluble				

Table-3.8

Hydrodynamic volume (voluminosity  $V_e$ ) and Simha shape factor ( $\psi$ ) of copolymers in solutions

Sample No.	30°C		40°C		50°C	
	$V_e$ ml/g	$\psi$	$V_e$ ml/g	$\psi$	$V_e$ ml/g	$\psi$
In DMF						
A 1	15.20	2.50	14.00	2.50	13.07	2.51
A 2	11.95	2.51	11.37	2.50	13.39	2.51
A 3	12.19	2.50	12.52	2.50	12.00	2.50
A 4	11.86	2.50	10.27	2.50	10.42	2.50
A 5	23.20	2.50	22.03	2.51	20.00	2.50
A 6	26.13	2.52	25.24	2.50	22.12	2.50
A 7	46.22	2.51	40.00	2.50	36.50	2.50
In DMSO						
A 1	12.71	2.51	11.84	2.50	12.73	2.50
A 2	10.46	2.50	10.06	2.50	10.41	2.50
A 3	12.08	2.50	13.25	2.49	12.79	2.53
A 4	12.04	2.50	11.59	2.51	11.36	2.51
A 5	23.10	2.50	22.92	2.52	21.88	2.50
A 6	24.26	2.50	24.26	2.50	23.64	2.50
A 7	40.80	2.51	42.70	2.50	39.74	2.51

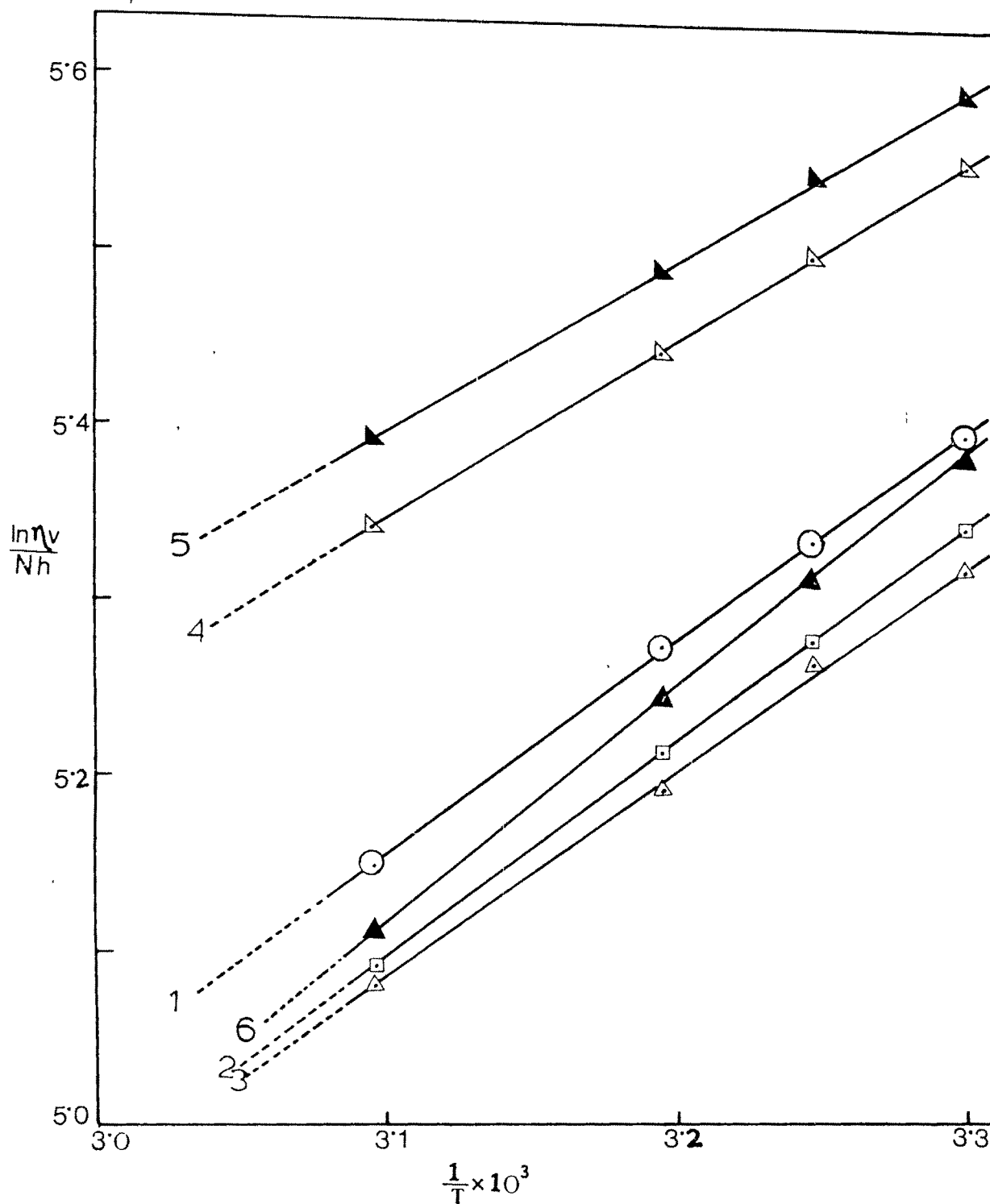


Fig.3.14  $\ln \frac{\eta_V}{Nh}$  versus  $1/T$  for 1.0 g/dl solution in DMF  
 1. A<sub>1</sub>, 2. A<sub>2</sub>, 3. A<sub>4</sub>, 4. A<sub>5</sub>, 5. A<sub>6</sub>, 6. A<sub>3</sub>

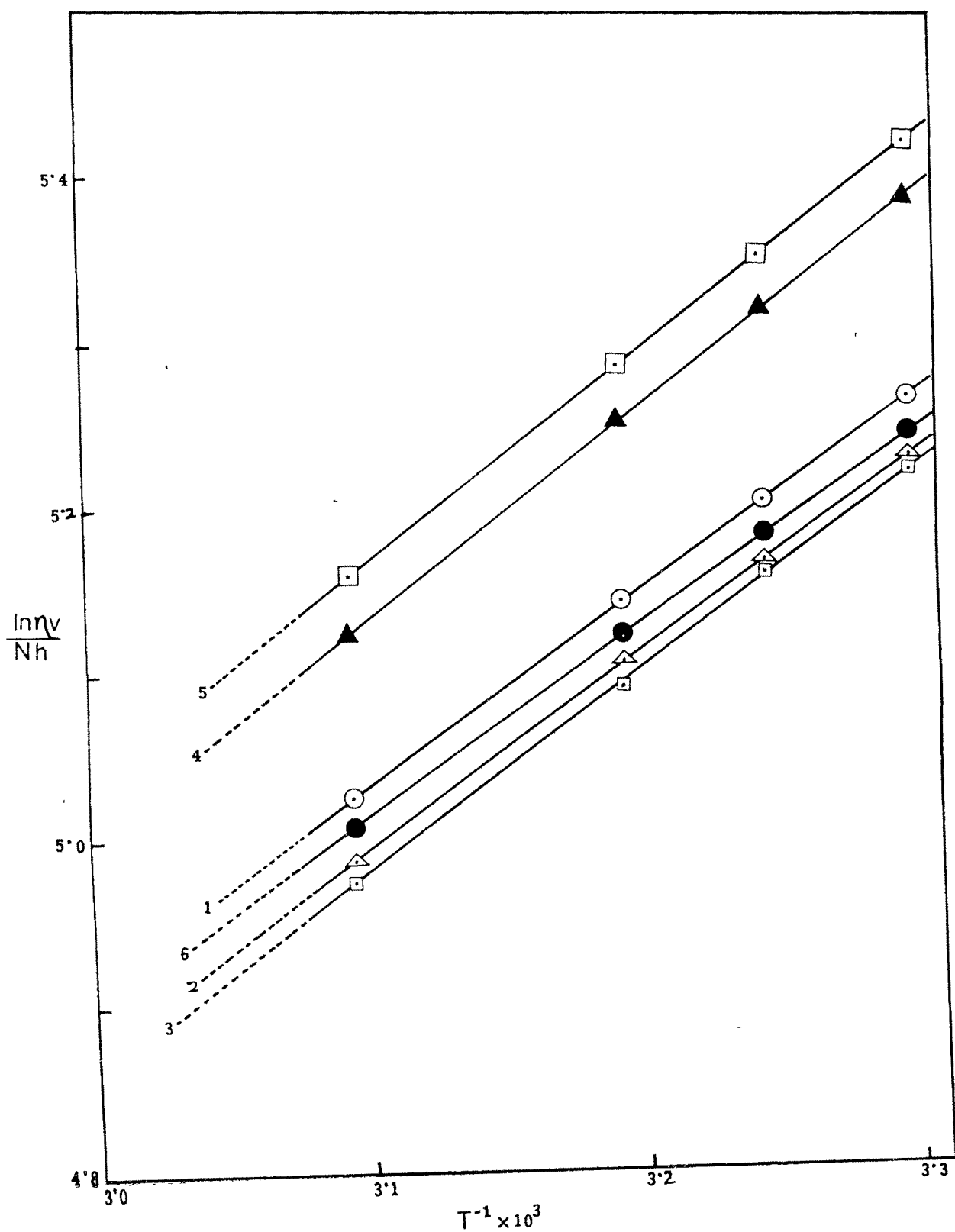


Fig. 3.15  $\ln \eta_V/N_h$  versus  $1/T$  for 0.6 g/dl solution in DMF  
 1.  $A_1$ , 2.  $A_2$ , 3.  $A_4$ , 4.  $A_5$ , 5.  $A_6$ , 6.  $A_3$

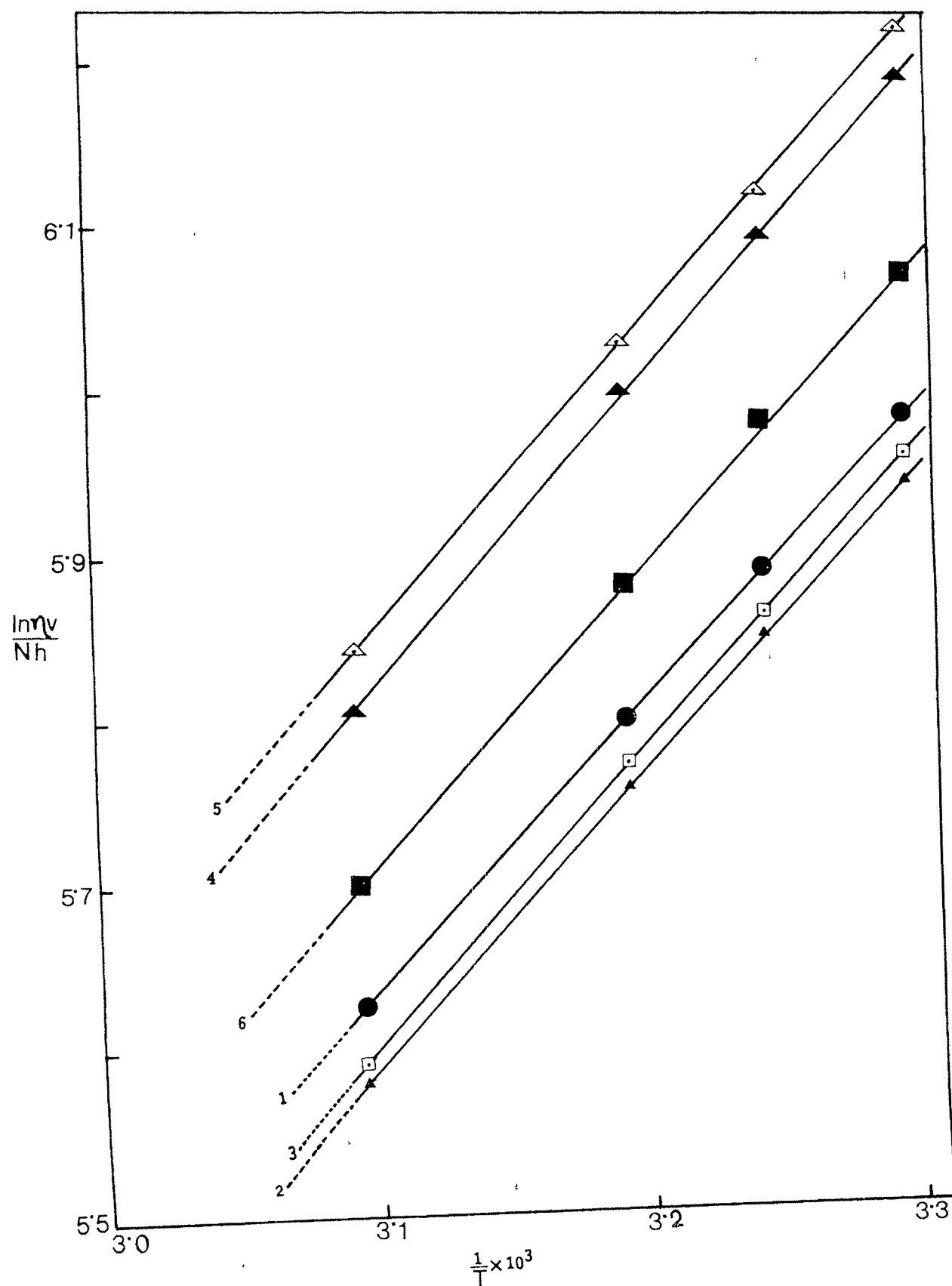


Fig.3.16  $\ln \frac{V}{Nh}$  versus  $1/T$  for 1.0 g/dl solution in DMSO  
 1.  $A_1$ , 2.  $A_2$ , 3.  $A_4$ , 4.  $A_5$ , 5.  $A_6$ , 6.  $A_3$

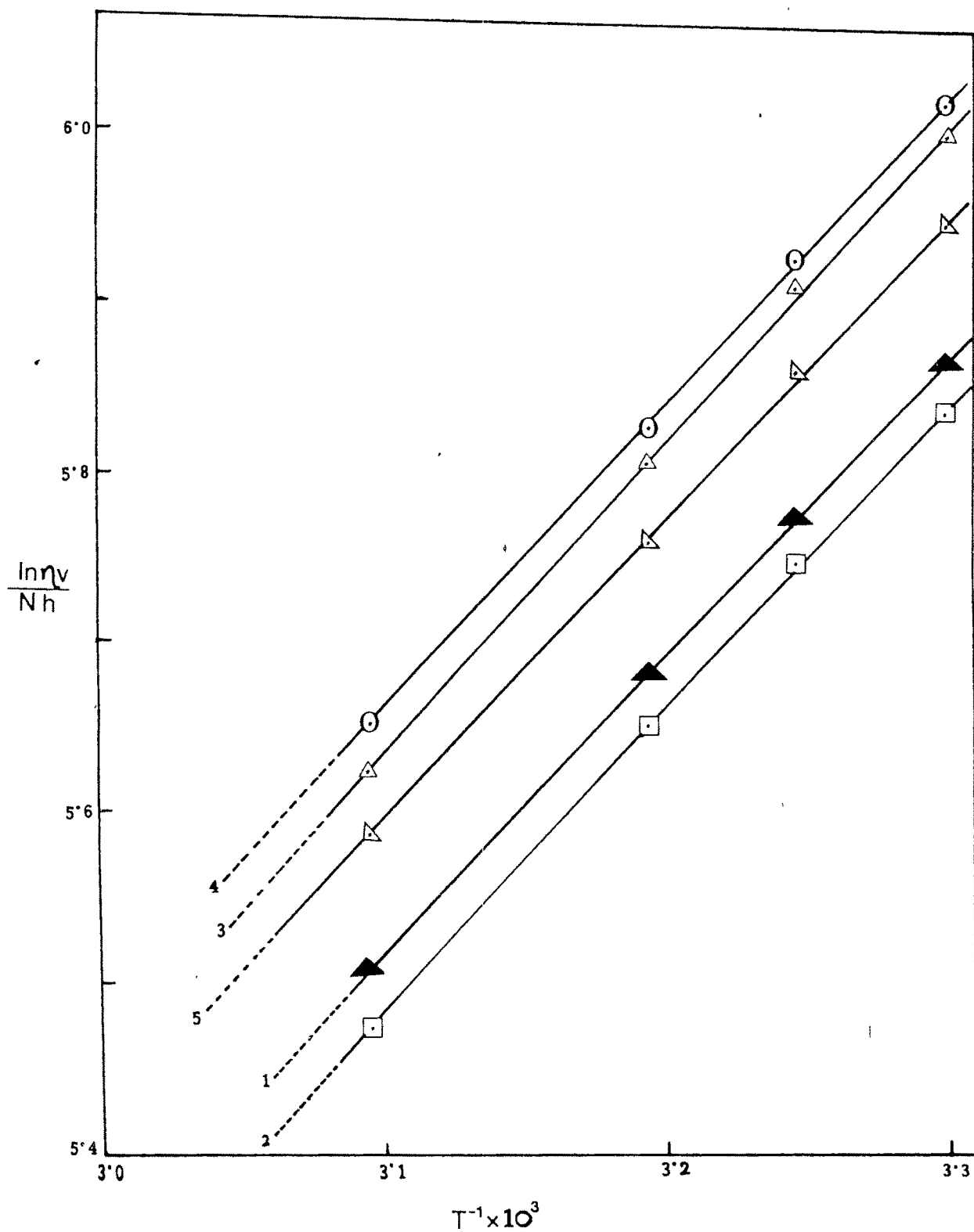


Fig.3.17  $\ln \eta_v / N h$  versus  $1/T$  for 0.6 g/dl solution in DMSO  
 1.  $A_1$ , 2.  $A_2$ , 3.  $A_5$ , 4.  $A_6$ , 5.  $A_3$ .

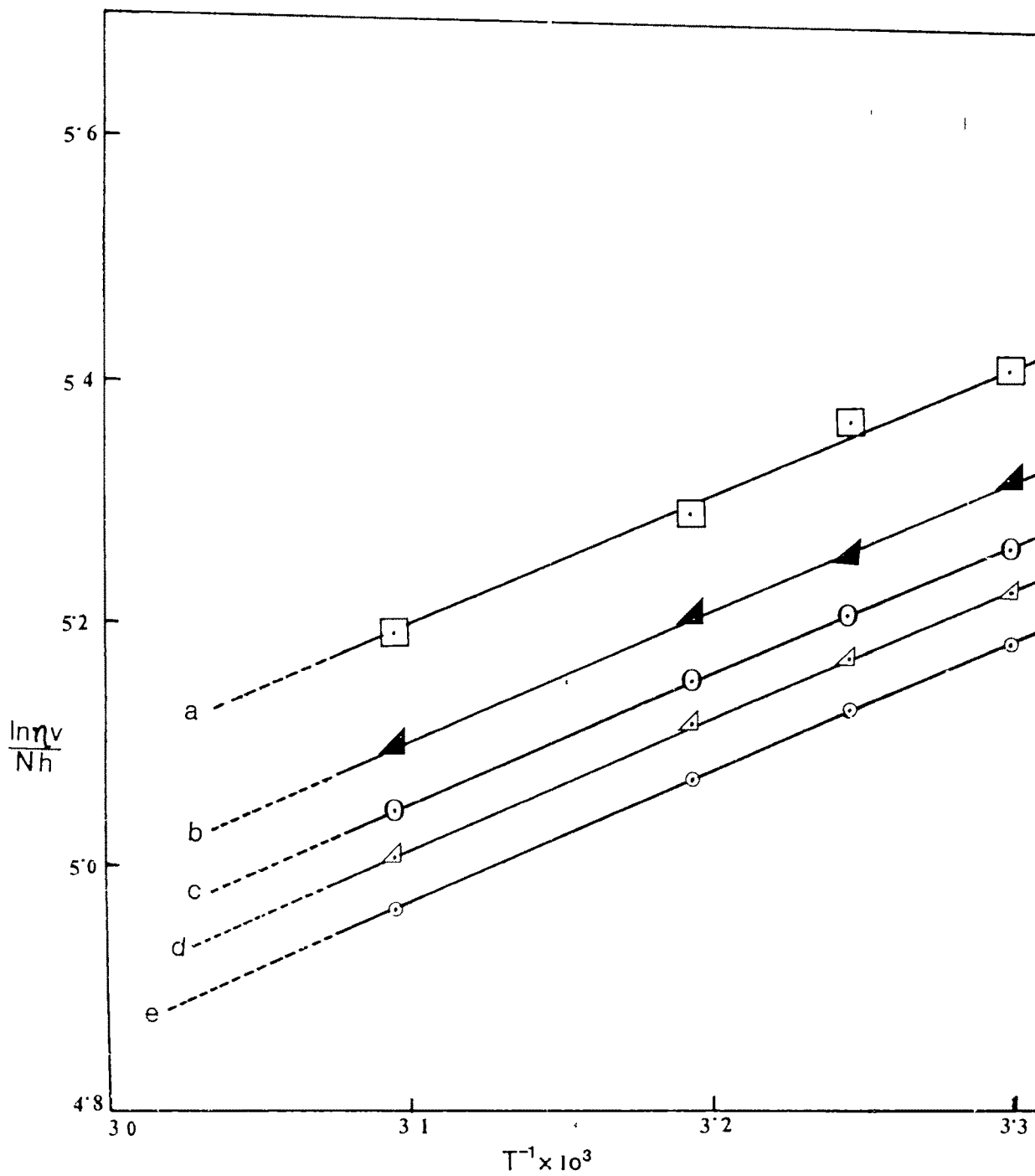


Fig.3.18  $\ln \eta_v/N_h$  versus  $1/T$  for PMMA in DMF  
 Concentration (g/dl): a. 1.0 b. 0.75, c. 0.60, d. 0.50 e. 0.375.

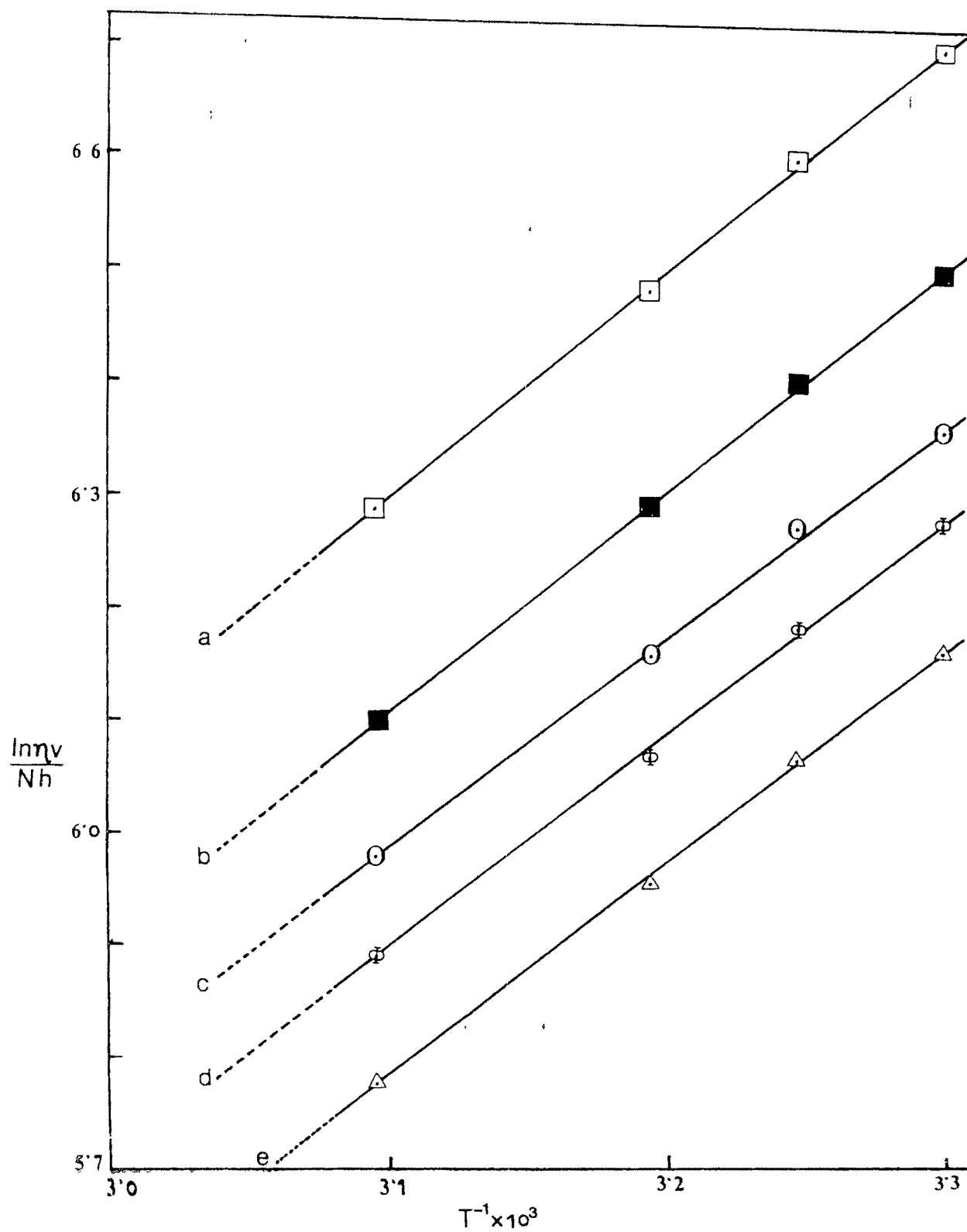


Fig.3.19  $\ln \eta/\eta_0$  versus  $1/T$  for PAN in DMSO  
 concentration (g/dl): a. 1.0, b. 0.75, c. 0.60, d. 0.50, e. 0.375

containing different composition of MMA and AN segments that  $\Delta H^\ddagger$  does not show noticeable change in a given solvent particularly for the copolymers rich in MMA. But the values of  $\Delta H^\ddagger$  for these copolymers are different in DMF and DMSO indicating that for the systems studied here, thermodynamic properties of the copolymer solutions are influenced by polymer solvent interactions. On the other hand, from the intrinsic viscosity data [Table 3.6] it was observed that the composition of the copolymers has more pronounced effect on viscosities than the nature of the solvent. The entropies of the copolymers though negative are small. Hence the copolymer systems are assumed to be poorly ordered. Increased disorder was observed in DMSO giving rise to smaller positive entropy values. A higher degree of order is observed with increasing mole-fraction of AN in the copolymer though the values do not vary from each other to a large extent. The calculated  $\Delta G^\ddagger$  values show little dependence on the temperature but about 8 % variation with respect to change in composition. The relative viscosity data were used to calculate the equivalent hydrodynamic volume (voluminosity  $V_e$ ), a measure of size of a solvated polymer molecule at infinite dilution. Recently, Narang et al. [19] have ~~reported~~ determined the shape of protein molecules (natural polymers) in solution. In the present study the same procedure has been followed for the determination of  $V_e$ , the hydrodynamic volume of the solvated polymer molecules by plotting  $Y = (\eta_r^{0.5} - 1) / C (1.35 \eta_r^{0.5} - 0.1)$  against  $C \text{ g.cm}^{-3}$ . Extrapolation to  $C=0$  gives  $V_e$ . Since  $[\eta] = \nu V_e$  [20], from  $V_e$ , the Simha shape factor  $\nu$  was calculated. A few representative systems are illustrated in Fig. 3.20. It was observed that value of  $\nu$  for all systems at all temperatures remains constant at 2.5 [Table 3.8] indicating that, in the concentration range under study, the copolymer molecules are spherical in the solution. Einstein computed a value of  $\nu$  as 2.5 for sphere [21], whereas for oblate or prolate shapes the values in solution differ widely from 2.5 [22,23].

The intrinsic viscosities of the homopolymers and copolymers in theta ( $\theta$ )

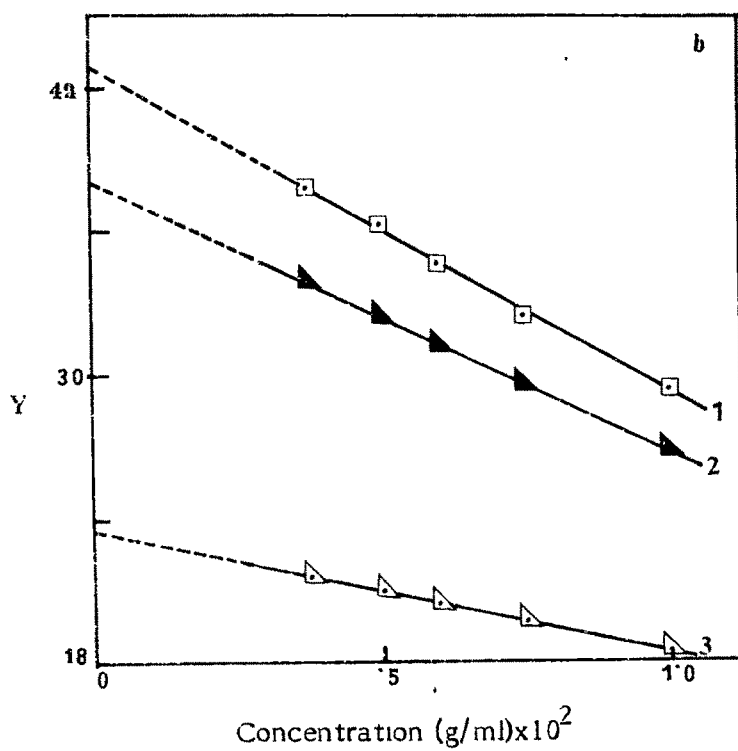
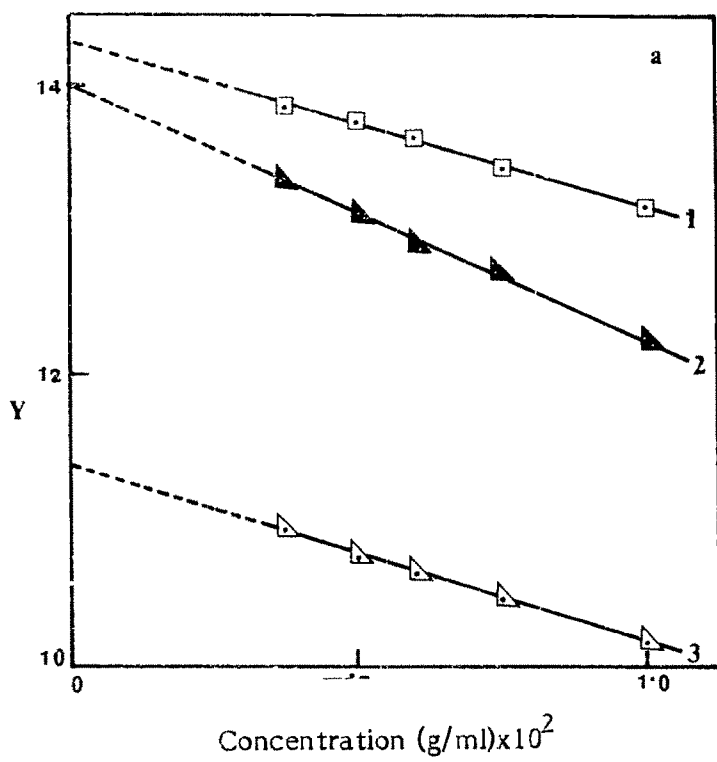


Fig.3.20 Y versus concentration curve for copolymers and homopolymers.  
 a. in DMF b. in DMSO.  
 a. 1.  $A_2$  at  $40^\circ$ , 2.  $A_1$  at  $40^\circ$ , 3. PMMA at  $30^\circ$   
 b. 1.  $A_6$  at  $30^\circ$ , 2.  $A_7$  at  $50^\circ$ , 3. PAN at  $30^\circ$ .

solvents, a solvent nonsolvent mixture of DMF and methanol at 30° were measured. The results are given in Table 3.9. The intra-molecular expansion factor  $\alpha$ , which is a measure of the flexibility of the polymer molecules was calculated from the relation,

$$\alpha^3 = [\eta] / [\eta]_0$$

The spatial distribution in the actual molecule is assumed to be expanded uniformly by the factor  $\alpha$  as the result of intramolecular interactions. From Table 3.9 it is observed that the intramolecular expansion factor for homopolymers, PAN and PMMA is higher than that for the copolymers of MMA and AN indicating that the homopolymers are more flexible than the copolymers. The variation in the composition of the copolymers does not affect  $\alpha$  considerably.

Viscosity molecular weights of the homopolymers and copolymers were calculated using K and  $\alpha$  values from literature. Inagaki et al. [ 23.a ] have reported K &  $\alpha$  values as  $29.6 \times 10^{-5}$  and 0.74 respectively for PAN in DMF at 30°. Cohn et al. [ 23.b ] have reported K and  $\alpha$  values as  $7.7 \times 10^{-5}$  and 0.7 respectively for PMMA in acetone at 30°. The molecular weights calculated from viscosity measurements in DMF and acetone were found to be 71700 and 40300 respectively for PAN and PMMA.

Cleland and Stockmayer [ 23.c ] have reported K and  $\alpha$  values for acrylonitrile - methyl methacrylate copolymers as  $3.92 \times 10^{-4}$  and 0.75 respectively. Hence using these values  $\bar{M}_n$  were calculated for the copolymers with different compositions. The results are given in Table 3.6. Due to higher molecular weight of PAN than PMMA copolymers with increasing AN content show higher molecular weights.

### 3.2.7 Differential Scanning Calorimetry (DSC)

The DSC analysis of all samples was carried out as described in section 2.4.3a.

Table-3.9

Intrinsic viscosities of polymers in theta ( $\theta$ ) solvent .

Temperature : 30°

Sample	Composition of $\theta$ -solvent		$[\eta]_{\theta}$ (dl/g)	$[\eta]$ in DMF at 30°C (dl/g)	Intramolecular expansion factor ( $\alpha$ )
	DMF (%)	Methanol (%)			
A <sub>1</sub>	34.0	66.0	0.16	0.38	1.334
A <sub>2</sub>	33.2	66.8	0.13	0.30	1.321
A <sub>3</sub>	40.0	60.0	0.13	0.31	1.336
A <sub>4</sub>	38.0	62.0	0.17	0.30	1.208
A <sub>5</sub>	61.2	38.8	0.21	0.58	1.403
A <sub>6</sub>	60.0	40.0	0.23	0.66	1.421
A <sub>7</sub>	58.4	41.6	0.39	1.16	1.438
PMMA	30.0	70.0	0.08	0.35	1.636
PAN	77.2	22.8	0.15	1.16	1.977

Representative DSC curves for homopolymers and copolymers are given in Figs. 3.21 - 3.25. From the literature it is observed that glass transition temperatures ( $T_g$ ) are  $100 - 105^\circ$  for both PMMA [24-37] and PAN [38-50]. Our samples show a glass transition temperature of  $99.3^\circ$  for PMMA. The difference in the value may be due to the variation in the synthetic procedure. Table 3.10 gives the values for crystallisation and melting temperatures of the copolymers and homopolymers. It is observed that all the copolymers irrespective of their composition show lower  $T_g$  values than the homopolymers. PAN being highly crystalline material, its crystallisation temperature ( $T_c$ ) is exhibited at  $268^\circ$ . PMMA is reported to be amorphous [28,29,32]. Incorporation of PMMA in PAN decreases the crystallinity index and hence samples  $A_1$  to  $A_5$  do not exhibit any crystallisation temperature. The copolymers rich in PAN show crystallisation temperature in their DSC studies. However, these values are higher than the  $T_c$  for PAN. For confirmation we have also taken DSC curve for the 1:1 molar mixture of PAN and PMMA (both dissolved in DMF and reprecipitated by methanol). This sample exhibits  $T_c$  at  $250^\circ$ . Therefore from our thermal studies we can say that the polymers synthesised are true copolymers and not the mixtures of homopolymers. Due to presence of MMA,  $T_c$  of copolymers are higher than that of PAN and gradually decreases as the PMMA composition in the copolymer goes on decreasing. The copolymers rich in PAN did not show any melting temperature resembling the parent compound polyacrylonitrile. The copolymers with higher composition of MMA show melting temperature of almost  $380^\circ$ .

### 3.2.8 Thermogravimetric analysis (TGA)

Dynamic thermogravimetric analysis was carried out using a nitrogen purge atmosphere as described in section 2.4.3b. The experimental conditions were

Sample: PMMA.  
Size: 13.3640 mg  
Method: DSC/500  
Comment: N2

# DSC

File: ALGY.22  
Operator: ALGY KAZLAUCIUNAS  
Run Date: 3-Jun-91 10:05

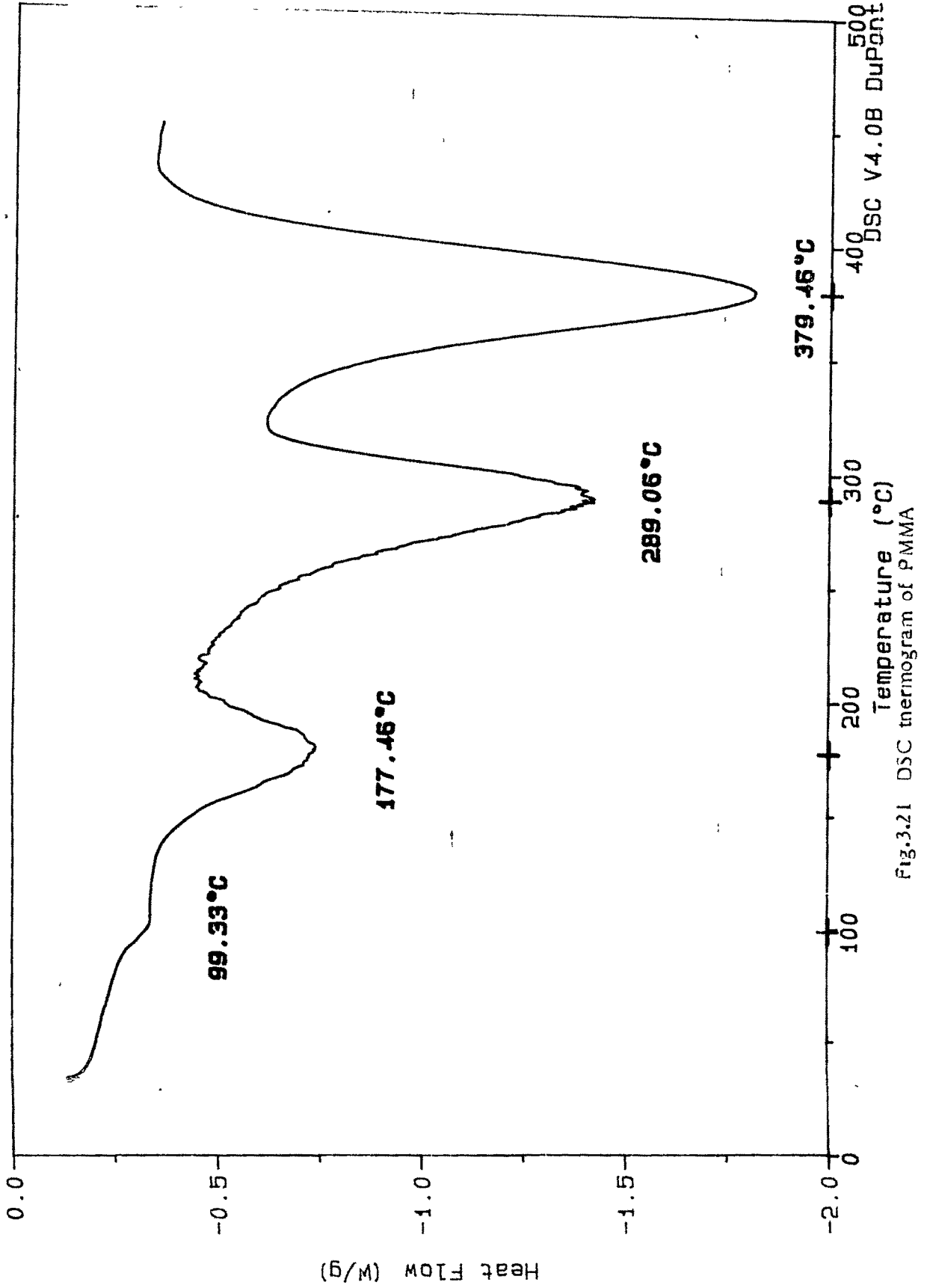


Fig.3.21 DSC thermogram of PMMA

# DSC

File: WOLF.57  
Operator: ALGY KAZLAUCIUNAS  
Run Date: 25-May-90 16:42

Sample: SAMPLE H2.  
Size: 2.6600 mg  
Method: STANDARD DSC RUN  
Comment: N2

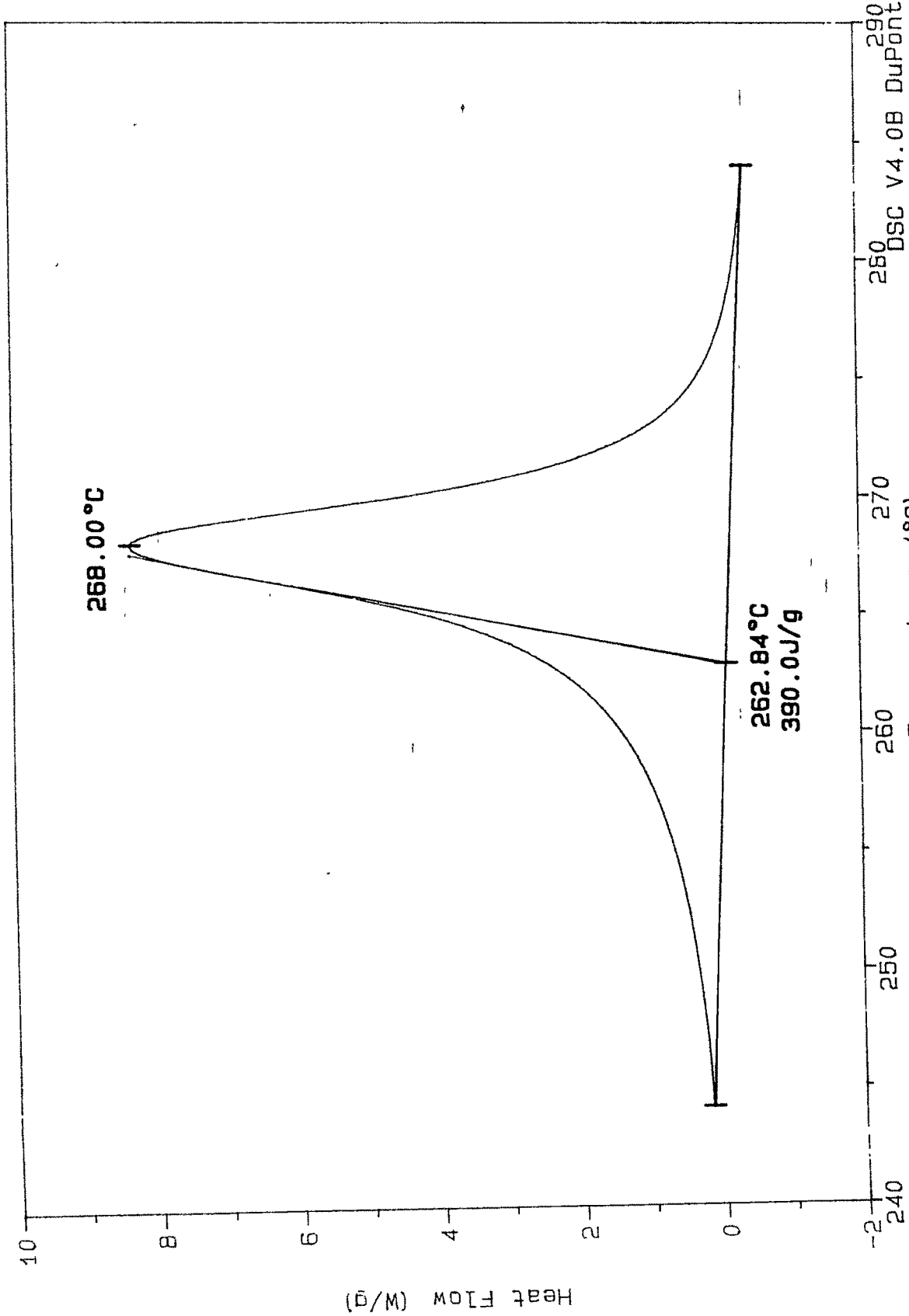


Fig. 3.22 DSC thermogram of PAN

Sample: MIXTURE OF PAN & PMMA.  
Size: 10.5220 mg  
Method: DSC/500  
Comment: N2

DSC

File: ALGY.23  
Operator: ALGY KAZLAUCIUNAS  
Run Date: 3-Jun-91 11:25

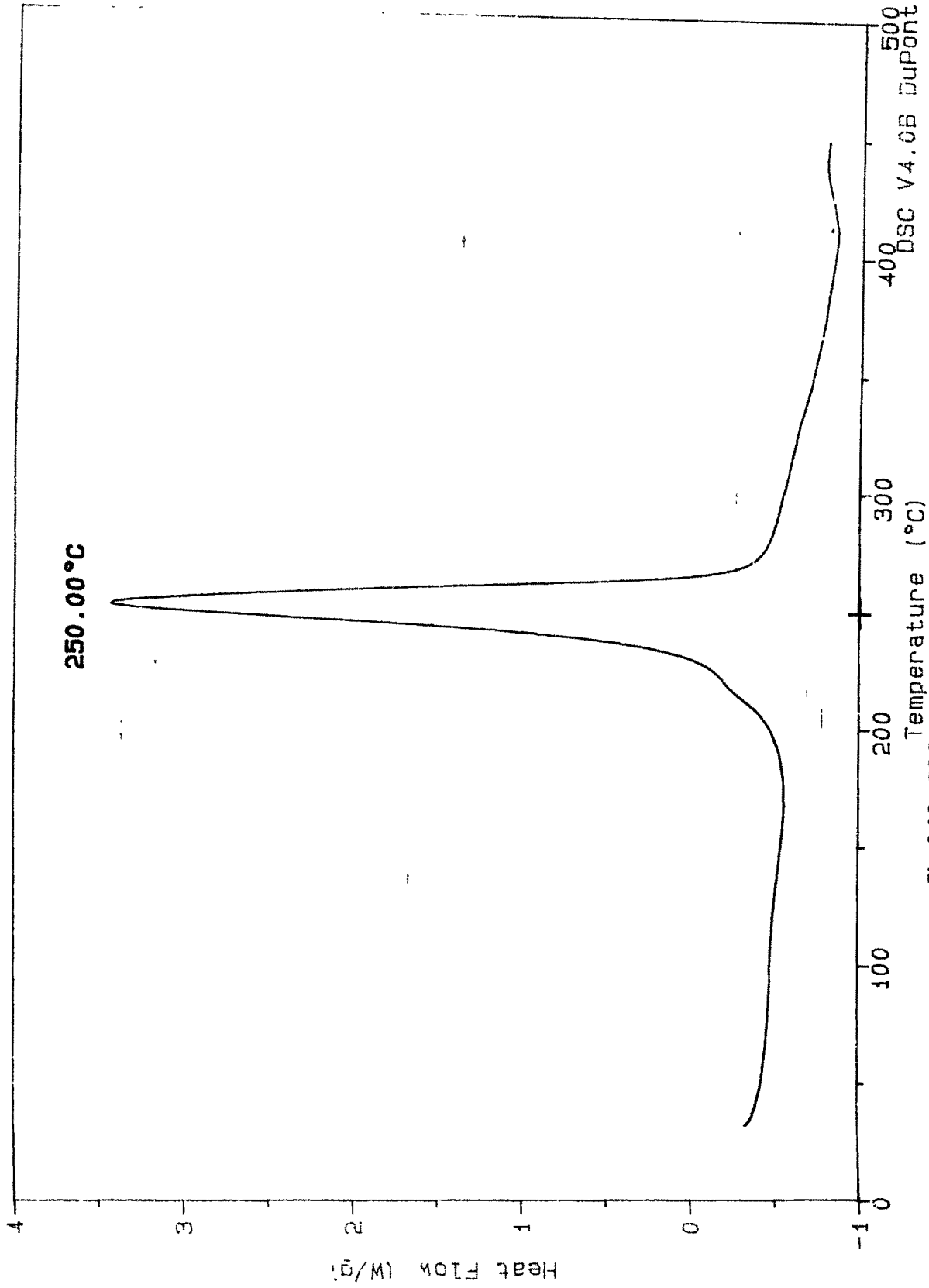


Fig.3.23 DSC thermogram of mixture of PMMA and PAN

Sample: SAMPLE A4  
Size: 9.3300 mg  
Method: STANDARD DSC RUN  
Comment: N2

# DSC

File: WOLF.42  
Operator: ALGY KAZLAUCIUNAS  
Run Date: 23-May-90 11:55

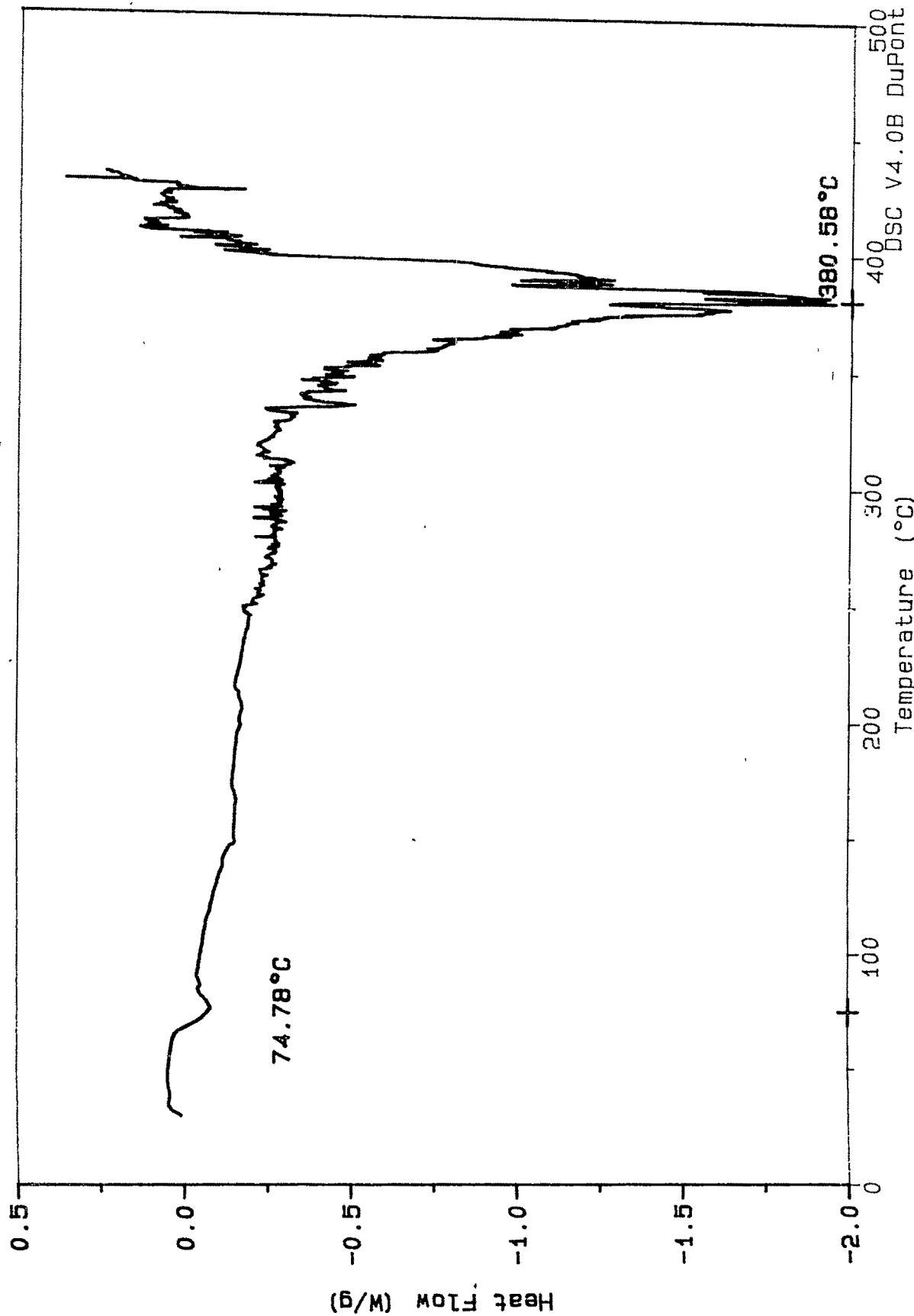


Fig. 3.24 DSC thermogram of sample A<sub>3</sub>

Sample: A6/2: 3.  
Size: 11.7100 mg  
Method: DSC/500  
Comment: N2.

# DSC

File: ALGY.25  
Operator: ALGY KAZLAUCIUNAS  
Run Date: 3-JUN-91 14:24

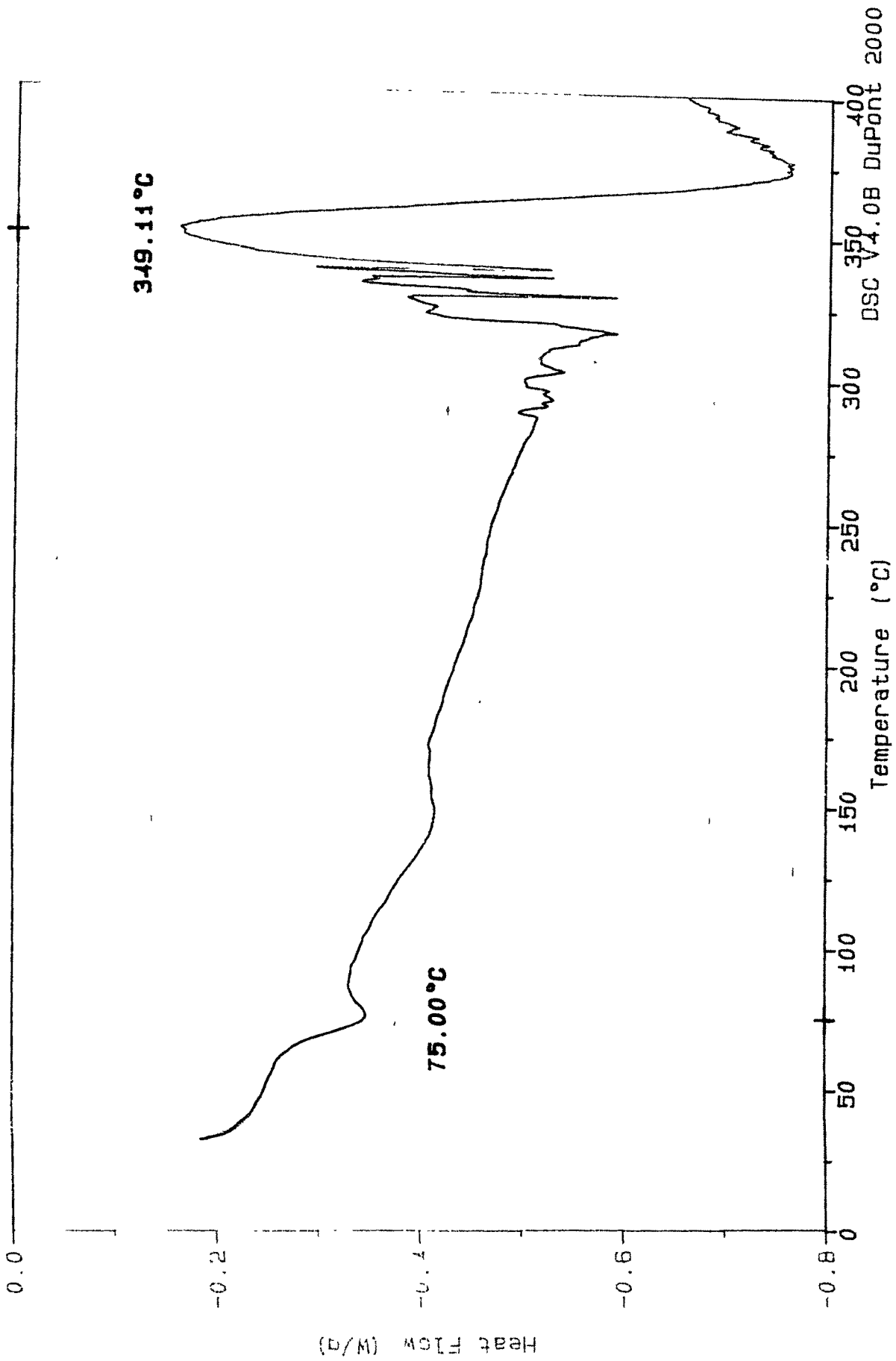


Fig.3.25 DSC thermogram of sample A5

Table-3.10

## Differential Scanning Calorimetry

Sample Code	Glass transition temperature $T_g$ (°C)	Crystallisation temperature ( $T_c$ ) (°C)	Heat of Crystallisation $H_c$ (J/g)	Melting temperature $T_m$ (°C)	Heat of fusion $H_f$ (J/g)
A <sub>1</sub>	71.66	-	-	379.50	-
A <sub>2</sub>	-	-	-	382.50	833.80
A <sub>3</sub>	73.46	-	-	380.10	308.20
A <sub>4</sub>	73.40	-	-	373.90	507.50
A <sub>5</sub>	68.82	375.00	277.10	-	-
A <sub>6</sub>	-	359.15	83.00	-	-
A <sub>7</sub>	-	319.2	364.70	-	-
PMMA	99.33	-	-	378.57	-
PAN	91.00	268.00	390.00	-	-
Mixture of PMMA+PAN		250.77	445.80		

identical for all samples. The thermogravimetric analysis and derivative thermogravimetric analysis thermograms for PMMA, PAN and some copolymers are given in Figs. 3.26 - 3.29. Examinations of the thermograms of the copolymers reveal that all the copolymers are quite stable upto 320°. The initial decomposition temperature (IDT) for PAN and PMMA are 270° and 160° respectively and for copolymers between 150-180°. From the derivative thermogravimetric analysis thermogram of PMMA (Fig. 3.26) it is observed that PMMA decomposes in three major stages at 168 - 194° at 301.5° and at 382.2°. The first stage is due to scission of head to head linkages. The second step by scission at the chain end initiation from vinylidene ends and the third step by random scission with the polymer chains. Kashiwagi et al. [51] and Bhuyan et al. [52] also observed three stage thermal degradation in the TGA of PMMA synthesised by free radical and chain transfer mechanism. However, McNeill et al. [53] observed in the TGA study of bulk polymerised PMMA prepared by using AIBN, that the thermal degradation was a two-stage process. On the other hand Babu et al. [54] observed one stage thermal degradation of PMMA and copolymers of MMA and vinyltriacetoxysilane.

PAN shows decomposition only in one stage at 279°. Bajaj et al. [55] observed that the decomposition of PAN occurred in two stages, one at 300° and the other around 600°. Since we have run TGA upto 500° the second stage decomposition at 600° was not observed. The weight loss in degradation at 279° could be associated with nitrile oligomerisation [56,57] which produces volatile products (such as NH<sub>3</sub>, HCN, CH<sub>3</sub>CN etc) and subsequent chain scission. The copolymers of MMA and AN decompose in two stages, the major portion being decomposed in second stage. The decomposition temperatures (T<sub>D</sub>) corresponding to 5%, 10%, 20%, 30%, 50%, 70%, 80%, and 90% weight losses are given in Table 3.11. T<sub>max</sub> the temperature for maximum rate of decomposition obtained from DTG thermograms and the char residue upto 500° are also given in the Table 3.11. The increased amount of char residue in AN rich copolymers is

Sample: H1  
Size: 8.1860 mg  
Method: TGA 10°C/min.  
Comment: N2 50 ml/min.

# TGA

File: H1.01  
Operator: L JOHNSON  
Run Date: 9-Jul-90 10:03

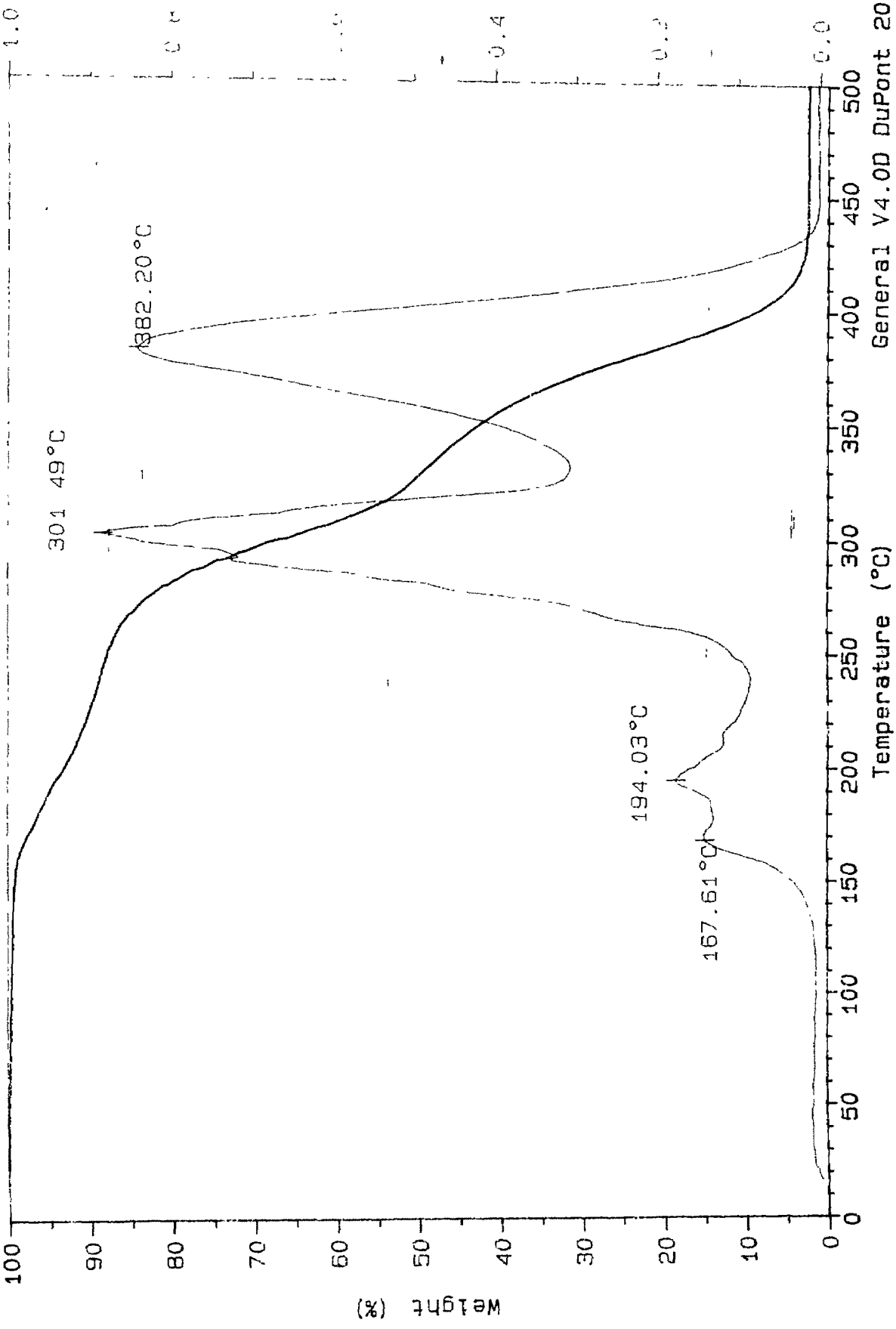


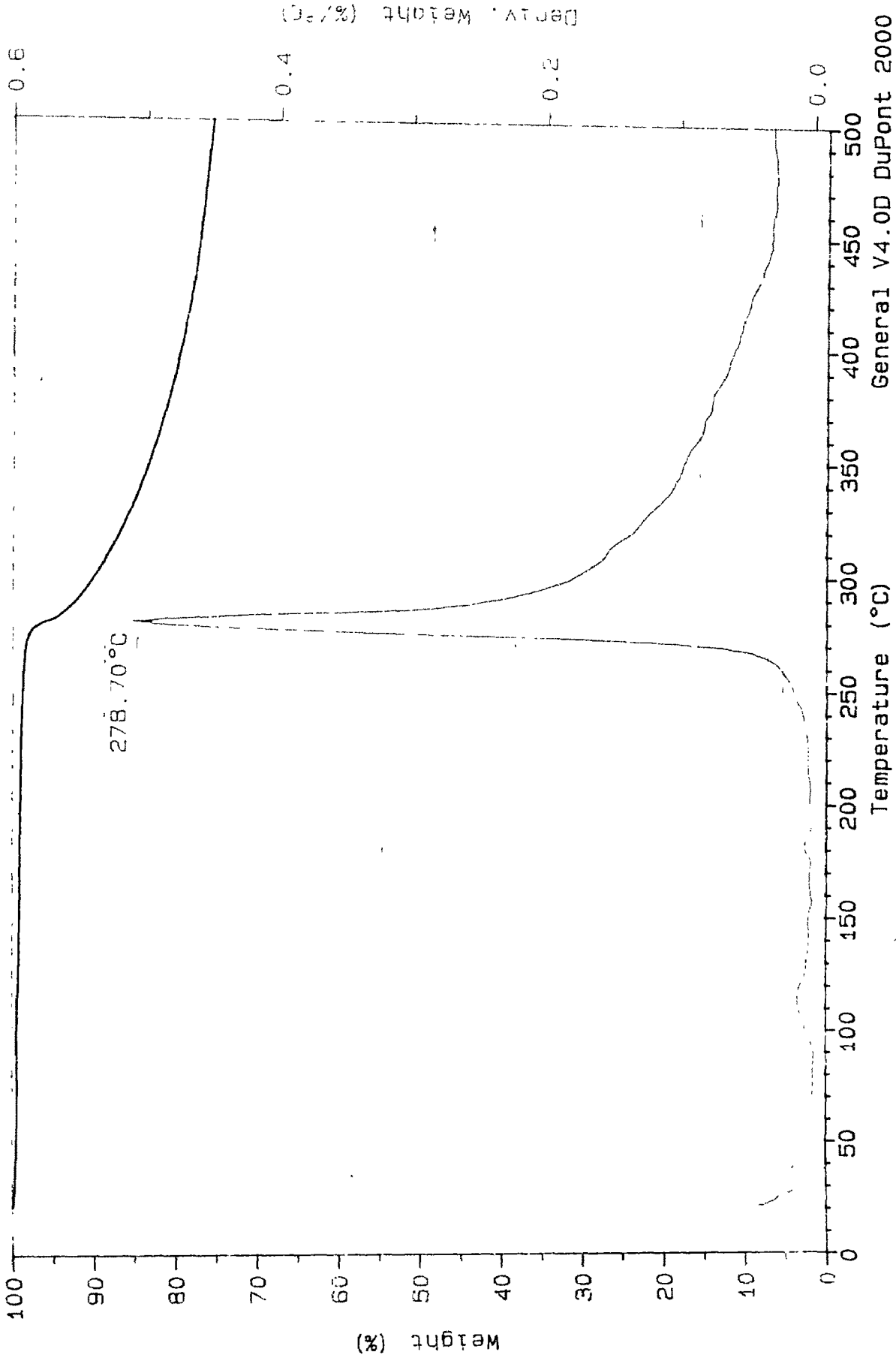
Fig.3.26 TGA of PMMA

General V4.0D DuPont 2000

Sample: H2  
Size: 8.2020 mg  
Method: TGA 10°C/min.  
Comment: N2 50 ml/min.

# TGA

File: H2.01  
Operator: L JOHNSON  
Run Date: 9-Jul-90 11:28



Sample: A-4 COLOUR CHEM  
Size: 7.3680 mg  
Method: TGA 10°C/min.  
Comment: N2 50 ml/min.

# TGA

File: A-4.01  
Operator: L JOHNSON  
Run Date: 6-Jul-90 10:50

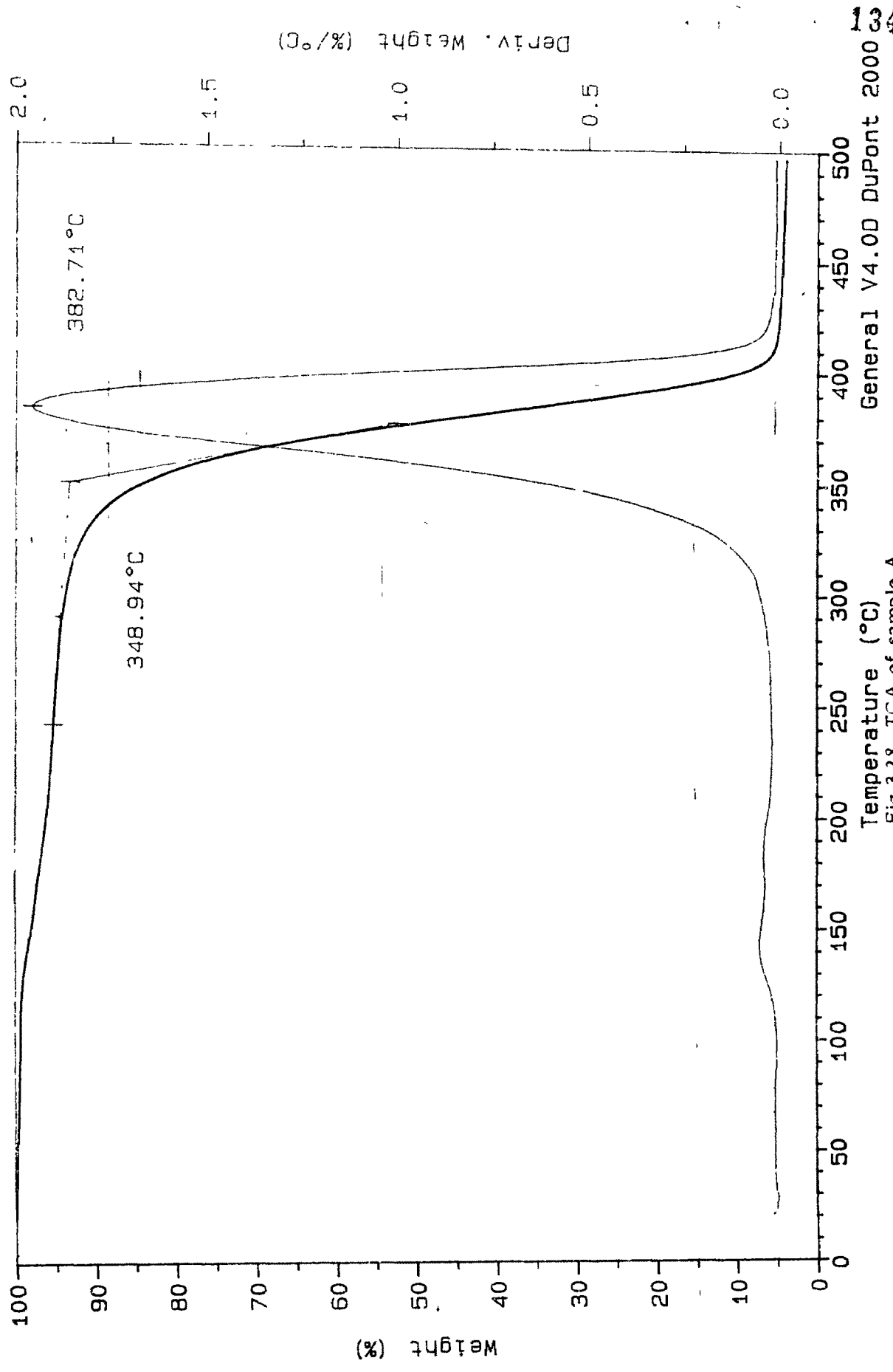


Fig.3.28 TGA of sample A<sub>3</sub>

Sample: A-6 COLOUR CHEM  
Size: 8.0900 mg  
Method: TGA 10°C/min.  
Comment: N2 50 ml/min.

# TGA

File: A-6.01  
Operator: L JOHNSON  
Run Date: 5-Jul-90 14:20

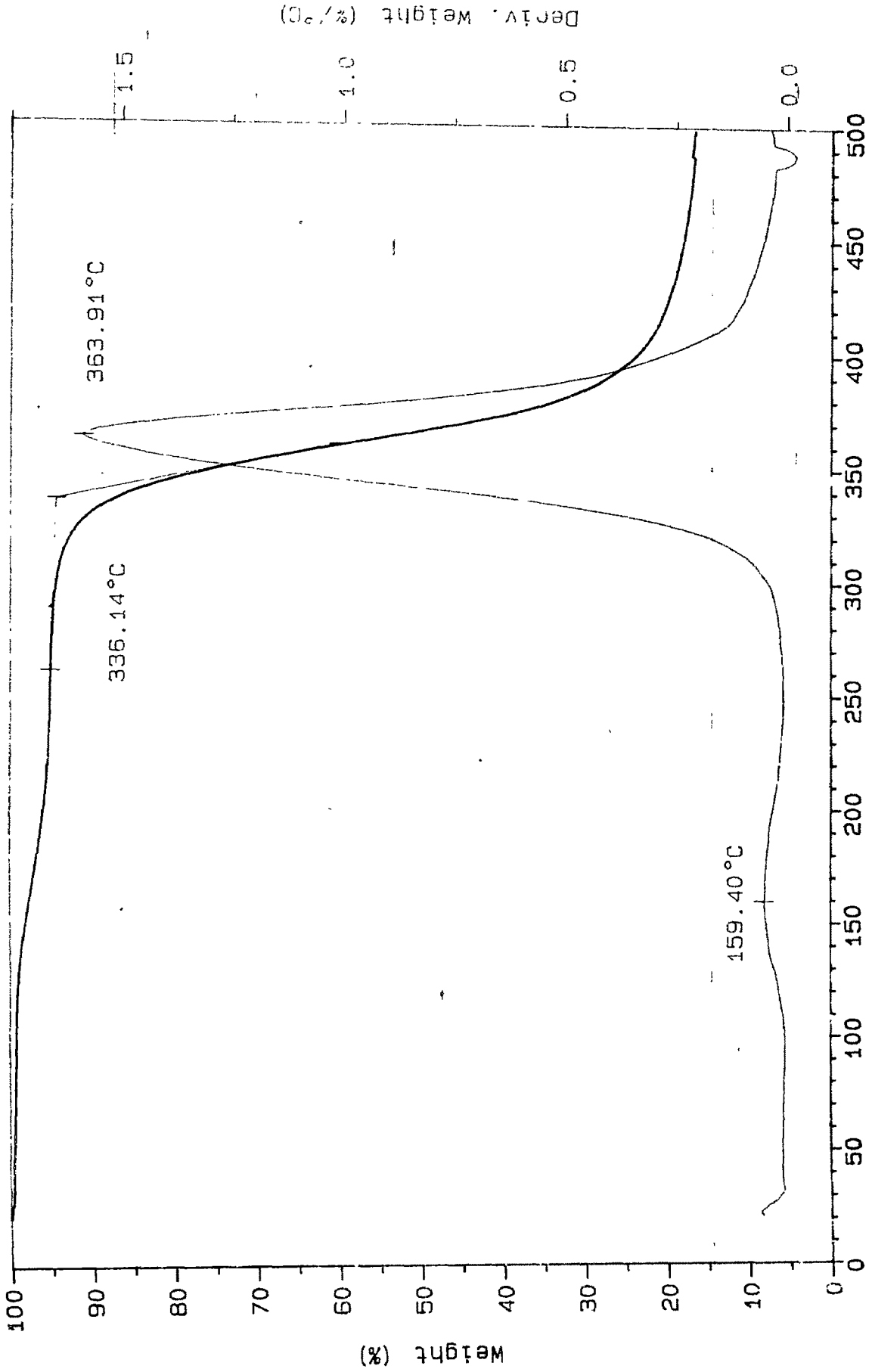


Fig.3.29 TGA of sample A5

Table-3.11

Thermogravimetric analysis :

Sample	(°C)									Char residue upto 500° (%)
	T <sub>5</sub>	T <sub>10</sub>	T <sub>20</sub>	T <sub>30</sub>	T <sub>50</sub>	T <sub>70</sub>	T <sub>80</sub>	T <sub>90</sub>	T <sub>max</sub> *	
PMMA	186	216	280	293	325	372	384	398	301.5	2.5
A <sub>1</sub>	166	278	346	362	378	393	398	405	387.8	-
A <sub>2</sub>	266	319	347	360	375	389	391	402	386.4	2.0
A <sub>3</sub>	290	331	355	365	378	389	399	401	382.7	5.0
A <sub>4</sub>	275	322	353	367	375	383	391	400	378.6	7.5
A <sub>5</sub>	291	326	349	355	367	383	428	-	363.9	17.5
A <sub>7</sub>	215	295	345	356	430	390	-	-	-	40.0
PAN	281	298	389	-	-	-	-	-	-	76.0

\* T<sub>max</sub> : Temperature for maximum rate of decomposition determined from DTG curves.

T<sub>5</sub>, T<sub>10</sub>..... etc. are the decomposition temperature corresponding to 5%, 10% .....weight loss.

Table-3.12

Activation energy of copolymers in thermal degradation.

Sample	Activation energy (KJ mol <sup>-1</sup> )
A <sub>1</sub>	131.6
A <sub>2</sub>	132.3
A <sub>3</sub>	165.5
A <sub>4</sub>	166.7
A <sub>5</sub>	168.4
A <sub>7</sub>	175.2

because of the higher stability of PAN in comparison with PMMA.

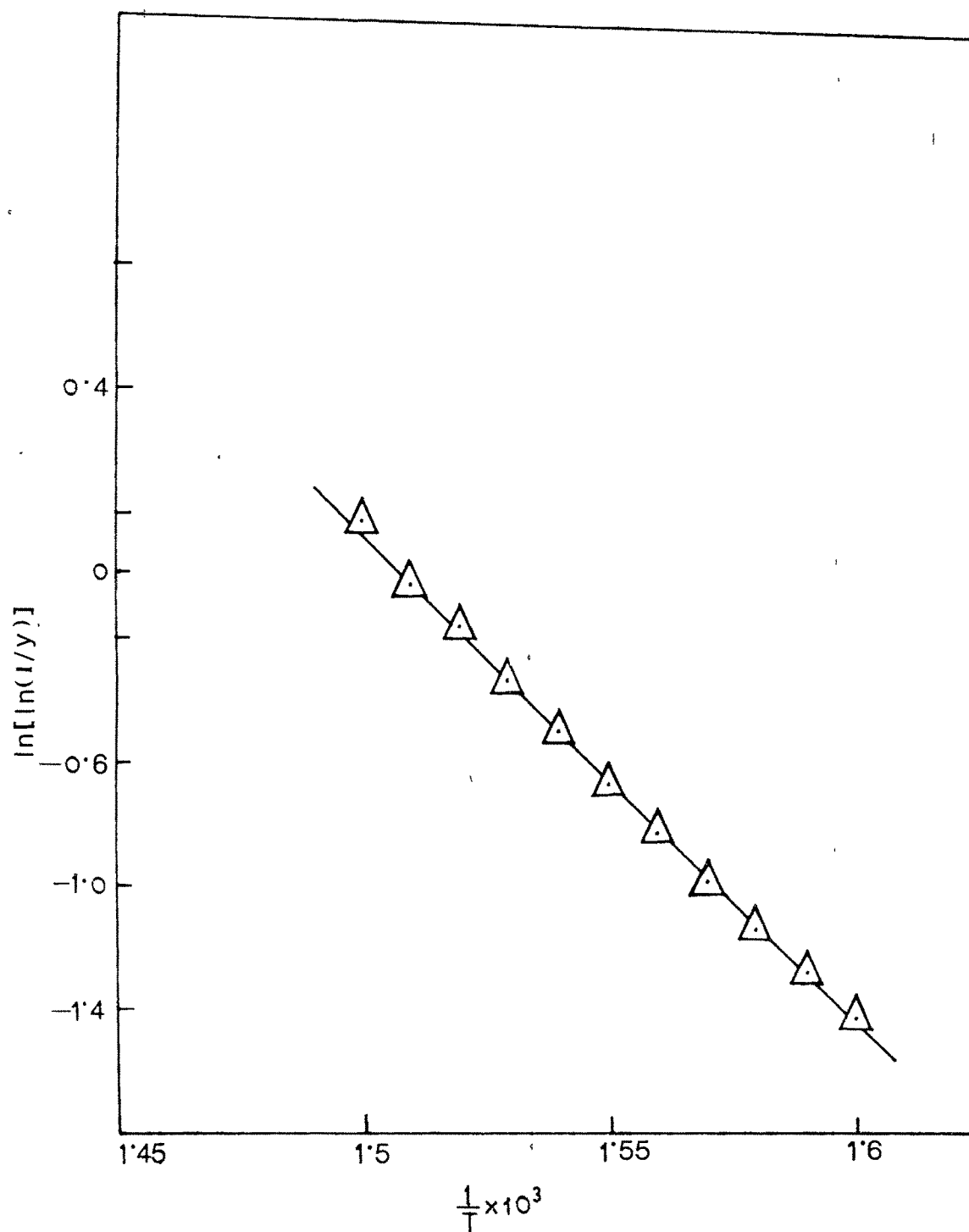
Graphical plots of the percentage of the original weight versus the incidental temperature were obtained for each sample analysed. Some typical examples of such a plots are presented in Figs. 3.30 - 3.32. Analysis of these traces using the method developed by Broido (discussed in section 2.4.3b) allows the calculation of activation energy associated with thermal breakdown. The activation energies of thermal breakdown were calculated by integrated Broido method using the equation.

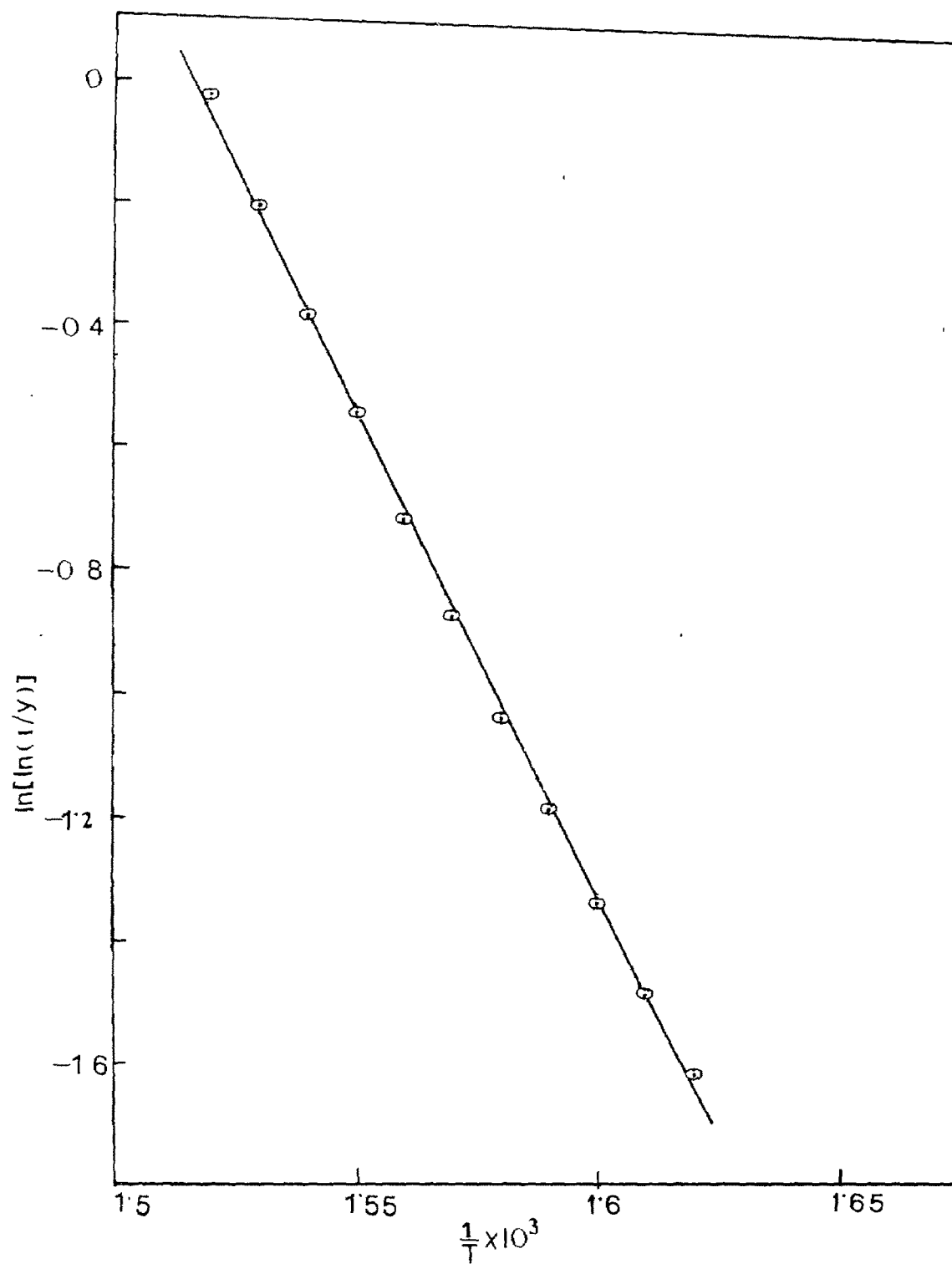
$$\ln [ \ln (1/Y) ] = -( E/R ). (1/T) + \text{Const.}$$

and are given in Table 3.12. As seen from the graphs a straight line plot of negative slope gradient was obtained when  $\ln [ \ln (1/Y) ]$  was plotted against  $1/T$ . The activation energy associated with thermal breakdown of copolymer was thus a positive quantity. It is observed from Table 3.12 that the activation energy of thermal breakdown gradually increases with the increase of acrylonitrile content in the copolymer. This may be due to the higher thermal stability of PAN than PMMA. PAN, being highly polar exhibits intermolecular attraction between polymer molecules and hence increases the stability.

### 3.2.9 Differential thermal analysis (DTA)

From DTA studies melting temperature ( $T_m$ ) and decomposition temperature ( $T_D$ ) for copolymers were calculated and are given in Table 3.13. DTA of PAN gave exothermic peak at  $310^\circ$ . Dunn and Ennis [68] and Huggins [59] also observed the exotherm for PAN at  $300^\circ$ . The observed difference in temperature may be due to the difference in the molecular weights of the polymers. Thompson [60] has also discussed the influence of molecular weight of the polymer on shape and position of the exothermic peaks. The results obtained by DTA for copolymers are agreeable with those obtained by DSC studies.

Fig.3.30 Broido plot for sample A<sub>1</sub>

Fig. 3.31 Broido plot for sample A<sub>2</sub>.

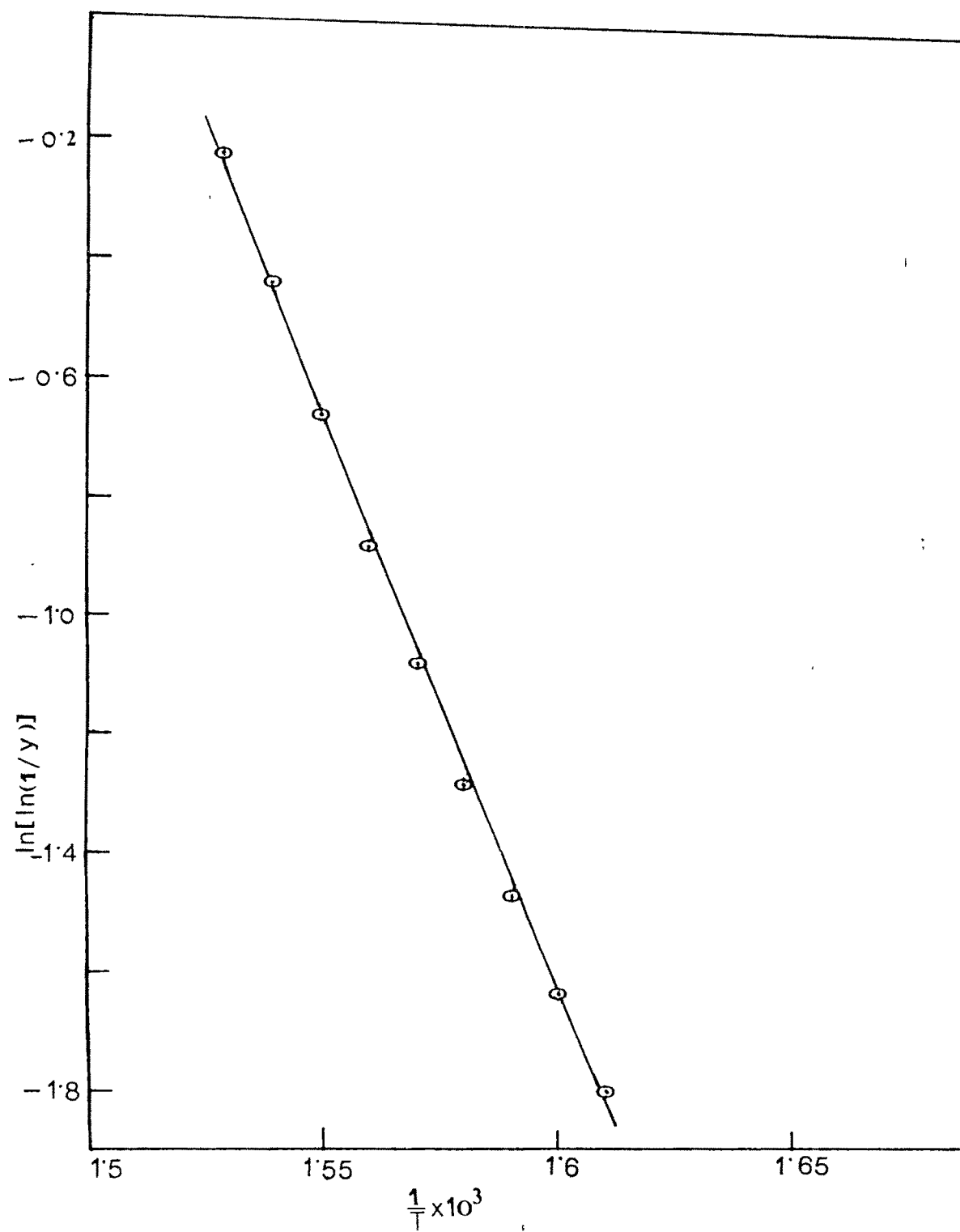
Fig. 3.32 Broido plot for sample A<sub>3</sub>

Table-3.13

Thermal Analysis : DTA

Sample	Melting temperature $T_m$ ( $^{\circ}\text{C}$ )	Decomposition temperature $T_D$ ( $^{\circ}\text{C}$ )
A <sub>1</sub>	380	468
A <sub>2</sub>	390	483
A <sub>3</sub>	380	477
A <sub>4</sub>	390	485
A <sub>5</sub>	-	490
A <sub>6</sub>	-	500
A <sub>7</sub>	-	510
PAN	310	380
PMMA	370	342

The observed increase in  $T_m$  and  $T_D$  of copolymer supports the better thermal stability on copolymerisation.

### 3.2.10 Wide angle X-ray diffraction study

Poly(methyl methacrylate) is an amorphous polymer under all conditions due to dl-isomerism of the bulky side groups. However, crystallisable stereospecific polymers are also known [61]. Heterogeneous system of polyacrylonitrile contains crystalline, quasicrystalline and amorphous phases [62,63]. Natta et al. [64] have demonstrated a hexagonal structure for the crystalline syndiotactic PAN. Mencik [65] obtained rather poor quality diffraction patterns of PAN which could not be interpreted in terms of hexagonal structure and hence he proposed an orthorhombic unit cell structure which was in agreement with the observed reflections and crystal density. Some x-ray diffraction [66] patterns of PAN have been shown to be capable of interpreting in terms of two crystalline phases formed by association of alternating syndiotactic and isotactic segments along the chain. On this basis orthorhombic unit cell is attributed to the syndiotactic polymer and tetrahedral unit cell to the isotactic.

The x-ray diffraction curves for PMMA, PAN and copolymers under this study are given in Figs. 3.33 - 3.36. X-ray scattering in PMMA is in the region of  $(\sin \theta) / \lambda = 0.08$  i.e. peak is at  $2\theta = 14.1^\circ$  arising from an intermolecular spacing of  $6.27 \text{ \AA}$ . Weak rings of PMMA are also observed at  $2\theta = 29.5^\circ$  and  $2\theta = 42.5^\circ$  corresponding to spacing of  $3.024$  and  $2.125 \text{ \AA}$  respectively which arise from intra-molecular scattering [67,68]. Beevers et al. [69] observed similar scattering pattern for PMMA but they got a weak peak at  $5 \text{ \AA}$  which was due to the presence of a small amount of crystalline PMMA polymer in the sample. Fox et al. [70] obtained the scattering pattern of a crystalline PMMA which shows weak rings at  $8.48 \text{ \AA}$  and  $5.1 \text{ \AA}$  with a stronger ring at  $6.68 \text{ \AA}$ . These rings are not observed in the x-ray diffraction pattern of the PMMA

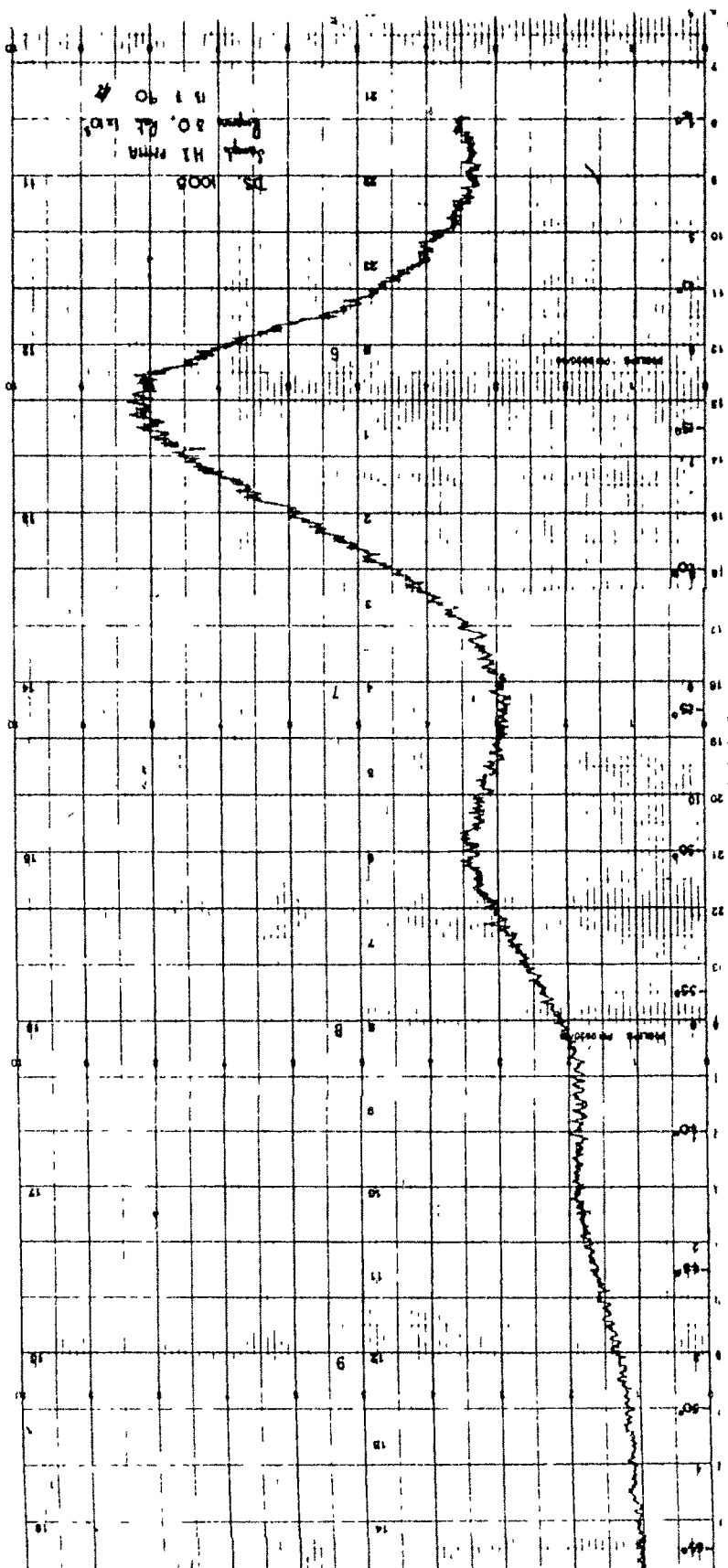


Fig. 3.33 X-ray diffraction pattern of PMMA.

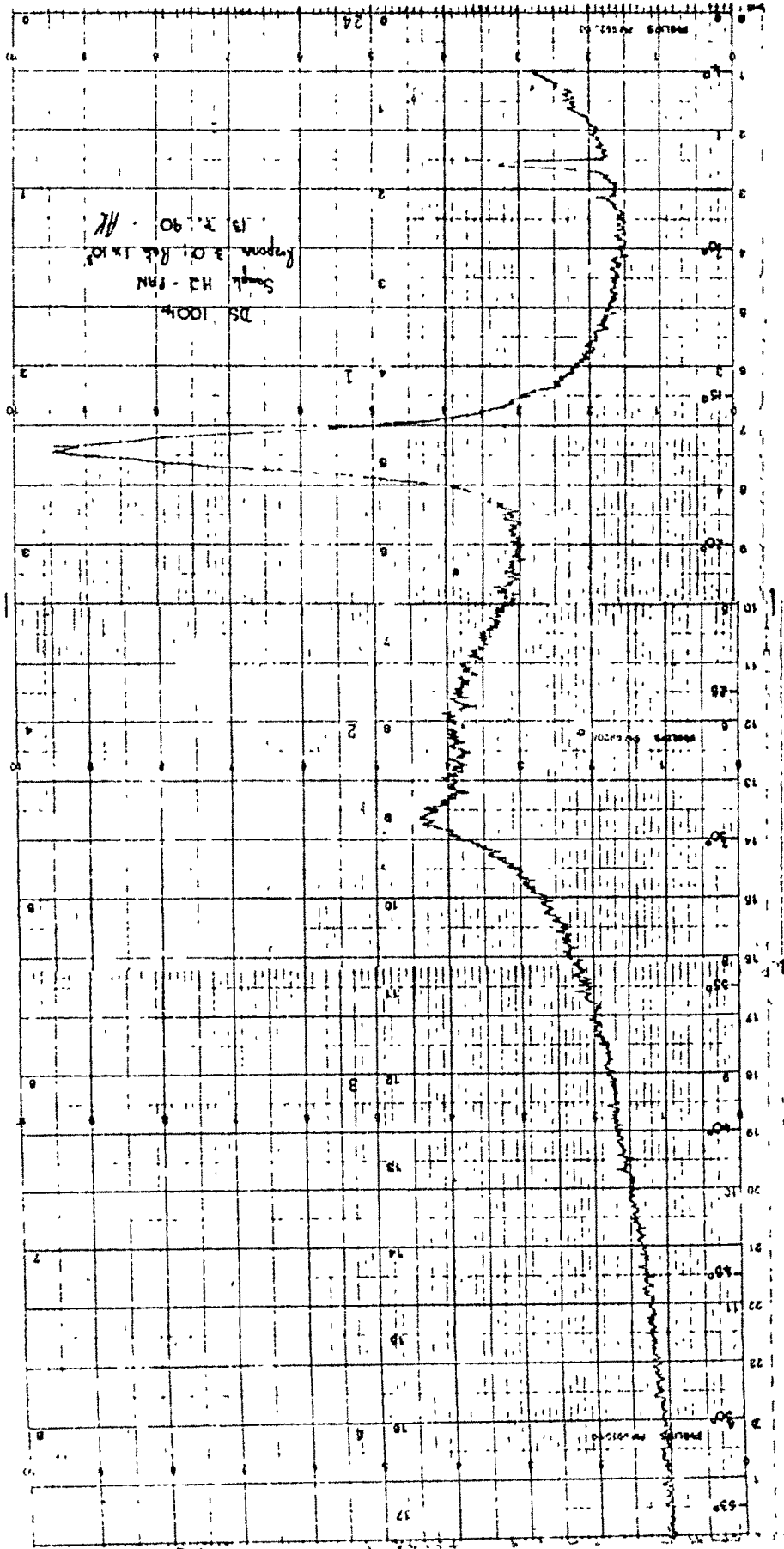


Fig. 3.34 X-ray diffraction pattern of PAN

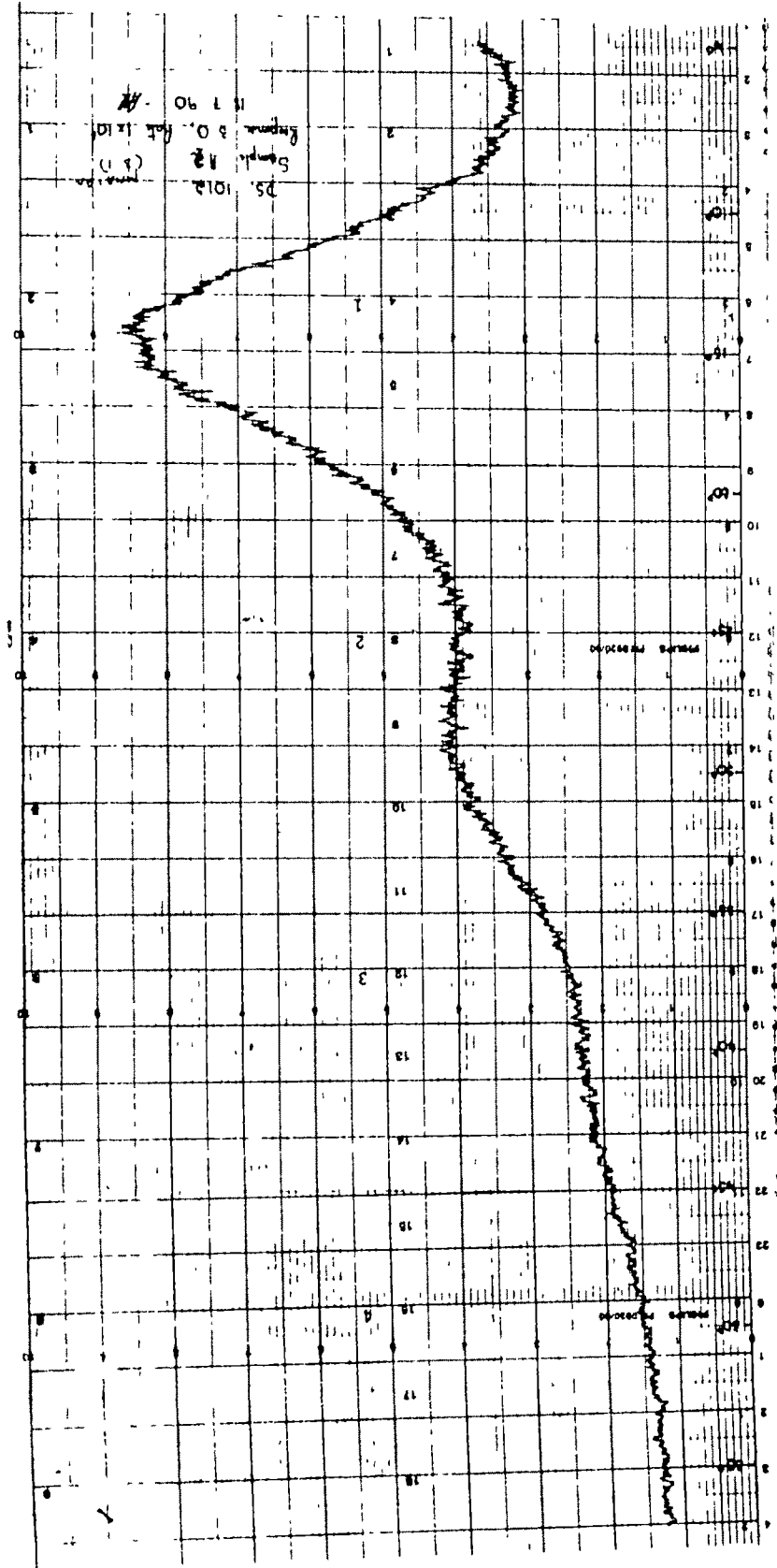


Fig. 3.35 X-ray diffraction pattern of sample A<sub>1</sub>

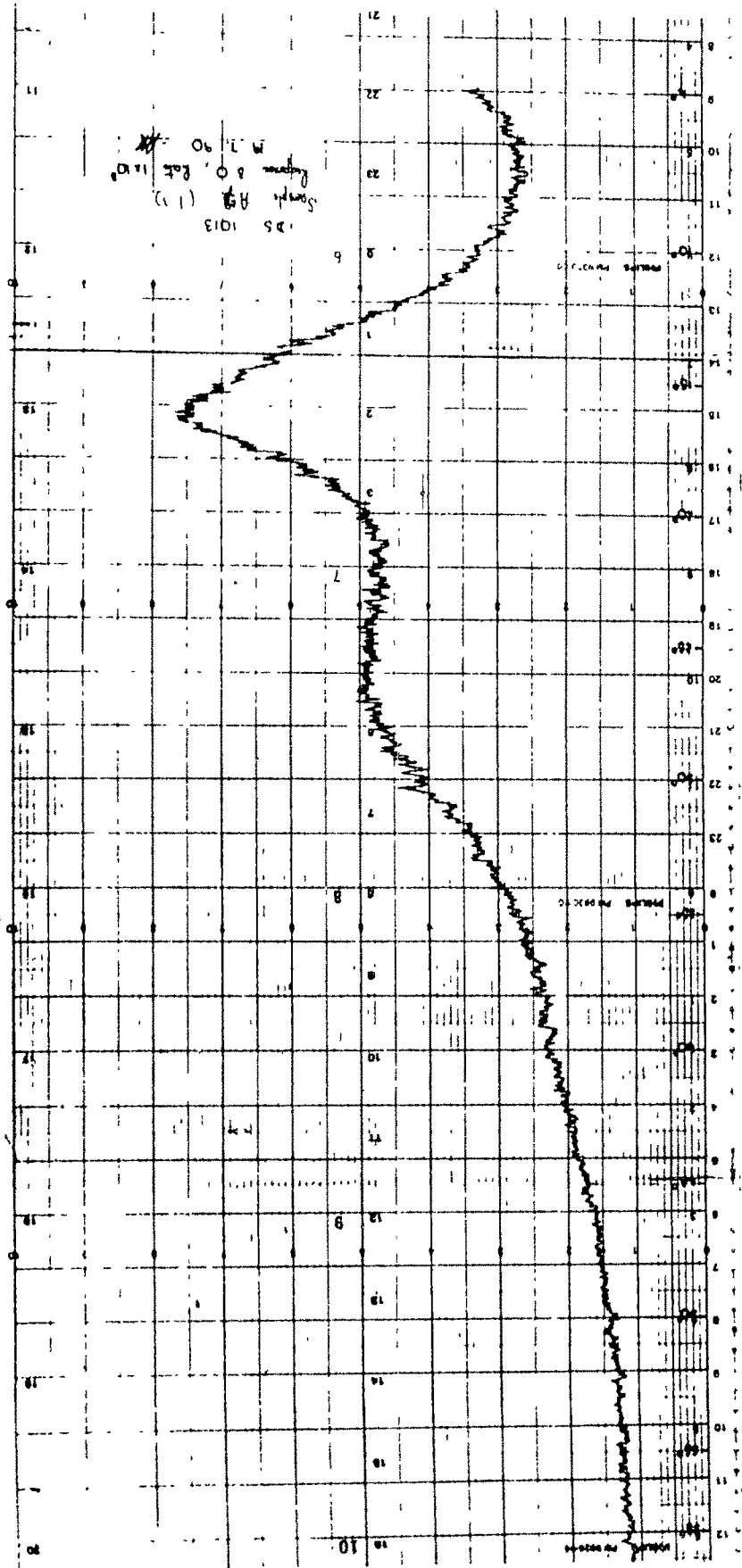


Fig.3.36 X-ray diffraction pattern of sample A7

does not contain any crystalline segments.

The X-ray scattering of PAN Fig. 3.34 shows a sharp peak at  $(\sin \theta)/\lambda = 0.095$  i.e. at  $2\theta = 16.8^\circ$  arising from intermolecular spacing of  $d = 5.27 \text{ \AA}$ . PAN has an additional unresolved peak in the region of  $2\theta = 29.4 - 22.0^\circ$  i.e. at  $d = 3-4 \text{ \AA}$ . Stefani et al. [71] reported a value of  $5.17 \text{ \AA}$  for polyacrylonitrile and have also suggested an orthorhombic unit cell structure. The sharpness of the  $5.27 \text{ \AA}$  peak of PAN under this study gives evidence of a reasonably crystalline polymer but the extent of the crystalline domain in PAN has not been determined.

The X-ray diffraction pattern of copolymers reveals that all the copolymers show reflections in between that of PAN and PMMA. It was also observed that the X-ray diffraction curves for copolymers show progressive changes with alteration in copolymer composition. As the methyl methacrylate fraction increases the curves show both a shift and broadening of the peak towards the scattering curves for PMMA. This is evident from the results of the analysis given in Table 3.14.

With the increase of MMA content in the copolymer  $\theta$  values gradually decrease and the corresponding d-spacing increases, indicating that with the increasing MMA content in the copolymer the distance (d-spacing) between two successive lattice planes increases due to bulky side groups of MMA. Similar observations were made by Beevers et al [69]. Okamura [72] has given evidence of a similar effect in AN-vinylidene copolymers. No marked difference was observed for copolymers containing 20% vinylidene chloride but a copolymer containing upto 60% vinylidene chloride had a noticeably enlarged spacing. Gremillion and Boulet [73] examined the X-ray scattering for vinylidene chloride - AN copolymers containing 0 to 40% AN. Their photometer traces suggest that the enlargement in spacing observed by Okamura [72] reaches a maximum value for a copolymer containing 10 - 20% AN. Nukushima and Sakurada [74] found a continuous in-

Table-3.14

Wide angle X-ray diffraction studies of copolymers and homopolymers of MMA and AN.

Mole fraction of MMA in the copolymer	Bragg angle $\theta$ (degree)	$\sin \theta / \lambda$	d-spacing (Å)
0.0	8.40	0.095	5.27
0.28	8.25	0.093	5.37
0.41	7.70	0.087	5.75
0.55	7.35	0.083	6.02
0.60	7.30	0.083	6.06
0.64	7.25	0.082	6.10
0.68	7.20	0.081	6.14
1.00	7.05	0.080	6.27

crease in spacing in X-ray diffractions of several vinyl acetate-vinyl chloride copolymers.

The shift in spacing observed in the copolymers under the present study is shown in Fig.3.37. It was observed that the intermolecular spacing in the copolymer chains shows reasonable linear relationship with composition in the range of 40-70 % MMA.

### 3.2.11 Microscopy :

Scanning electron microscopic studies were carried out for homopolymers and copolymers to see the change in the morphology of the copolymers. Some representative results are given in Figs. 3.38 - 3.41. Figs. 3.38 and 3.41 represent PAN and PMMA respectively. Due to the crystalline nature of PAN surface of the polymer exhibited very little particulates concentration which has contributed towards the lowering of the crystallinity of PAN. Fig. 3.41 representing PMMA shows exclusively fiber and network type of structure which may be due to amorphous nature of PMMA. Fig. 3.40 represents copolymer with higher (75%) MMA composition and hence shows resemblance towards PMMA, whereas Fig.3.39. represents copolymer with 75% AN in feed composition and hence exhibits the morphology identical to PAN.

### 3.2.12 Contact angle measurement :

One way of characterising polymer surface is to measure the contact angle ( $\theta$ ) made by a drop of liquid on the surface at the point where the two phases meet. The surface tension of solid surface and that of a liquid determines whether the liquid will wet the surface when applied to it. Perfect wetting occurs when  $\cos\theta = 1$ , i.e. when  $\theta = 0$ . Critical surface tension provides information related to the solvents which have wettability for the surface. Table 3.15

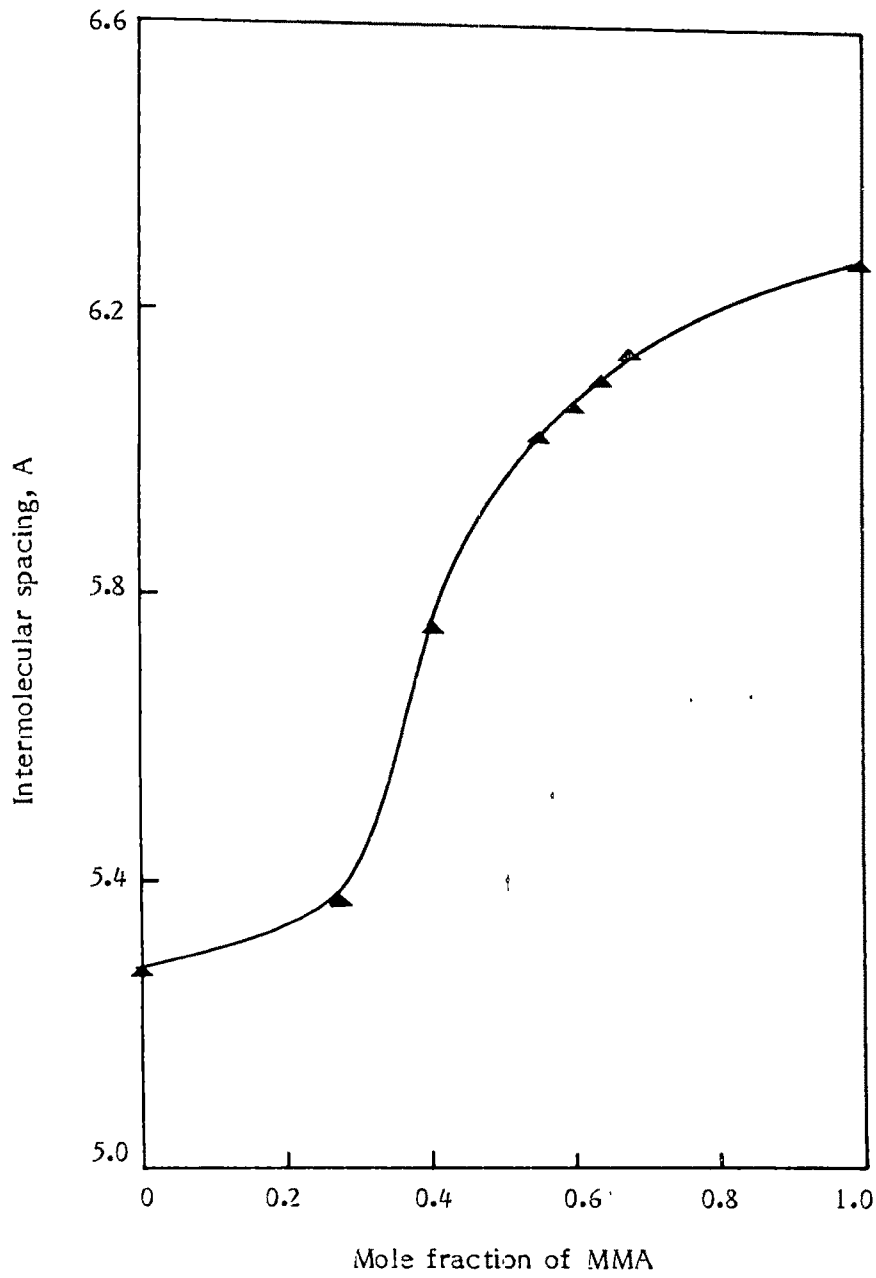


Fig.3.37 Effect of copolymer composition on the intermolecular spacing in random copolymer.

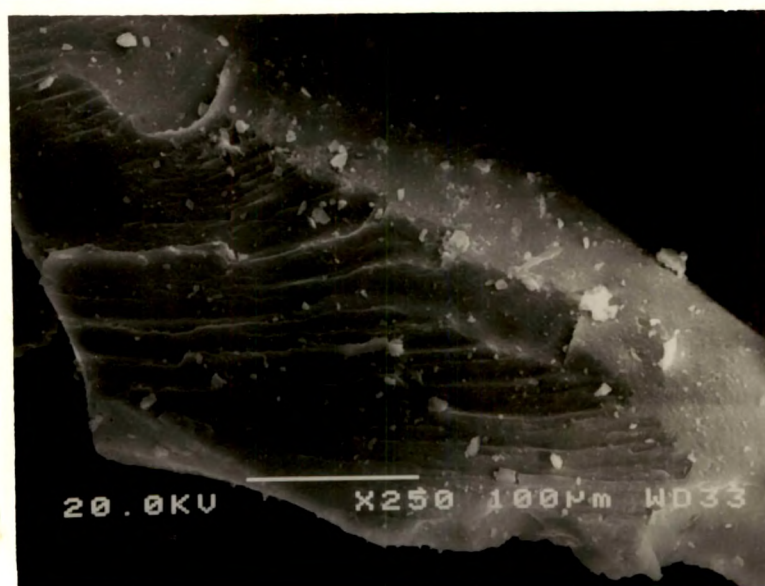


Fig. 3.38 : SEM micrograph of PAN (x250)

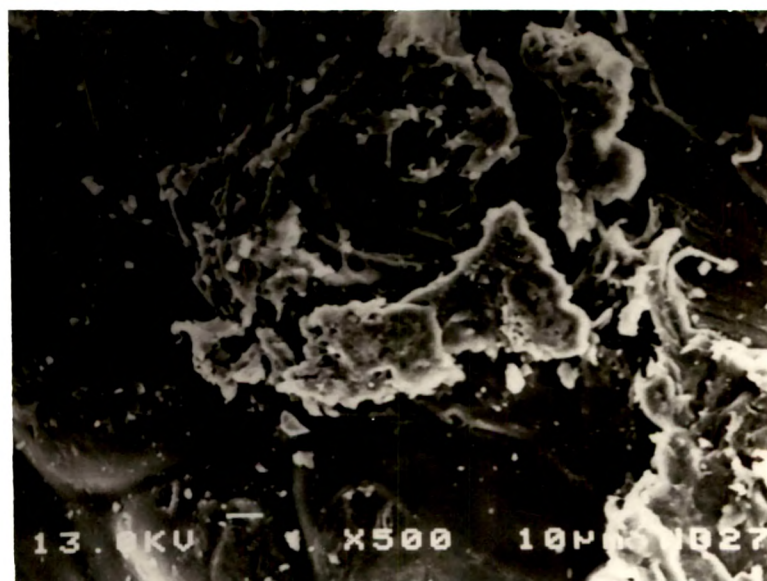


Fig.3.39 : SEM micrograph of sample A<sub>7</sub>.  
( 75% AN, v/v ) x 500

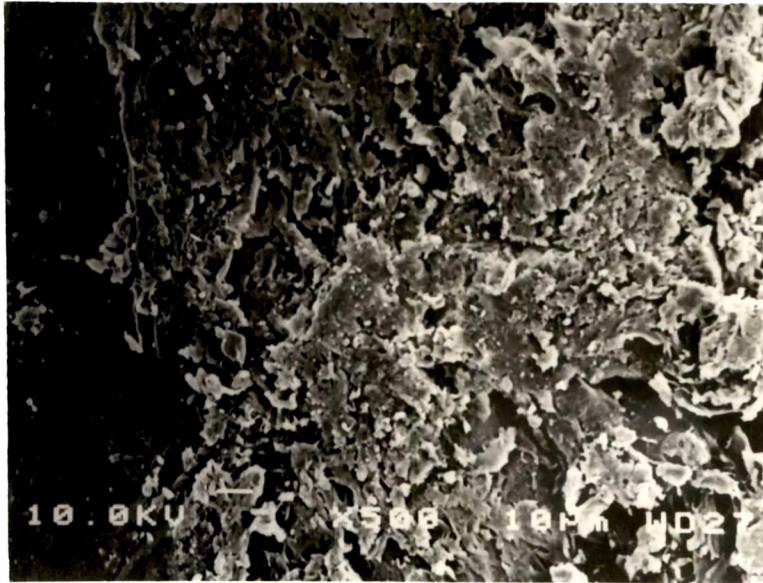


Fig.3.40 : SEM micrograph of sample A<sub>1</sub>  
( 75% MMA, v/v ) x 500

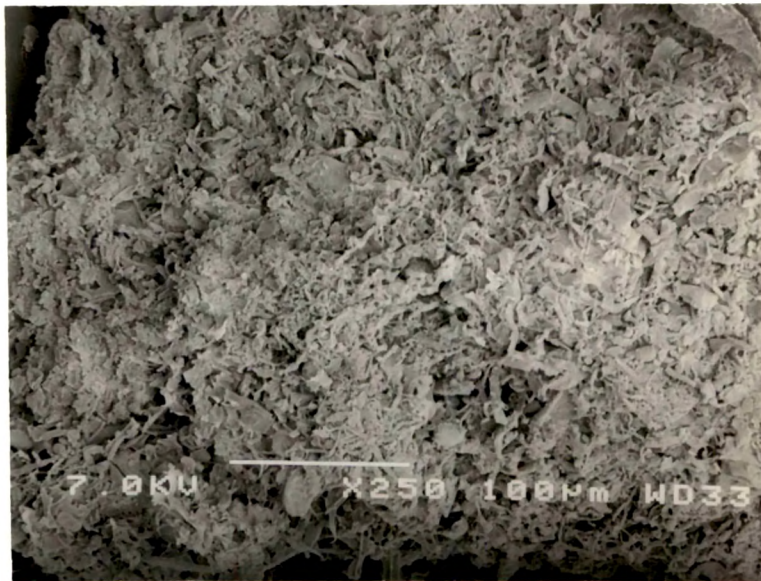


Fig. 3.41 : SEM micrograph of PMMA x 250

Table-3.15

Contact angles of copolymers and homopolymers in different solvents.

Solvent	Angle of contact ( $\theta$ ) of polymer (degree)				
	A <sub>1</sub>	A <sub>3</sub>	A <sub>6</sub>	A <sub>7</sub>	PMMA
Ethylene glycol	46.0	51.8	55.5	64.0	35.0
Glycerol	61.7	63.0	70.9	71.7	54.0
Acetaldehyde	48.0	50.0	54.1	60.3	45.0
Water	65.4	69.3	73.9	75.8	63.0
30% Ethanol.	47.4	49.0	54.0	59.0	43.0

gives the contact angles of the copolymers of various compositions for different solvents. It is observed from the results that in a particular solvent, the angle of contact gradually increases as the acrylonitrile content in the copolymer increases. Figures 3.42, 3.43 show the plots of  $\cos\theta$  versus surface tension of the contacting liquids. From these graphs the critical wetting tension of the copolymers having various compositions were determined. It is evident from the graph of critical wetting tension ( $\gamma_c$ ) versus mole fraction of AN in the copolymer [ Fig.3.44 ] that as the mole fraction of acrylonitrile in the copolymer increases, the critical wetting tension decreases. But for a given polymer contact angle with respect to various solvents increases with increasing polarity of the solvent. In terms of dielectric constants and hence polarity water > glycerine > ethylene glycol > acetaldehyde. The  $\theta$  values obtained for the copolymer films show that all the surfaces are hydrophobic irrespective of polymer composition. Hence polymer surface properties are totally different than their bulk properties. Casting of PAN films as well as films of polymers rich in PAN were very difficult. *Hydrophobicity of films is due to their casting in DMF which leads to cyclisation as discussed earlier.*

### 3.2.13 Solubility parameter of copolymer :

The solubility parameter for copolymers of MMA and AN were evaluated by studying the intrinsic viscosity in different solvents. The intrinsic viscosity is plotted against the solubility parameter of the solvents. Since the chain conformation is most expanded in the best solvent, the intrinsic viscosity will be the highest for the best match in solubility parameter. In the present study six fractions of 2:3 (MMA:AN, v/v),  $A_5$  copolymer were undertaken. The fractions were collected by precipitating the copolymer from its 2% solution in DMF by successive addition of methanol. The dependence of intrinsic viscosity on the solubility parameter of solvents has been used for estimating solubility parameter of the copolymer. The intrinsic viscosity of the copolymer solution

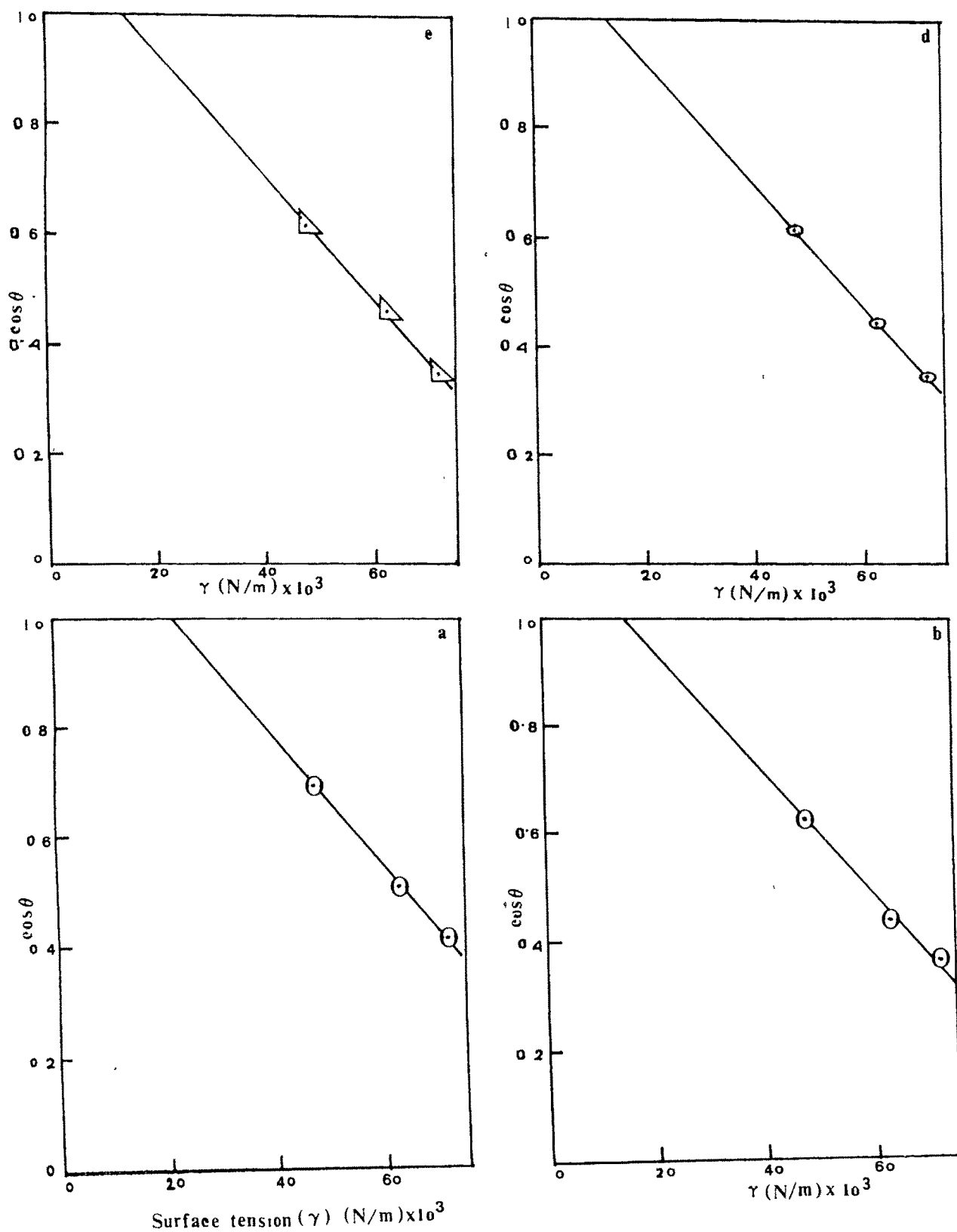


Fig.3.42 Cos of angle of contact ( $\cos \theta$ ) versus surface tension of liquids.  
 a.  $A_1$  b.  $A_2$ , c.  $A_3$ , d.  $A_4$ ,

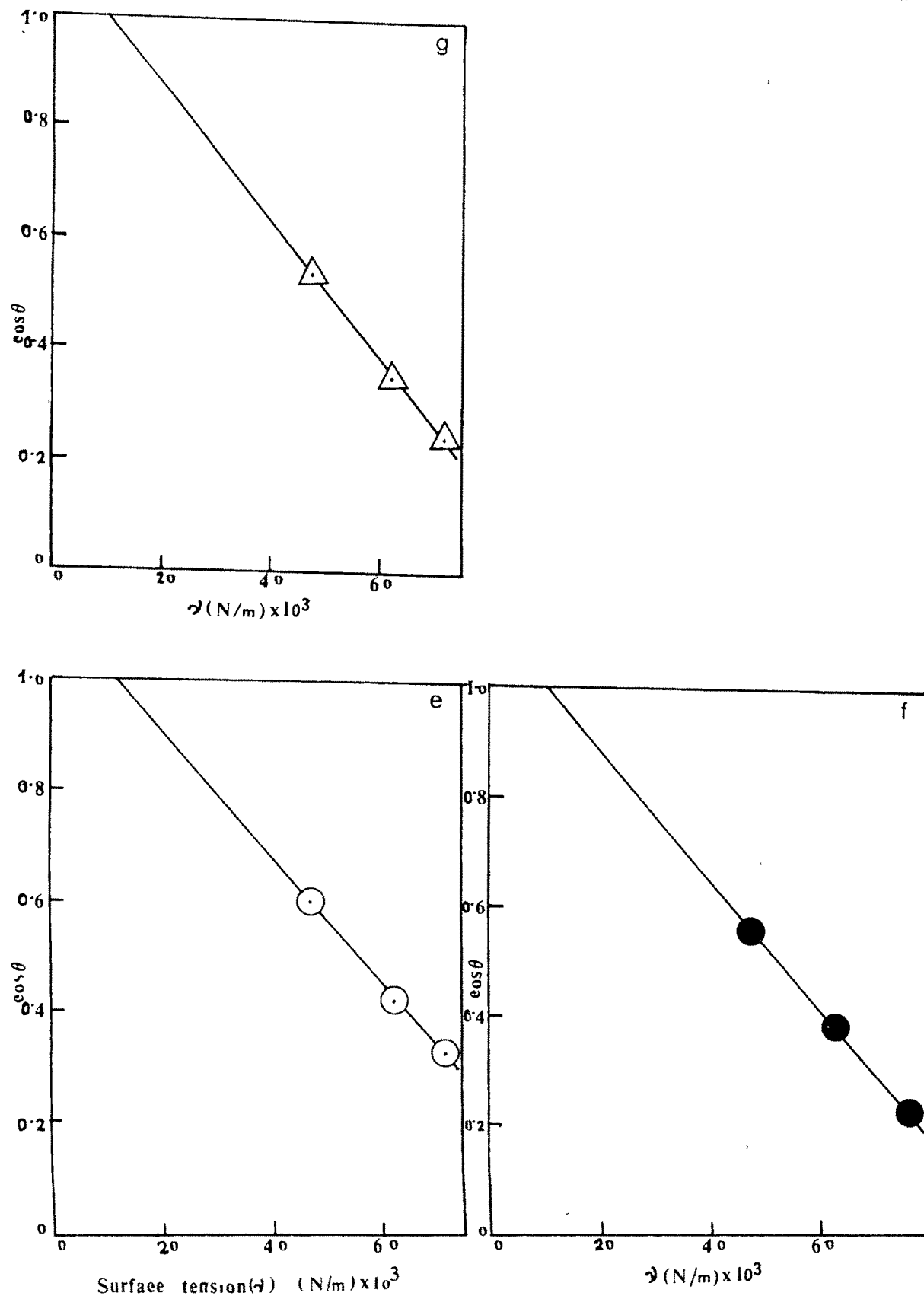


Fig. 3.43  $\cos \theta$  versus surface tension of liquids.  
e.  $A_5$ , f.  $A_6$ , g.  $A_7$

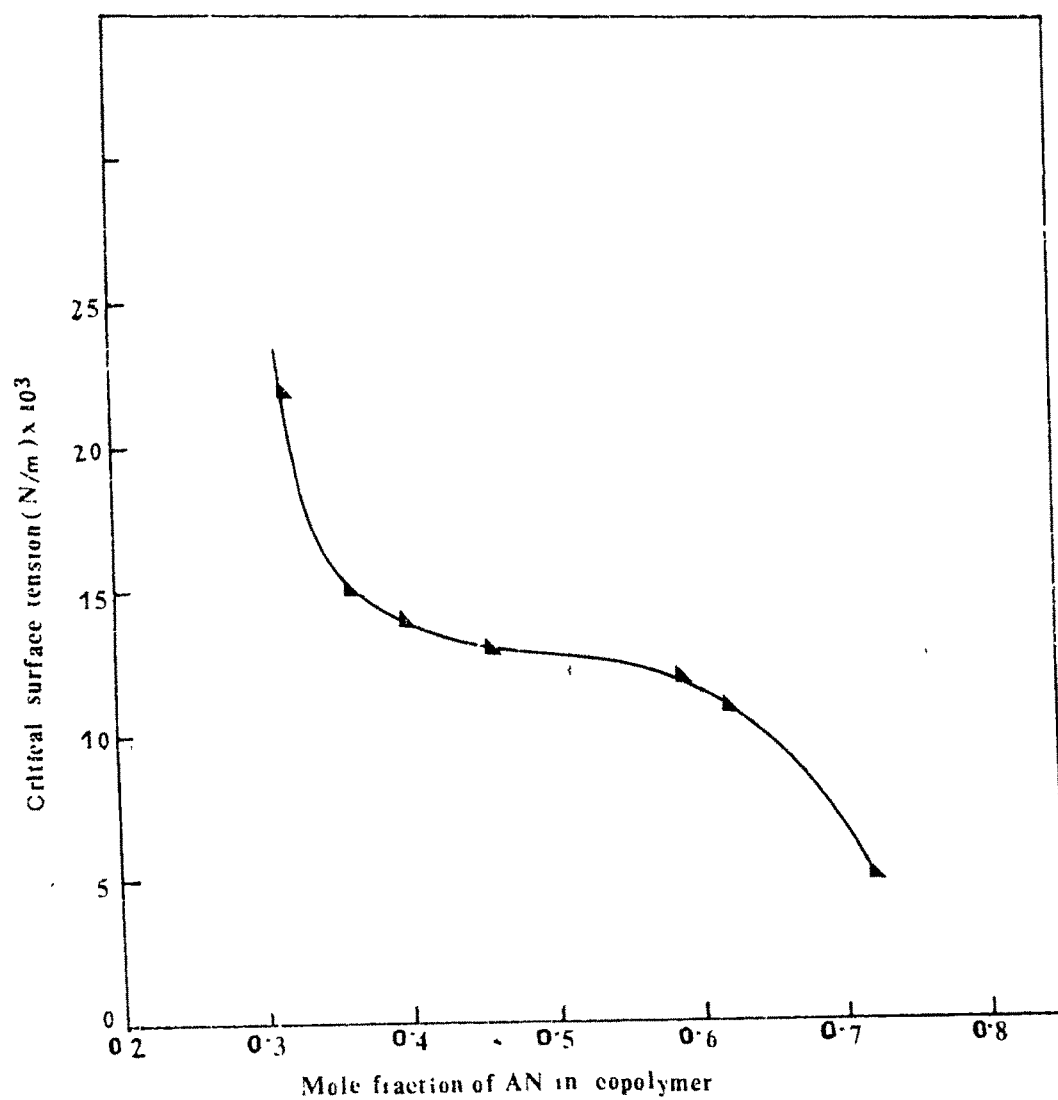


Fig.3.44 Dependence of critical surface tension on copolymer composition.

attains maximum value when solubility parameter of the copolymer falls in the vicinity of that of the solvents  $\delta_p$ . The solubility parameter of the copolymer has been estimated by equating it to that of the solvent at which intrinsic viscosity has the maximum value in the plot of  $[\eta]$  versus  $\delta$  (Fig. 3.45). The intrinsic viscosities of the six fractions and the solubility parameter of the solvents are shown in Table 3.16. The value of solubility parameter for all the fractions of MMA-AN system is  $10.0 \text{ (cal/cc)}^{1/2}$ . This value lies between the solubility parameters  $9.5$  and  $15.4 \text{ (cal/cc)}^{1/2}$  reported for PMMA and PAN respectively [75,76].

#### 3.2.14 Swelling :

Results from studies of swelling of random copolymers are shown in Figures 3.46, 3.47. It is observed from the figures that percentage swelling increases in water with the increase of acrylonitrile content in the copolymer ; whereas it goes on decreasing with other less polar solvents like methanol, absolute alcohol, 1-propanol and cyclohexane. Due to hydrogen bonding character of water as well as polyacrylonitrile , swelling extent increases with increasing acrylonitrile concentration in copolymer. It has also been observed that, for a particular sample of copolymer, the percent swelling goes on decreasing in methanol, absolute alcohol, 1-propanol and cyclohexane. This may be due to decreasing order of polarity of these solvents. Copolymer with strong polar  $-\text{C}\equiv\text{N}$  group allows the polar solvent to penetrate into it. Hence penetration of solvent molecules into polymer molecules increase with increasing polarity of the solvent which results into increasing swelling extent. It has also been observed that though water is most polar solvent among the five solvents used, the copolymers do not show the maximum extent of swelling in water. This may be due to the unmatched solubility parameter of the copolymer ( $10 \text{ (cal/cm}^3$ )

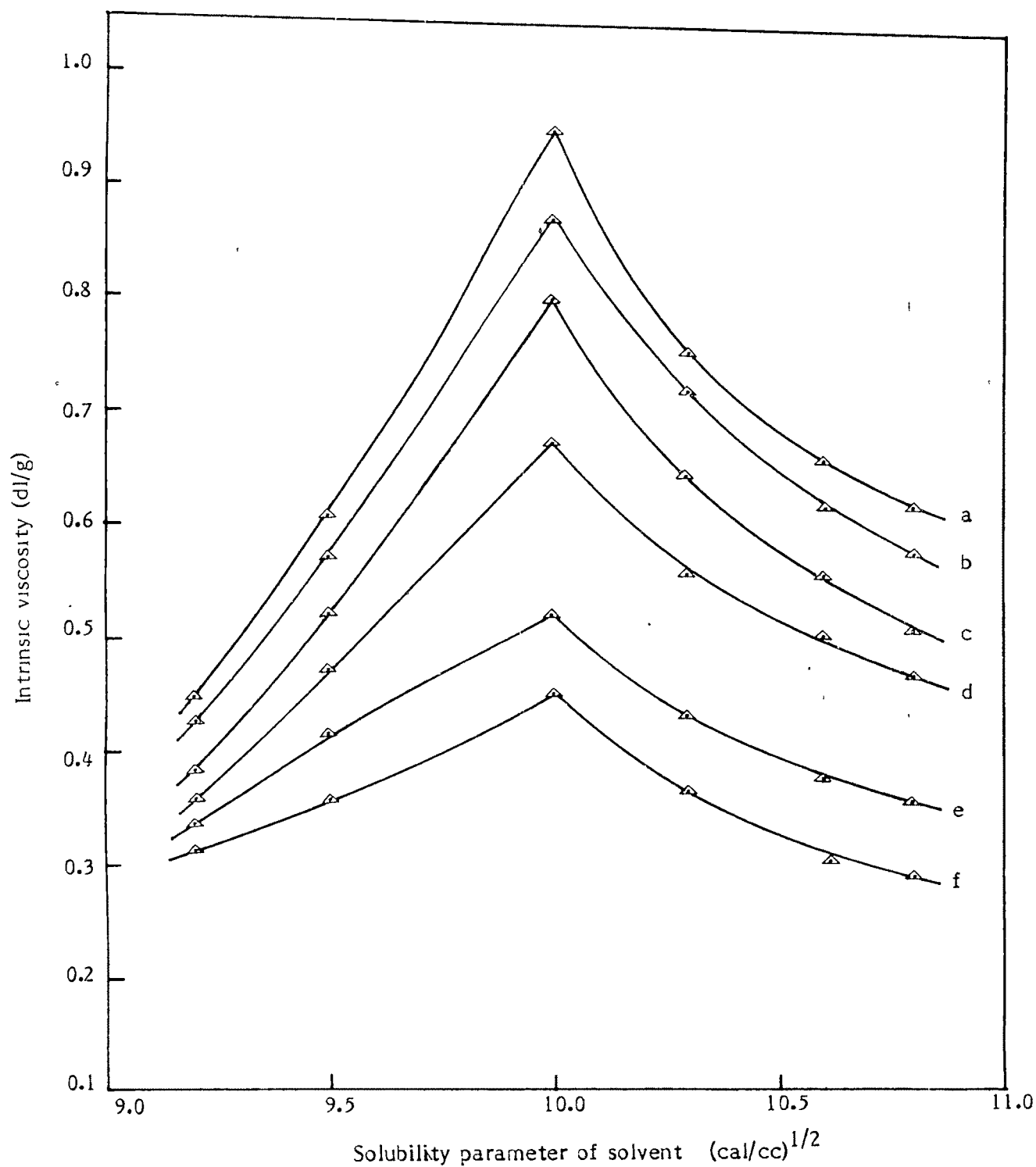


Fig.3.45 Plot of intrinsic viscosity versus solubility parameter of sample  $A_5$  in different solvents at  $30^\circ$ . a,b,c,d,e, & f, represents fraction 1,2,3,4,5,& 6 respectively.

Table-3.16

Intrinsic viscosity  $[\eta]$  and their dependence on solubility parameter ( $\delta$ ) of solvents.

$[\eta]$  at 30° ; Six fractions of A<sub>5</sub> sample (2:3 (v/v) MMA:AN)

Solvents	Solubility parameter ( $\delta$ ) (Cal/cc) <sup>1/2</sup>	[ $\eta$ ]dl/g of copolymer fraction in different solvents					
		F <sub>1</sub>	F <sub>2</sub>	F <sub>3</sub>	F <sub>4</sub>	F <sub>5</sub>	F <sub>6</sub>
Benzene	9.2	0.450	0.430	0.385	0.360	0.340	0.315
Chloro-benzene	9.5	0.610	0.575	0.525	0.475	0.420	0.360
1,4-Dioxane	10.0	0.954	0.875	0.805	0.675	0.525	0.455
Acetic anhydride	10.3	0.760	0.725	0.650	0.565	0.440	0.370
Diethyl-formamide	10.6	0.665	0.625	0.565	0.510	0.385	0.305
Dimethyl acetamide	10.8	0.625	0.585	0.515	0.475	0.365	0.295

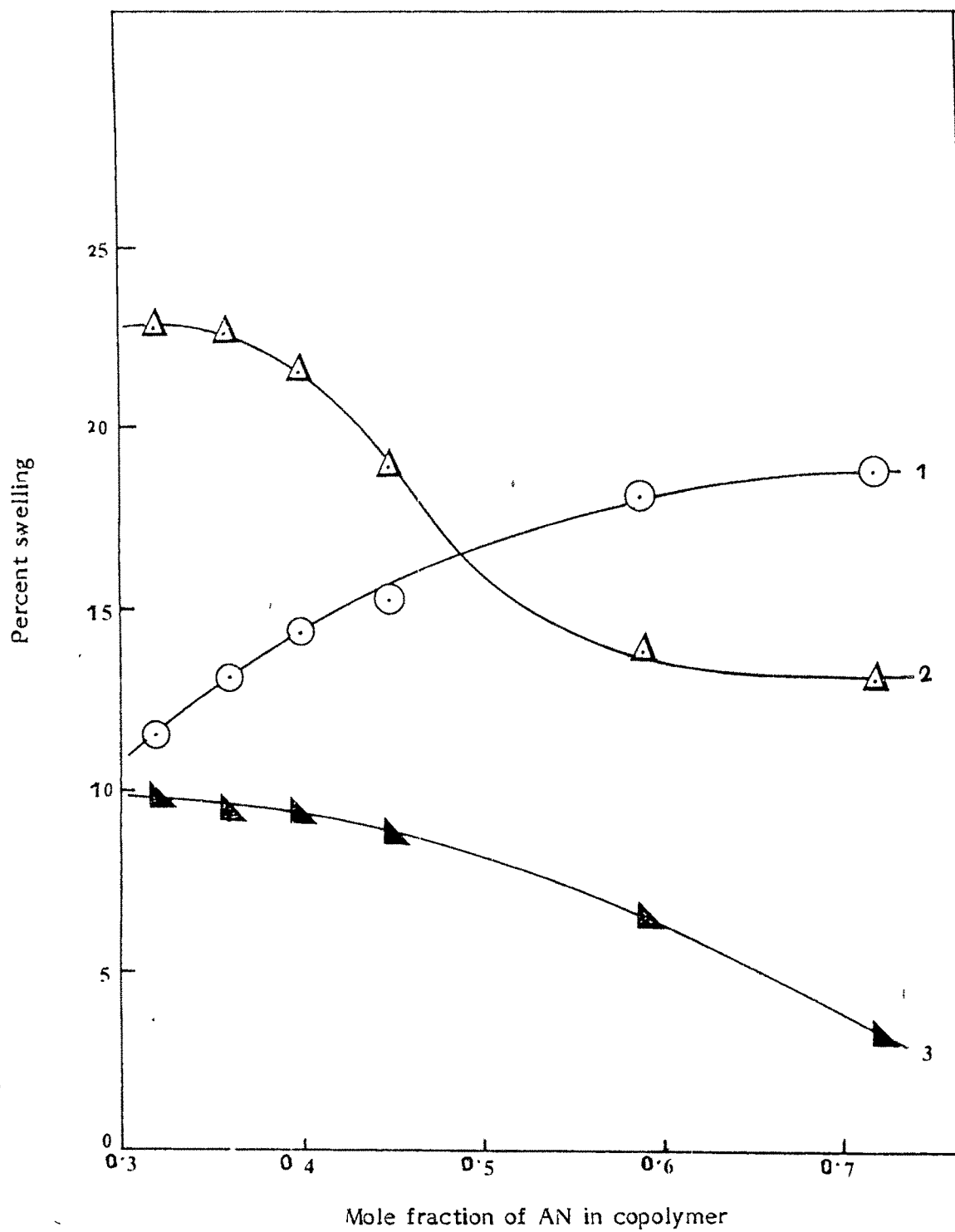


Fig. 3.46 Effect of copolymer composition on percent swelling in 1. water, 2. methanol, 3. cyclohexane.

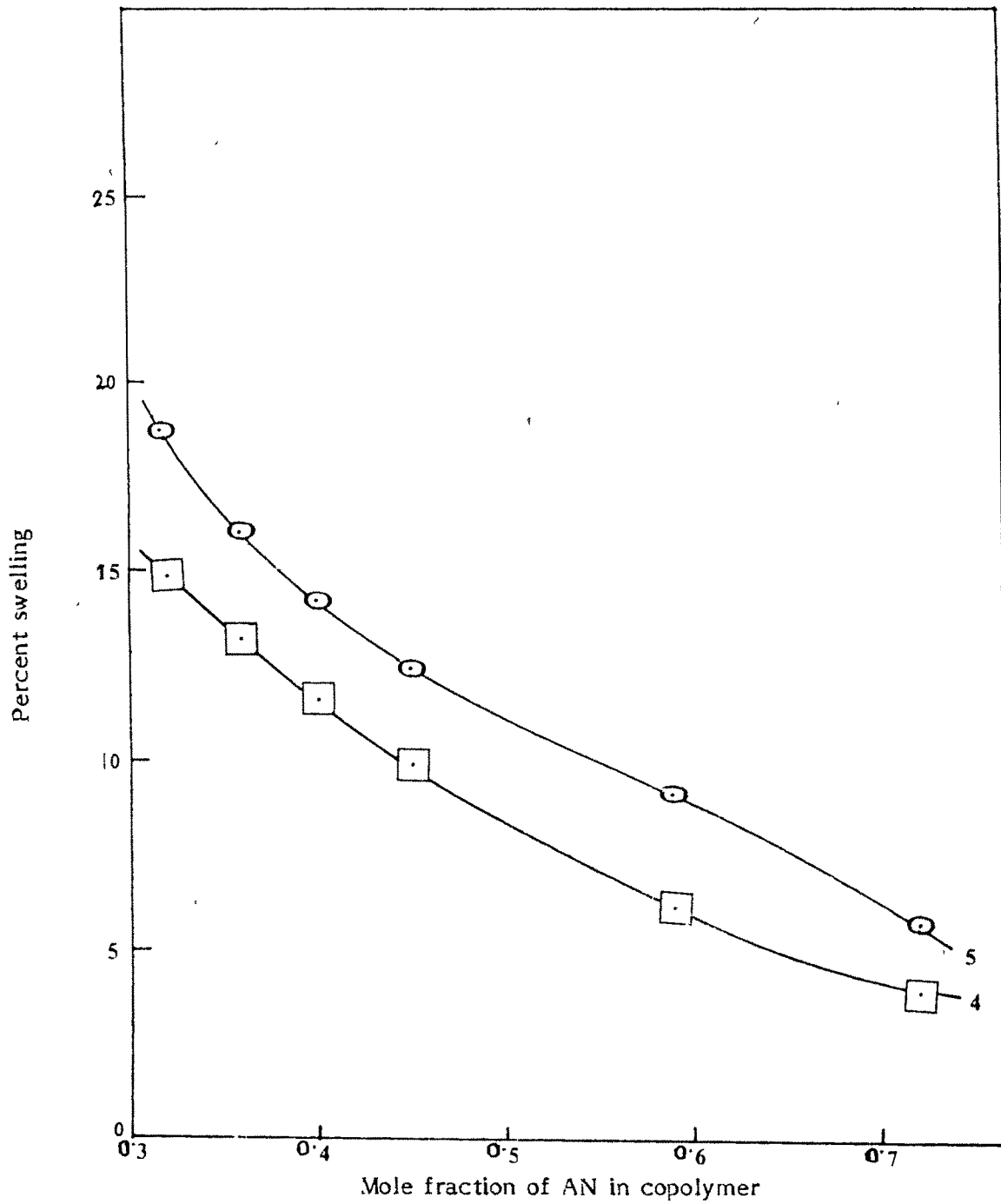


Fig.3.47 Effect of copolymer composition on percent swelling in  
4. 1-propanol, 5. absolute alcohol

with that of water,  $[23.4(\text{cal}/\text{cm}^3)^{1/2}]$ . It is expected that the maximum swelling will take place when solubility parameter of the copolymer matches of the solvent. The solvents reported here have solubility parameters between 8.2 to  $14.5(\text{cal}/\text{cm}^3)^{1/2}$

### 3.2.15 Differential refractometry

The  $dn/dc$  values of MMA-AN copolymers, PAN and PMMA were calculated at 632.8 nm as described in section 2.4.11. DMF was used for preparing polymer solutions. Five different dilutions were used for each system examined. The systems studied showed very little concentration dependence. Some representative graphs are given in Fig. 3.48. The  $dn/dc$  values observed for the individual copolymer in DMF are given in Table 3.17. The  $dn/dc$  values calculated by assuming that the individual components of the copolymer contributes to the  $dn/dc$  in proportion to their known weight fractions, are also given in Table 3.17. The theoretical values of  $dn/dc$  were calculated according to equation,

$$\nu_{\text{copolymer}} = dn/dc = W_A \nu_A + W_B \nu_B$$

Where  $\nu_A$ ,  $\nu_B$  are the specific refractive index increments of component A and B of the copolymer and  $W_A$  and  $W_B$  are their corresponding weight fractions. The weight fraction values required for the calculations were obtained from gravimetric analysis of nitrogen and  $\nu_A$  and  $\nu_B$  were determined experimentally. The  $dn/dc$  values calculated and observed experimentally are presented in Fig. 3.49. It is observed that the experimental values show 25 % deviation from the calculated values except for the copolymer where MMA : AN composition is 1:2 (i.e.  $A_0$ ). These results indicate that only weight fraction of the individual component is not contributing towards the  $dn/dc$  values, but the morphological arrangements of the components in the copolymer is equally

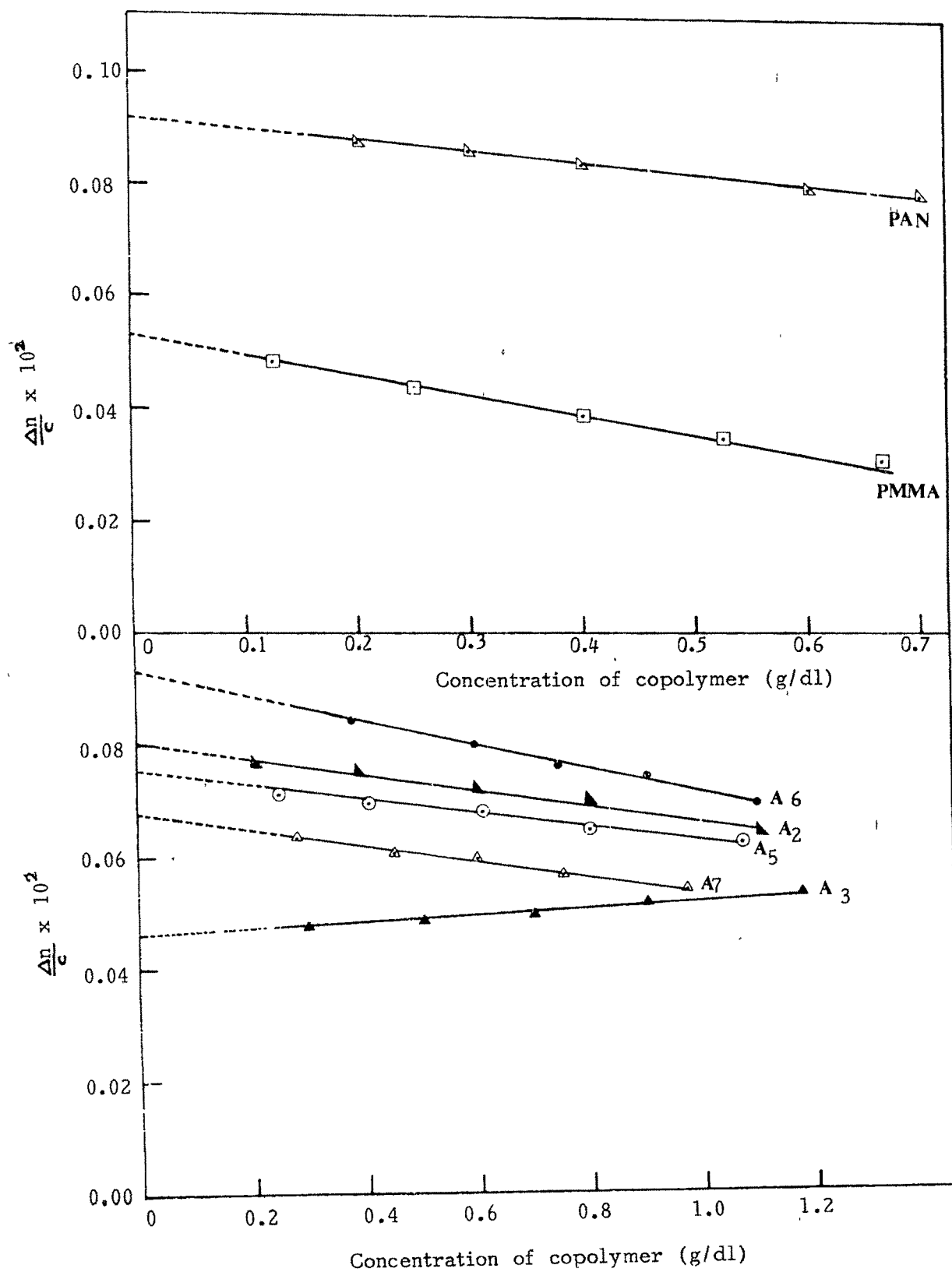


Fig. 3.48 Plot of  $\Delta n/c$  versus concentration of copolymer in differential refractometry.

Table-3.17

Differential refractometric analysis :  
 dn/dc values for copolymers, PMMA and PAN  
 Cell constant = 0.0008

Copolymer sample	Weight fraction of AN	Weight fraction of MMA	dn/dc calculated	dn/dc observed
A <sub>1</sub>	0.202	0.798	0.061	0.081
A <sub>2</sub>	0.227	0.773	0.062	0.046
A <sub>4</sub>	0.299	0.701	0.065	0.076
A <sub>5</sub>	0.437	0.563	0.070	0.093
A <sub>6</sub>	0.466	0.534	0.071	0.068
A <sub>7</sub>	0.578	0.422	0.076	0.059
PAN	-	-	-	0.092
PMMA	-	-	-	0.053

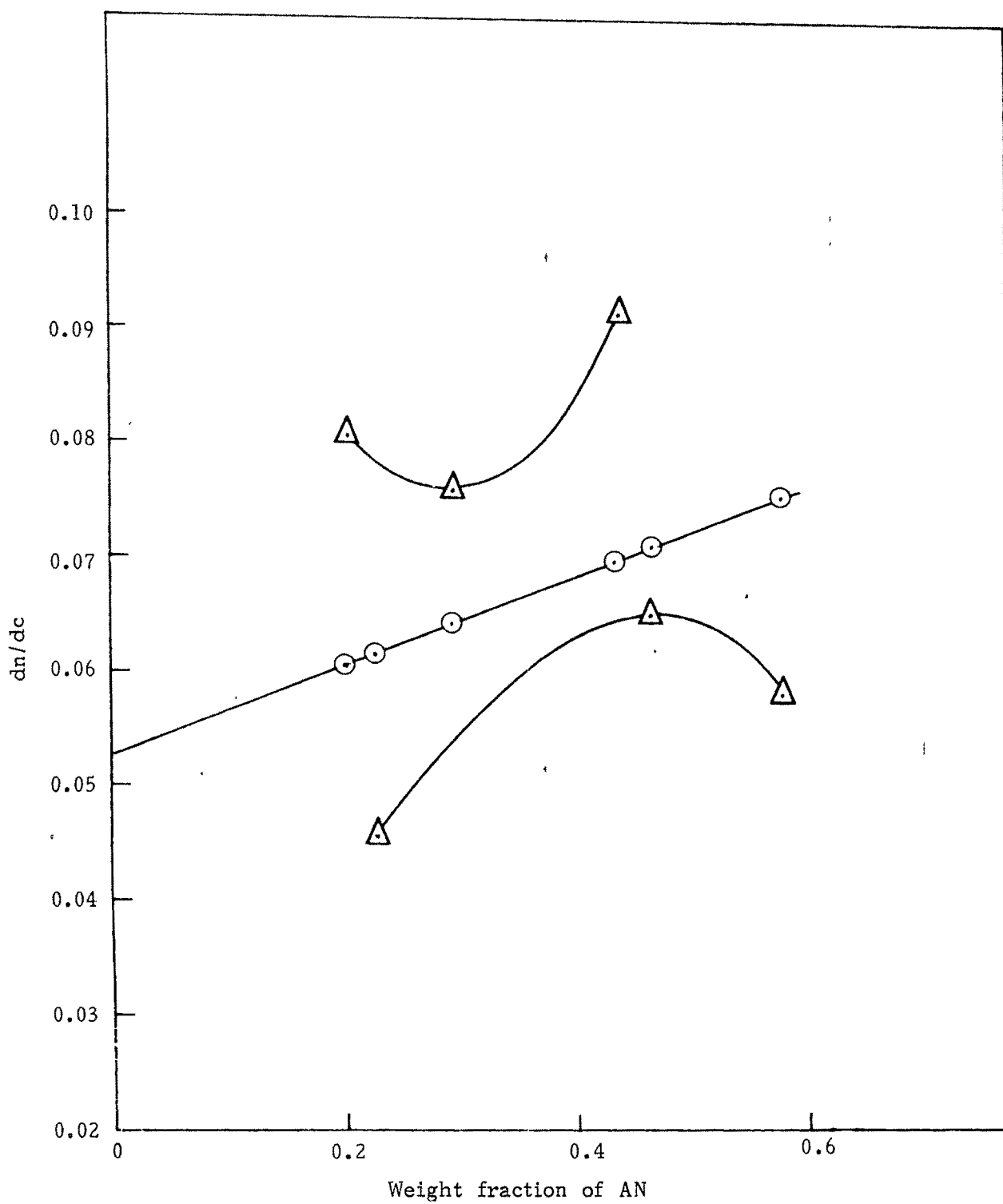


Fig.3.49 Effect of copolymer composition on  $dn/dc$  values in differential refractometry.  $\Delta$  Experimental  
 $\odot$  Calculated

responsible for  $dn/dc$  values. In the present study the copolymer being random, deviation of values from the ideal behaviour is observed. However, this deviation is not very high ( $\sim 25\%$ ), indicating the randomness or disorder in copolymer conformation within 25%.

### 3.2.16 Adiabatic Compressibility :

Table 3.18 shows the results of the measurements of adiabatic compressibility of the copolymers and homopolymers of MMA and AN and also of DMF. It is observed that the adiabatic compressibility of the solvent is not much affected by the polymer in solution. Compressibility of the solvent DMF is increased to 0.8% by polyacrylonitrile and 5.21% by poly(methyl methacrylate) ; whereas copolymers show an increase in compressibility of the solvent from 1.8 to 4.21%. It has also been observed that with the increase of AN content in the copolymer the compressibility gradually decreases though the change is very low. This may be due to the less number of bulky methyl groups. Copolymers with higher MMA content have greater number of bulky methyl groups which allow the solution to be compressed when pressure is applied to it. So with the decrease of MMA content i.e. with the increase of AN content in the copolymer, compressibility gradually decreases.

### 3.2.17 Measurement of Zeta Potential

Table 3.19 shows the positive zeta potential values of the copolymers. It is observed from the data that the zeta potential increases with the increase of acrylonitrile content in the copolymer. This may be due to the increasing polarity of the copolymer with the increase of acrylonitrile content. When the polarity of the copolymer increases the thickness of the electrical double layer at the solid liquid interface also increases because of the increase of

Table-3.18

Adiabatic compressibility of copolymers and homopolymers

Sample	wave length ( $\lambda$ )	Adiabatic compressibility $\text{Sec}^2 \text{ cm}^{-1} \text{ g}^{-1} \times 10^7$
PMMA	1.434	5.25
A <sub>1</sub>	1.432	5.18
A <sub>2</sub>	1.434	5.17
A <sub>3</sub>	1.436	5.15
A <sub>4</sub>	1.436	5.13
A <sub>5</sub>	1.442	5.11
A <sub>6</sub>	1.444	5.10
A <sub>7</sub>	1.446	5.08
PAN <sup>*</sup>	1.454	5.03
DMF	1.458	4.99

Table-3.19

Zeta potential measurement of the copolymers

Copolymer	Zeta potential (mV)
A <sub>1</sub>	474.5
A <sub>3</sub>	587.2
A <sub>5</sub>	765.8
A <sub>7</sub>	931.2

electrical charge density at the solid-liquid interface. Since zeta potential depends on the thickness of the double layer, increase in the thickness of the double layer increases the zeta potential.

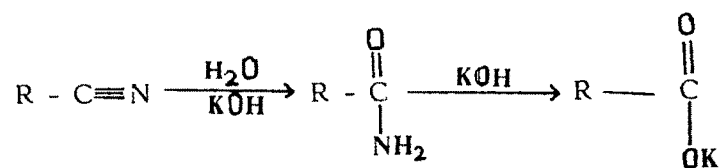
### 3.2.18 Hydrolysis of copolymer

Hydrolysed acrylates and graft copolymers have shown remarkable change in their behaviour as support for enzyme immobilisation. The behaviour depends on the extent of hydrolysis. Hence we have undertaken a brief study of hydrolysis of MMA-AN copolymers.

Hydrolysis of copolymers of MMA and AN was carried out with potassium hydroxide at various conditions, by changing hydrolysis time, temperature and KOH concentration. During hydrolysis reaction the following compounds are supposed to be formed.

- (i) Polymethacrylic acid salt.
- (ii) Poly acrylamide
- (iii) Poly acrylic acid salt.
- (iv) cross-linked poly acrylonitrile etc.

In the copolymer containing nitrile group, hydrolysis should occur according to the same pattern as for low molecular weight nitriles.



Similarly the ester group ( $-\text{COOCH}_3$ ) of the copolymer should undergo hydrolysis following the mechanism of low molecular weight esters. Potassium ion ( $\text{K}^+$ ) content in the hydrolysed product was considered as a measurement of extent of hydrolysis and the former was calculated by using a flame photometer.

### 3.2.18 a. Effect of time on hydrolysis

Figure 3.50 shows the effect of time on hydrolysis of the copolymers. It is observed from the figure that with the increase of reaction time from 15 to 480 minutes with 20 % KOH ( 20cm<sup>3</sup> ), the amount of potassium ion in the hydrolysed product gradually increases upto 160 minutes reaction time and then remains constant ; indicating the progress of hydrolysis with time. The lowering of the rate of hydrolysis after 2 hours may be due to the hindering role of newly formed carboxylate groups on the saponification of nitrile groups. This agrees with the previous reports [77,78] for the hydrolysis of polyacrylonitrile.

### 3.2.18 b. Effect of KOH concentration

The effect of KOH concentration on the hydrolysis of copolymer was studied for 60 minutes hydrolysis time at 40° and by varying the KOH concentration in the range of 1 % - 20 % ( 20cm<sup>3</sup> ). The results obtained are illustrated in Fig.3.51. It is observed that increase in the KOH concentration increases the potassium ion content in the hydrolysed product which indicates the increase of extent of hydrolysis.

During hydrolysis copolymer specimen change colouration from pale yellow to dark red. The extent of colour change increases with the increase of KOH concentration. The appearance of intense colouration is due to polymerisation through nitrile groups with formation of chromophoric azopolyene structure  $(-\overset{|}{\text{C}} = \text{N} - )_n$ , which are subsequently hydrolysed by alkali with the formation of units containing  $-\text{CONH}_2$  and  $-\text{COOK}$  group [79].

### 3.2.18 c. Effect of temperature

The effect of temperature on the hydrolysis was investigated by treating the

copolymer with 20 % KOH solution for a fixed reaction time of 60 minute and varying the temperature in the range of 10-80°. It is observed from the results presented in Fig. 3.52 that the hydrolysis of the copolymer substrate strongly depends on temperature. With the increase of temperature, the amount of potassium ion in the the hydrolysed product increases which indicates the increase of extent of hydrolysis with increase of temperature.

The hydrolysed products were insoluble in organic solvents such as DMF, DMSO, acetone, chloroform etc and hence viscosity characterisation was not carried out. However, the hydrolysed products have been observed to be good supports in immobilisation of enzymes from our preliminary studies.

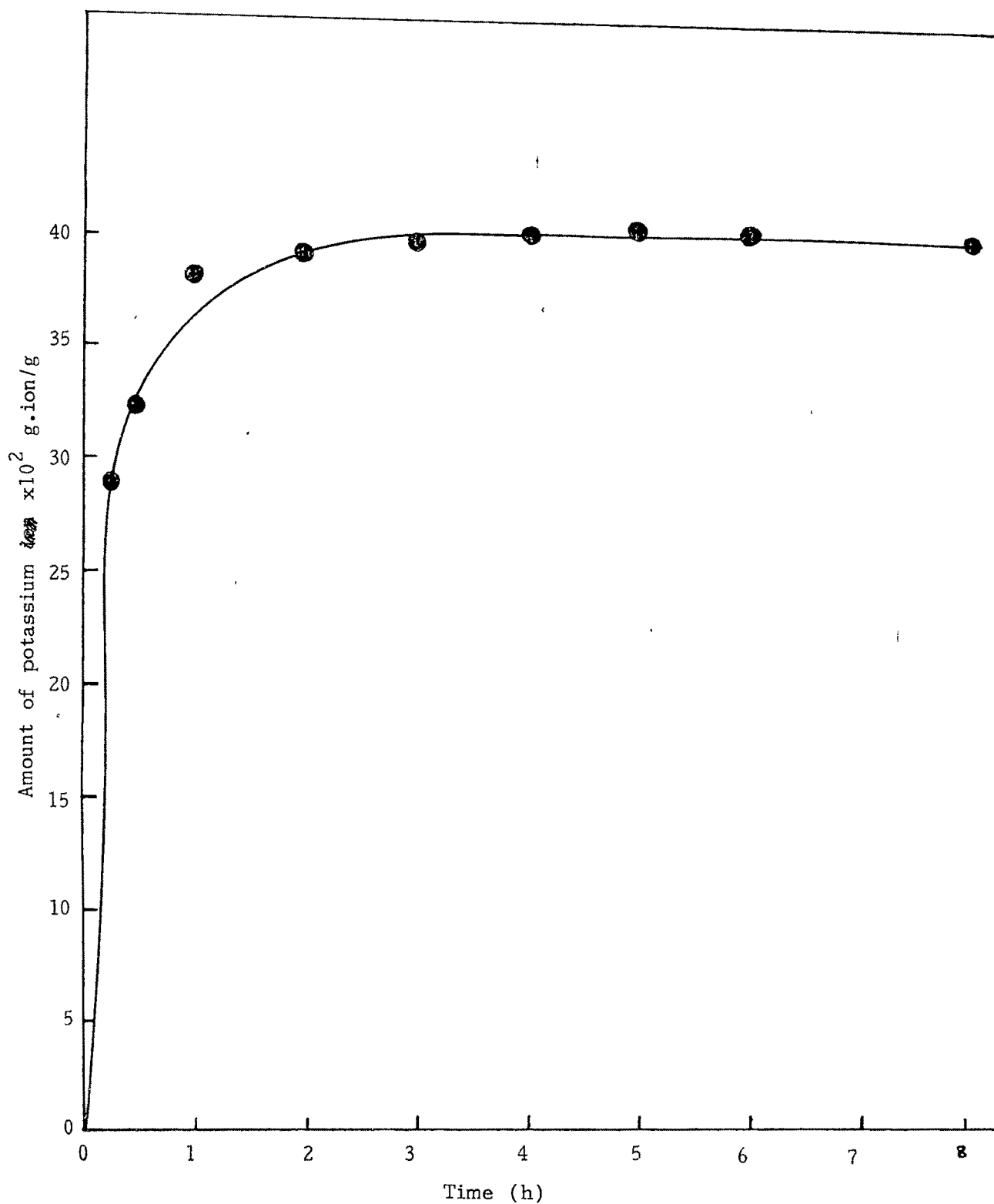


Fig.3.50 Effect of time on hydrolysis of copolymer (1.4 MMA:AN, v/v)  
concentration of KOH : 20%, temperature :  $40^\circ$

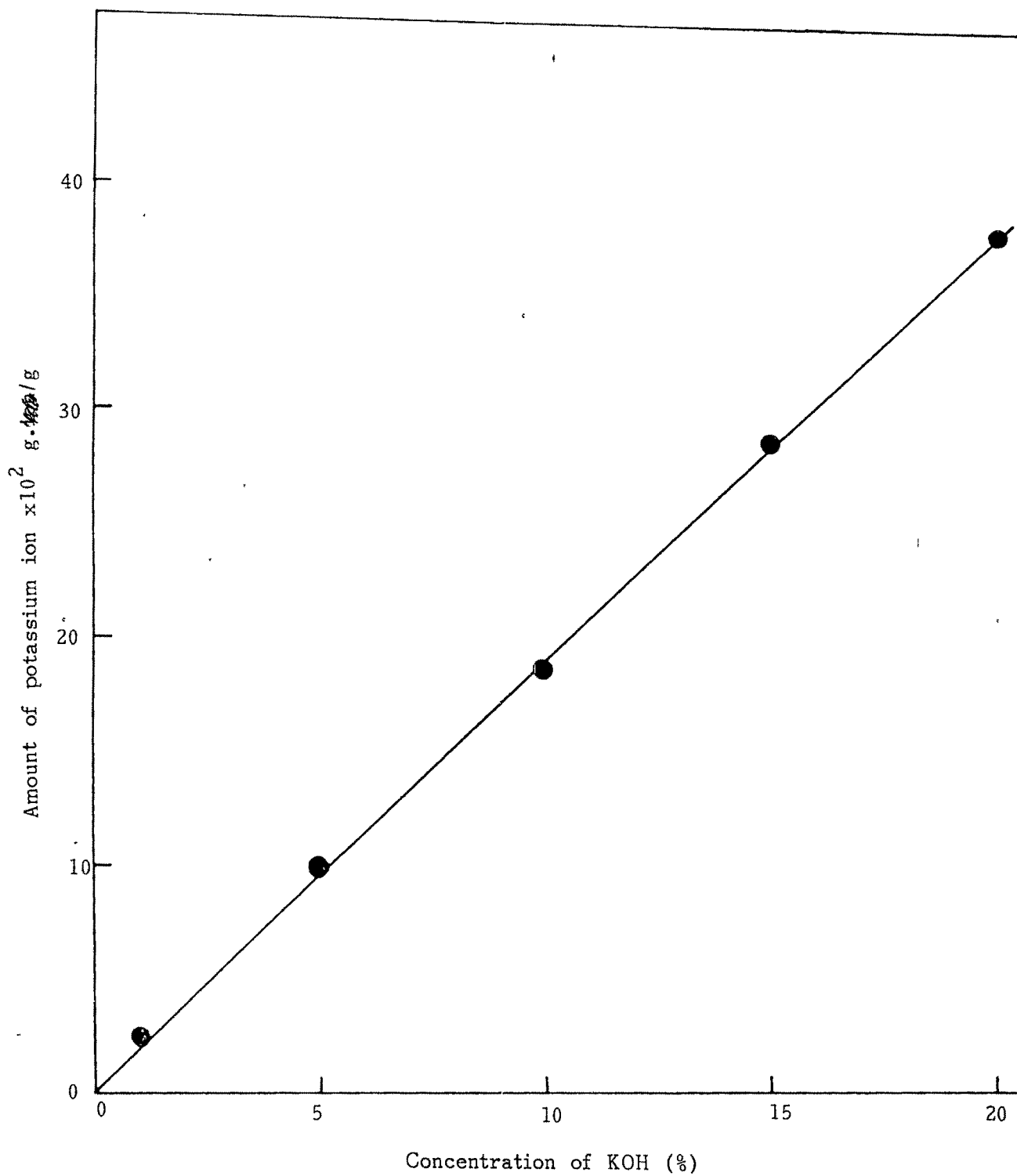


Fig.3.51 Effect of KOH concentration on hydrolysis of copolymer.  
hydrolysis time : 1h, temperature :  $40^\circ$

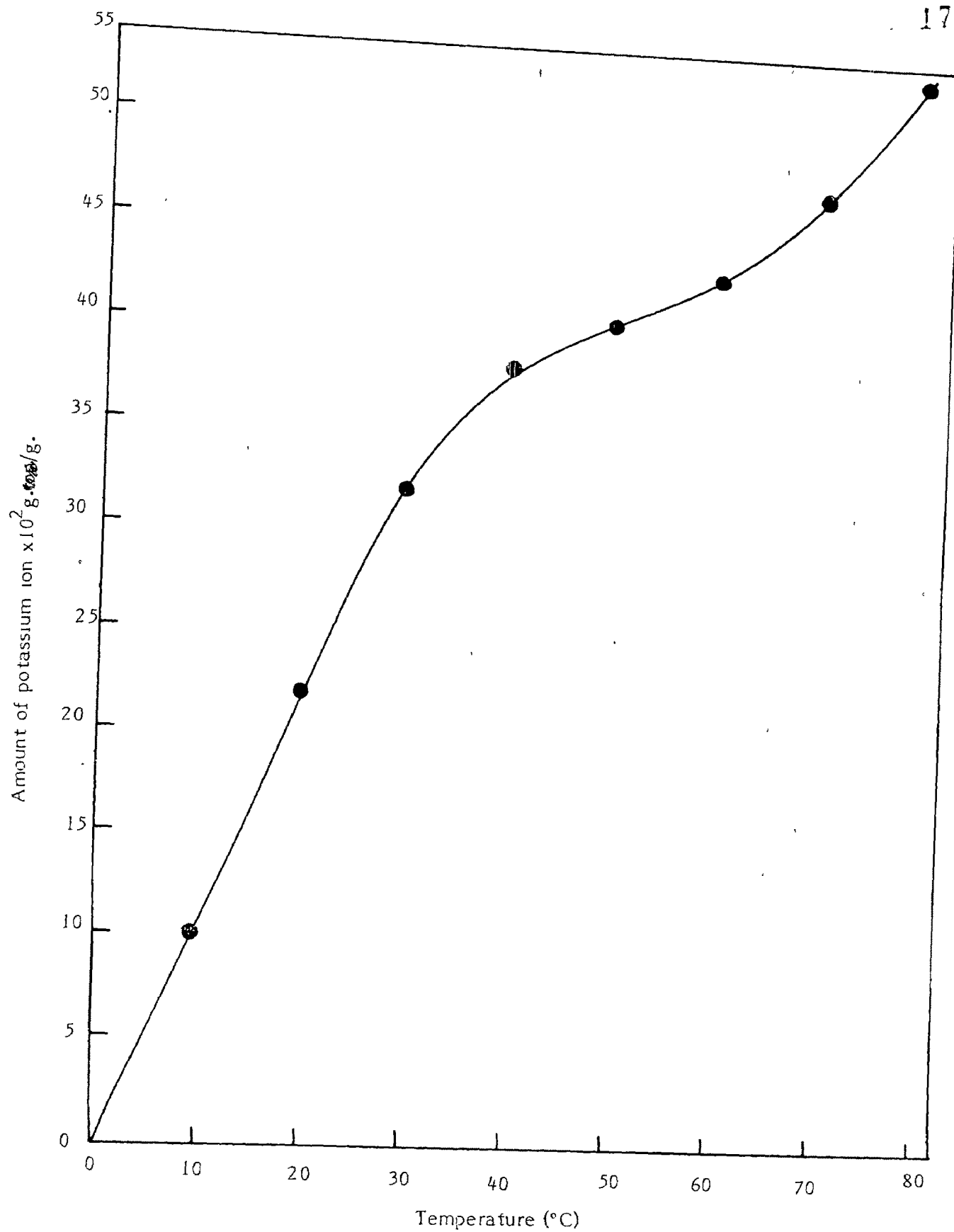


Fig. 3.52 Effect of temperature on hydrolysis of copolymers. Concentration of KOH : 20%, hydrolysis time : 1h

## References

1. F. Dawans and G. Smets, *Makromol. Chem.* **59**, 163 (1963)
2. J. McCartney, "Polymer Degradation mechanism", *Natl. Bur. Std. Publ.* **525**, 123 (1953)
3. R. Houtz, *Textile Res. J.* **20**, 781 (1950).
4. F. R. Mayo and C. Walling, *Chem Revs.* **46**, 191 (1950)
5. T. Alfrey, Jr, J. J. Bohner, And H. Mark, "Copolymerisation". Interscience publishers, New York, 1952.
6. L. Kucher, "Polymerisation Skinetik", Springer-verlag, Berlin, 1951, p.160.
7. I. Skeist, *J. Am. Chem. Soc.* **68**, 1781 (1946).
8. M. Fineman and S.r. Ross, *J. Poly, Sci, Polym. Lett.* **5**, 259 (1950)
9. T. Kelen and F. Tudos, *J. Macromol. Sci, Chem. A-9*, 1(1975)
10. F. M. Lewis, F.R. Mayo and W.F. Hulse, *J. A t. Chem. Soc.* **67**, 1701 (1945).
11. L. S. Luskin, in *Copolymerisation*, G.E. Ham, Ed. Interscience, New York, 1964 p. 655
12. M. L. Huggins, *ibid*, **64**, 2716 (1942).
13. E. O. Kraemer, *Ind. Eng. Chem.* **30**, 1200 (1938)
14. A. Tager, "Physical Chemistry of Polymers". Mir Publishing, Moscow, 1979, p. 459, 467.
15. C. Price and R.B. Stubbersfield, *Eur. Polym. J.* **23**, 177 (1987).
16. J. S. Higgins, S. Bake, P.E. Tomlins, S.B. Ross-Murphy, E. Staples, J. Penfold, and J.V. Dawkins, *polymer* **29**, 1968 (1988)
17. C. Price, A. L. Hudd, R. B. Stubbersfield and B. Wright, *Polym*, **21**, 9 (1989)
18. H. Tompa, "Polymer solutions", Butter worth publications, London, 1956, p.287.
19. A. S. Narang and V.C. Garg, *J. Ind. Chem. Soc.* **66**, 214 (1989)

20. R. Simha, *J. Phys. Chem.* **44**, 25 (1940)
21. A. Einstein, *Ann. Phys.* **19**, 289 (1906).
22. J. W. McBain, *Collid Science*, D.C. Heath, and Co. Boltan, 1950.
23. A. B. Mandal, S. Ray, A. M. Biswas and S.P. Moulík, *J. Phys. Chem.* **84**, 856 (1980)
- 23.a H. Inagaki, K. Hayashi and J. Matsu, *Makromol. Chem.* **84**, 80 (1965)
- 23.b E. Cohn-Ginsberg, T. G. Fox and H.F. Mason, *Polym.* **3**, 97 (1962):
- 23.c. Cleland and Stockmayer, *J. Polym. Sci.* **17**, 473 (1955).
24. R. H. Wiley and G.M. Brauer. *J. Polym. Sci.* **3**, 455 (1948)
25. A. E. Woodward, *Trans. N.Y. Acad. Sci.*, **24**, 250 (1962)
26. R. B. Beevers, *Trans. Faraday. Soc.* **58**, 1465 (1962)
27. R.B. Beevers and E.F.T. white, *Trans. Faraday Soc.* **56**, 744 (1960)
28. R. W. Warfield, M.C. Petree, and P. Donovan, *Soc. Plastics Eng. J.* **15**, 1055 (1959).
29. E. H. Riddle, "Monomeric Acrylic Esters". Reinhold, N.Y. 1954, p.59.
30. F. E. Wiley, *Ind. Eng. Chem*, **34**, 1052 (1942)
31. L. J. Hughes and G. L. Brown, *J. Appl. Polym. Sci.* **51**, 580 (1961)
32. C.E. Rehberg and C.H. Fisher, *Ind. Eng. Chem.* **40**, 1429(1948)
33. J. A. Shetter, *J. Polym. Sci*, **B1**, 209 (1963)
34. F. Wurstlin and H. Thurn, in H.A. Stuart , Ed. "Die Physik der Hochpolymeren", Springer-Verlag, Berlin, 1956.
35. S. S. Rogers and L. Mandelkern, *J. Phys. Chem.* **61**, 985 (1957)
36. T. G. Fox and S. Loshaek, *J. Polym. Sci.*, **15**, 371 (1955)
37. G.M. Martin, S.S. Rogers, and L. Mandelkern, *J. Polym. Sci.* **20**, 579 (1956).
38. L.E. Nielsen, "Mechanical properties of polymers," Reinhold, 1962.
39. R.F. Boyer, "Changements des phases", *Soc. de Chim. Physc. Paris.* 1952
40. J.J. Keavney and E.C. Ebelin, *J. Appl. Polym. Sci.* **3**, 47 (1960)
41. H. J. Kolb and E.F. Lyman, *J. Polym. Sci*, **B1** 317 (1963)

42. R. B. Beevers and E.F.T. White, *Trans. Faraday Soc.* **56**, 1529 (1960)
43. R.H. Gerke, *J. Polym. Sci.* **13**, 295 (1954).
44. K. Schmieder and K. Wolf, *Kolloid. Z.* **134**, 149 (1953)
45. S. Saito and T. Nakajima, *J. Appl. Polym. Sci.*, **2**, 93(1959)
46. R. B. Beevers and E.F.T. White, *J. Polym. Sci.* **B1**, 171 (1963)
47. W. J. Wolf, "Fibres, Plastics and Rubbers", Academic Press, New York, 1956.
48. U. S. 2, 651, 627, Sept. 8, 1953
49. W. H. Howard, *J. Appl. Polym. Sci.*, **5**, 303 (1961)
50. L.V. Holroyd, R.S. Codrington, B. A. Mrowca, and E. Guth, *Rubber Chem. Technol* **25**, 767 (1952)
51. T. Kashiwagi, A. Inaba, J. E. Brown, K. Hatada, T. Kitayama, and E. Masuda, *Macromolecules*, **19**(8), 2160 (1986)
52. K. Bhuyan and N.N. Dass. *J. Poly. Mat.* **12**, 261 (1990)
53. I.C. McNeill, T. Straiton and P. Anderson, *J. Polym. Sci. Polym. Phys.* **18**, 2085 (1980)
54. G.N. Babu, A.R. Atodaria, and A. Deshpande, *J. Inorg. Nucl. Chem.* **25**, 1067(1963)
55. P. Bajaj and M. Padmanban, *Eur. Polym. J.* **21**, 93(1985)
56. N. Grassie and R. McGuchan, *Eur. Polym. J.* **7**, 1091 (1971)
57. M. Tomescu, I Demetroscu and E. Segal, *J. Appl. Polym. sci.*, **26**, 4103 (1981)
58. P. Dunn and B.C. Ennis, *J. Appl. Polym. Sci.*, **14**, 1795 (1970)
59. M. L. Huggins, *J. Am. Chem. Soc.* **64**, 2716 (1942)
60. E.V. Thompson, *J. Polym. Sci, Part B* **4**, 361 (1966)
61. F.W. Billmeyer, Jr. "Text book of Polymer chemistry", Interscience Publishers, Inc. New York, 1957, p. 297
62. S. Minami, *Appl. Polym. Symp.* **25**, 145 (1974)
63. A. S. Kenyon and Mc.C. Rayford. *J. Appl. Polym. Sci.* **23**, 717 (1979)

64. G. Natta, G. Mazzanti, and P. Carradini, *Atti. Acad. Nazl. Lincei, Mem. Classe Sci. Fis. Mat. Nat.* **25**, 3(1958)
65. Z. Mencik, *Vysokomolekul. Soedin*, **2**, 1635 (1960)
66. R. Stefani, M. Chevreton, M. Garnier, and C. Eryraud, *Compt. Rend.* **251**, 2174 (1960)
67. Bjorhaug, Ellefsen and Tonnesen, *J. Polym. Sci.* **12**, 621 (1954), *Norsk. Skogind*, **6**, 402 (1952)
68. Charlesby, *J. Polym. Sci.* **10**, 201 (1953)
69. R. B. Beevers, E.F.T. White and L. Brown. *Trans. Faraday Soc.* **56**, 1535 (1960)
70. Fox, Goode, Gratch, Huggett, Kincaid, Spell and Troupe, *J. Polym. Sci.* **31**, 173 (1958)
71. Stefani, Chevreton, Terrier and Eryraud, *Compt. Rend.* **248**, 2006 (1959)
72. Okamura, *Sen-i Gakkaishi*, **14**, 205 (1958)
73. Gremillion and Boulet, *J. Phys. Chem*; **62**, 94 (1958)
74. Nukushima and Sakurada, *Bull. Inst. Chem. Res. Japan*, **31**, 426 (1953)
75. A. Beerbower, L.A. Kaye, and D.A. Pattison *Chem. Eng.* p.118, Dec, 18, 1967.
76. H. Burrel, *Interchem. Rev.* **14(1)**, 3 (1955)
77. Oya Sanlı , *Eur. Polym. J.* **26**, 9(1990)
78. M.F. Mamedov, B.R. Serabryakov, A.A. Buniyatzade and T.B. Dadashev, *Polym. Sci. USSR*, **14**, 127 (1972)
79. E.A. Ziberman, A.A. Starkov, D.E. Zlotick, A.P. Arbastskii, E.G. Pomerantseva and G.N. Luzyanina, *Zh. Prikl. Khim.* **47**, 2610 (1970).